DISCLAIMER

This contractor document was prepared for the U.S. Department of Energy (DOE), but has not undergone programmatic, policy, or publication review, and is provided for information only. The document provides preliminary information that may change based on new information or analysis, and represents a conservative treatment of parameters and assumptions to be used specifically for Total System Performance Assessment analyses. The document is a preliminary lower level contractor document and is not intended for publication or wide distribution.

Although this document has undergone technical reviews at the contractor organization, it has not undergone a DOE policy review. Therefore, the views and opinions of authors expressed may not state or reflect those of the DOE. However, in the interest of the rapid transfer of information, we are providing this document for your information per your request.

18

NM5507

OFFICE OF CIVILIAN RADIOACTIVE WASTE MANAGEMENT
ANALYSIS/MODEL COVER SHEET
Complete Only Applicable Items

1. QA: QA
Page: 1 of: 88

2. ☒ Analysis	☐ Engineering	3. ☒ Model	☒ Conceptual Model Documentation
	☐ Performance Assessment		☒ Model Documentation
	☒ Scientific		☒ Model Validation Documentation

4. Title:
CSNF Waste Form Degradation: Summary Abstraction

5. Document Identifier (including Rev. No. and Change No., if applicable):
ANL-EBS-MD-000015 REV 00

6. Total Attachments:	7. Attachment Numbers - No. of Pages in Each:
1	I. Document Input Reference Sheet (DIRS), 10 pages

	Printed Name	Signature	Date
8. Originator	Steven A. Steward	Steven A. Steward	Jan. 12, 2000
9. Checker	James C. Cunnane	[illegible]	1/12/00
10. Lead/Supervisor	Christine Stockman	Christine Stockman	1/12/2000
11. Responsible Manager	David Stahl	David Stahl	1/12/00

12. Remarks

INFORMATION COPY
LAS VEGAS DOCUMENT CONTROL

AP-3.10Q.3 Rev. 06/30/1999

Enclosure 18

OFFICE OF CIVILIAN RADIOACTIVE WASTE MANAGEMENT
ANALYSIS/MODEL REVISION RECORD

Complete Only Applicable Items

2. Analysis or Model Title:

CSNF Waste Form Degradation: Summary Abstraction

3. Document Identifier (including Rev. No. and Change No., if applicable):

ANL-EBS-MD-000015 REV 00

4. Revision/Change No.	5. Description of Revision/Change
00	**Initial Issue**

CONTENTS

Page

ACRONYMS 9

1. PURPOSE 11

2. QUALITY ASSURANCE 13

3. COMPUTER SOFTWARE AND MODEL USAGE 15

4. INPUTS 17
   - 4.1 DATA AND PARAMETERS 17
     - 4.1.1 Chemical Basis of Spent Fuel Dissolution 17
     - 4.1.2 Flow-Through Dissolution Data 17
     - 4.1.3 Unsaturated Drip Tests 20
       - 4.1.3.1 Definitions of Data Terms for the Unsaturated Drip Tests 21
     - 4.1.4 Batch (Semi-Static) Tests 31
     - 4.1.5 Gap and Grain Boundary Radionuclide Inventories of Light-Water Reactor (LWR) Spent Fuels 32
     - 4.1.6 Natural Analogs 35
   - 4.2 CRITERIA 37
   - 4.3 CODES AND STANDARDS 37

5. ASSUMPTIONS 39

6. ANALYSIS/MODEL 41
   - 6.1 CHEMICAL BASIS OF SPENT FUEL DISSOLUTION 41
   - 6.2 FLOW-THROUGH DISSOLUTION TESTS AND MODELS 43
     - 6.2.1 Flow-Through Test Results 45
     - 6.2.2 Modeling of Flow-Through Dissolution Data 46
       - 6.2.2.1 Development of the Flow-Through Dissolution Model 46
       - 6.2.2.2 Regression Fit of Alkaline Data to Models 47
       - 6.2.2.3 Abstraction Model at Alkaline Conditions 53
       - 6.2.2.4 Intrinsic Dissolution Model at Acidic Conditions 54
       - 6.2.2.5 Model Validation 55
   - 6.3 UNSATURATED DRIP TESTS 63
     - 6.3.1 High-Drip-Rate Tests 63
     - 6.3.2 Low-Drip-Rate Tests 64
     - 6.3.3 Vapor Tests 65
     - 6.3.4 Estimation of Dissolution Rates from the ANL Unsaturated Drip Tests 65
   - 6.4 BATCH (SEMI-STATIC) TESTS 68
   - 6.5 GAP AND GRAIN BOUNDARY RADIONUCLIDE INVENTORIES OF LWR SPENT FUELS 74
   - 6.6 NATURAL ANALOGS 76
     - 6.6.1 Studies of Natural Analog Sites 76
     - 6.6.2 Spent-Fuel Corrosion Products in Laboratory Tests 77

CONTENTS (Continued)

Page

6.6.3 Comparison of Mineral Formation Between Laboratory Tests and Nopal I Studies 78

7. CONCLUSIONS 81

8. INPUTS AND REFERENCES 85

ATTACHMENT

I DOCUMENT INPUT REFERENCE SHEET (DIRS) I-1

FIGURES

Page

1. Inventories as a Percentage of Total Inventories versus Fission-Gas Release 33
2. Abstracted Dissolution Model 55

INTENTIONALLY LEFT BLANK

TABLES

Page

1. Test Parameters and Dissolution Measurement Results for YMP-Sponsored UO_2 and Spent-fuel Studies 18
2. Measured UO_2 Flow-Through Dissolution Data with Variation of Oxygen and pH 20
3. ATM-103 High-Drip-Rate Test: Interval Fractions, Cumulative Fractions, Interval Release Rate, and Concentration of Isotopes 23
4. ATM-106 High-Drip-Rate Test: Interval Fractions, Cumulative Fractions, Interval Release Rate, and Concentration of Isotopes 25
5. ATM-103 Low-Drip-Rate Test: Interval Fractions, Cumulative Fractions, Interval Release Rate, and Concentration of Isotopes 27
6. ATM-106 Low-Drip-Rate Test: Interval Fractions, Cumulative Fractions, Interval Release Rate, and Concentration of Isotopes 28
7. ATM-103 Vapor Test: Interval Fractions, Cumulative Fractions, and Interval Release Rate of Isotopes 29
8. ATM-106 Vapor Test: Interval Fractions, Cumulative Fractions, and Interval Release Rate of Isotopes 30
9. Unsaturated Tests: pH at Each Time Interval 31
10. LWR Spent-Fuel Gap and Grain-Boundary Inventories Used in Figure 1 34
11. Paragenesis of Uranium Minerals at Nopal I 35
12. Summary of UO_2 Alteration Phases 36
13. Identification of Alteration Phases in Unsaturated Tests from Electron and X-ray Diffraction and Crystal Morphology 37
14. Coefficients and Statistics for the Best Fit Alkaline Spent-Fuel Dissolution Model (Eq. 11) 49
15. Coefficients and Statistics for the Alkaline Spent-Fuel Dissolution Model in Table 14 without Interaction Terms 50
16. Coefficients and Statistics for the Alkaline Spent-Fuel Dissolution Model in Table 15 after Removing Less Important Terms 50
17. Coefficients and Statistics for the Alkaline Spent-Fuel Dissolution Model in Table 16 after Removing Least-Important Carbonate Term 50
18. Coefficients and Statistics for the Alkaline Spent-Fuel Dissolution Model in Table 17 with Temperature as the Only Variable 51
19. Coefficients and Statistics for the Alkaline UO_2 Dissolution Model 51
20. Coefficients and Statistics for the Alkaline Spent-Fuel-Only Dissolution Model 51
21. Standard Error of Terms in Equation 16 53
22. Comparison of Model Fitting to Alkaline CSNF dissolution data 57
23. Comparison of Model Fitting to Alkaline UO_2 Data 58
24. Single-Measurement Dissolution Data 59
25. Measured UO_2 Flow-Through Dissolution Data in Brines with Variation of Temperature and Carbonate Concentration 61
26. Comparison of Data from Tait and Luht (1997) with the Alkaline Models Equations 11 and 16 62
27. Estimates of Dissolution Rates Based on Unsaturated Drip-Test Cumulative Release Fractions 67

TABLES (Continued)

Page

28. Calculations of Equivalent Intrinsic Dissolution Rates of H. B. Robinson Fuel at 25°C..... 71
29. Calculations of Equivalent Intrinsic Dissolution Rates of H. B. Robinson Fuel at 85°C..... 72
30. Calculations of Equivalent Intrinsic Dissolution Rates of Turkey Point Fuel at 85°C 73

ACRONYMS

ANL	Argonne National Laboratory
ATM	approved testing material
BWR	boiling water reactor
CANDU	Canada deuterium uranium
CSNF	commercial spent nuclear fuel
DIW	deionized distilled water
DOE	U.S. Department of Energy
DR	dissolution rate
EBS	Engineered Barrier System
EDS	energy-dispersive x-ray spectroscopy
EJ-13	Water from well J-13, equilibrated with tuff at 90°C
EM	Error metric = $\log_{10}(DR_c/DR_m)$, log of the ratio of the calculated to measured dissolution rates
FGR	fission gas release
GI	gap inventory
GBI	grain boundary inventory
HBR	H. B. Robinson (fuel source)
IRMR	interval release mass rate
IRSR	Issue Resolution Status Report
LBU	log10(burnup)
LDR	log10(dissolution rate)
LLNL	Lawrence Livermore National Laboratory
LWR	light-water reactor
NNWSI	Nevada Nuclear Waste Storage Investigations (NNWSI)
PNNL	Pacific Northwest National Laboratory
PMR	Process Model Report
PWR	pressurized water reactor
QA	Quality Assurance
QARD	Quality Assurance Requirements Document
RMS	root mean square

ACRONYMS (Continued)

SA	surface area
SCE	saturated calomel electrode
SEM	scanning electron microscopy/microscope
TCD	time to complete dissolution
TEM	transmission electron microscopy/microscope
TP	Turkey Point (fuel source)
UDT	unsaturated drip test
WBS	work breakdown structure
WFCR	Waste Form Characteristics Report
WFDPMR	Waste Form Degradation Process Model Report
XPS	x-ray photoelectron spectroscopy
XRD	x-ray diffraction
YMP	Yucca Mountain Project

1. PURPOSE

The purpose of this analysis is to provide a current summary of data and updated models for commercial spent nuclear fuel (CSNF) intrinsic (forward) dissolution (high water-flow) rates. A summary of the chemical interaction of UO_2 with groundwater and its components is given in the initial analysis section. This analysis also provides a comparison of the three types of CSNF dissolution measurements available within and outside of the program. The three types of dissolution tests available are semi-static/batch, low-flow/drip, and high-flow/flow-through tests. This analysis also provides a summary of the gap and grain boundary radionuclide inventories of clad spent fuel. The final analysis topic is a comparison of the current knowledge of uranium mineral phases that form in laboratory tests with spent fuel and UO_2 with the mineral assemblages found in natural uranium-bearing sites. This analysis will be incorporated into the *Waste Form Degradation Process Model Report* (PMR) for the Total Systems Performance Assessment–Site Recommendation. This report was developed in accordance with the technical product development plan *Waste Package Materials Department Analysis and Modeling Reports Supporting the Waste Form PMR* (CRWMS M&O 1999c).

These models of CSNF degradation are bounding models that apply to all UO_2-based spent fuel expected to be disposed in a repository. These models are valid within the range of qualified experimental data: pH down to 3 and up to 10, oxygen pressure from 0.002 to 0.2 atmospheres, carbonate/bicarbonate concentrations from $2x10^{-4}$ to $2x10^{-2}$ molar. At pHs less than or equal to 7, these models are only shown to be valid at CO_2 pressures of 10^{-3} atmospheres. Corroborating data outside of these ranges indicate that the valid ranges may extend beyond those stated.

INTENTIONALLY LEFT BLANK

2. QUALITY ASSURANCE

The Quality Assurance (QA) program applies to this analysis. All types of waste packages and their structures, systems or components were classified (per QAP-2-3 REV 10) as Quality Level-1 in *Classification of the MGR Uncanistered Spent Nuclear Fuel Disposal Container System* (CRWMS M&O 1999b, p. 7). This analysis applies to all of the waste package designs included in the MGR Classification Analyses. Reference CRWMS M&O (1999b) is cited as an example. The development of this analysis is conducted under activity evaluation *1101213FM3 Waste Form Analyses & Models - PMR* (CRWMS M&O 1999a), which was prepared per QAP-2-0 REV 5. The results of that evaluation were that the activity is subject to the *Quality Assurance Requirements and Description* (DOE 1998) requirements. This analysis and model report was prepared in accordance with AP-3.10Q REV 1 ICN 1, Analyses and Models.

INTENTIONALLY LEFT BLANK

3. COMPUTER SOFTWARE AND MODEL USAGE

The software used to support the analysis and modeling activities is not subject to the requirements of the *Quality Assurance Requirements Document* (QARD) because only industry standard software were used in this analysis. Those programs are Microsoft Excel, versions 5 at Lawrence Livermore National Laboratory (LLNL) and Excel version 98 at Argonne National Laboratory (ANL), and the RS series of data analysis software (LLNL) from the Domain Manufacturing Corporation (formerly BBN software). No software routines or macros were used with the software, only built-in regression functions. No external models are used in the development of this analysis and model report.

INTENTIONALLY LEFT BLANK

4. INPUTS

4.1 DATA AND PARAMETERS

Three types of dissolution studies have been sponsored by YMP. The first type, flow-through dissolution studies on spent fuel and UO_2 performed at Pacific Northwest National Laboratory (PNNL) and LLNL, provides direct dissolution measurements over a wide range of aggressive conditions that bracket the typical Yucca Mountain groundwater and environmental conditions. Flow-through tests are designed to eliminate the influence of back-reactions or secondary phase formation. The available data are in Section 4.1.2.

The second type, batch or semi-static dissolution tests, was performed over a decade ago on available spent-fuel samples. The tests involved placing a few grams of spent fuel in various configurations in less than a liter of synthetic J-13 groundwater, periodically sampling the solution, and analyzing for various radionuclides. These data allowed an estimate of the spent-fuel dissolution rate based on the fraction of radionuclide released per unit time and also provided an estimate of the solubility limit for the radionuclides. These static-type tests are still commonly performed in the international community. This type of test is also a prototype of the "bathtub" scenario of a failed fuel container in the repository that leaks groundwater into the container faster than it leaves and, over time, allows the fuel to be immersed in standing water. Data used to estimate spent-fuel dissolution rates are discussed in Section 4.1.4. These dissolution estimates are used in Section 6.4 to confirm the intrinsic dissolution model.

The third type of test, the unsaturated drip test performed at ANL, is intended to be an "in-service" type of test, in which spent-fuel degradation processes over time can be observed and measured, and in which the likely failure scenario of groundwater from a failed container drips onto the fuel, reacts with it, and dissolves away soluble components and perhaps forms solid corrosion products. Cumulative concentrations of the released soluble radionuclides in these tests can be used as a marker for fuel dissolution. Summaries of the fractional and cumulative released radionuclide concentrations are given in Section 4.1.3 and used in Section 6.3 to estimate dissolution rates for confirmation of the intrinsic dissolution model as a bounding measure of the release of radionuclides from spent fuel.

4.1.1 Chemical Basis of Spent Fuel Dissolution

This section is included to establish a one to one correspondence between the input sections 4.1.1 through 4.1.6 and analysis sections 6.1 through 6.6. Section 6.1 is provided for information only and contains no directly relied upon data.

4.1.2 Flow-Through Dissolution Data

The available YMP-sponsored qualified UO_2 and spent-fuel flow-through dissolution data are given in Table 1. Runs 1-31 for spent fuel and runs 39-60 for UO_2 are from Stout and Leider (1998). Runs 32-38 were reported recently (DTN: LL990707151021.075). Runs 61-64 are new runs for a very high-burnup fuel (ATM-109, DTN: LL990901851021.084). The ATM-109 burnup measurements are still uncertain with an approximate value of 70 MWd/kgU (Wolf et al. 1999).

Table 1. Test Parameters and Dissolution Measurement Results for YMP-Sponsored UO_2 and Spent-Fuel Studies

Run	BU[a]	LBU	T (°C)	T (K)	IT (K^{-1})	Total CO_3	pCO_3	O_2	pO_2	$[H^+](M)$	pH	DR	LDR
1	30	1.48	50	323	3.09E-03	0.002	2.70	0.2	0.7	1E-09	9	6.34	0.802
2	30	1.48	50	323	3.09E-03	0.002	2.70	0.2	0.7	1E-09	9	7.05	0.848
3	30	1.48	50	323	3.09E-03	0.002	2.70	0.2	0.7	1E-09	9	5.07	0.705
4	30	1.48	22	295	3.39E-03	0.020	1.70	0.2	0.7	1E-08	8	3.45	0.538
5	30	1.48	74	347	2.88E-03	0.020	1.70	0.2	0.7	1E-10	10	14.20	1.152
6	30	1.48	74	347	2.88E-03	0.0002	3.70	0.2	0.7	1E-08	8	8.60	0.934
7	30	1.48	21	294	3.40E-03	0.0002	3.70	0.2	0.7	1E-10	10	0.63	–0.201
8	30	1.48	22	295	3.39E-03	0.02	1.70	0.2	0.7	1E-09	9	2.83	0.452
9	30	1.48	22	295	3.39E-03	0.002	2.70	0.2	0.7	1E-10	10	2.04	0.310
10	30	1.48	27	300	3.33E-03	0.0002	3.70	0.02	1.7	1E-08	8	1.79	0.253
11	30	1.48	78	351	2.85E-03	0.0002	3.70	0.02	1.7	1E-10	10	1.49	0.173
12	30	1.48	25	298	3.35E-03	0.02	1.70	0.02	1.7	1E-10	10	2.05	0.312
13	30	1.48	77	350	2.86E-03	0.02	1.70	0.02	1.7	1E-08	8	2.89	0.461
14	30	1.48	23	296	3.38E-03	0.02	1.70	0.003	2.5	1E-08	8	2.83	0.452
15	30	1.48	74	347	2.88E-03	0.02	1.70	0.003	2.5	1E-10	10	0.69	-0.16
16	30	1.48	78	351	2.85E-03	0.0002	3.70	0.003	2.5	1E-08	8	1.98	0.297
17	30	1.48	19	292	3.42E-03	0.0002	3.70	0.003	2.5	1E-10	10	0.51	-0.29
18	30	1.48	50	323	3.09E-03	0.02	1.70	0.003	2.5	1E-10	10	1.04	0.017
19	30	1.48	21	294	3.40E-03	0.002	2.70	0.003	2.5	1E-09	9	1.87	0.272
20	30	1.48	75	347	2.88E-03	0.02	1.70	0.02	1.7	1E-10	10	4.75	0.677
21	31	1.49	50	323	3.10E-03	0.002	2.70	0.2	0.7	1E-09	9	6.60	0.82
22	50	1.70	25	298	3.39E-03	0.02	1.70	0.2	0.7	1E-08	8	1.50	0.18
23	31	1.49	25	298	3.36E-03	0.02	1.70	0.2	0.7	1E-08	8	4.00	0.60
24	31	1.49	75	348	2.87E-03	0.02	1.70	0.2	0.7	1E-08	8	9.10	0.96
25	31	1.49	25	298	3.36E-03	0.0002	3.70	0.2	0.7	1E-08	8	2.60	0.41
26	31	1.49	75	348	2.87E-03	0.0002	3.70	0.2	0.7	1E-08	8	11.00	1.04
27	44	1.64	25	298	3.36E-03	0.02	1.70	0.2	0.7	1E-08	8	3.50	0.54
28	50	1.70	25	298	3.36E-03	0.02	1.70	0.2	0.7	1E-08	8	3.80	0.58
29	50	1.70	75	348	2.87E-03	0.02	1.70	0.2	0.7	1E-08	8	6.90	0.84
30	50	1.70	25	298	3.36E-03	0.0002	3.70	0.2	0.7	1E-08	8	2.90	0.46
31	50	1.70	75	348	2.87E-03	0.0002	3.70	0.2	0.7	1E-08	8	9.50	0.98
32	50	1.70	25	298	3.36E-03	0.02	1.70	0.002	2.7	1E-08	8	4.1	0.61
33	50	1.70	75	348	2.87E-03	0.02	1.70	0.002	2.7	1E-08	8	1.4	0.15
34	50	1.70	25	298	3.36E-03	0.0002	3.70	0.002	2.7	1E-08	8	1.9	0.28
35	50	1.70	75	348	2.87E-03	0.0002	3.70	0.002	2.7	1E-08	8	3.5	0.54
36	15	1.18	25	298	3.36E-03	0.02	1.70	0.20	0.7	1E-08	8	3.2	0.51
37	15	1.18	75	348	2.87E-03	0.02	1.70	0.20	0.7	1E-08	8	11.9	1.08
38	15	1.18	25	298	3.36E-03	0.0002	3.70	0.20	0.7	1E-08	8	3.7	0.57
61	**70**	**1.85**	25	**298**	**3.36E-03**	**0.02**	**1.70**	**0.20**	0.7	**1E-08**	8	**3.8**	**0.58**
62	**70**	**1.85**	75	**348**	**2.87E-03**	**0.02**	**1.70**	**0.20**	0.7	**1E-08**	8	**4.6**	**0.66**
63	**70**	**1.85**	25	**298**	**3.60E-03**	**0.0002**	**3.70**	**0.20**	0.7	**1E-08**	8	**2.9**	**0.46**
64	**70**	**1.85**	75	**348**	**2.87E-03**	**0.0002**	**3.70**	**0.20**	0.7	**1E-08**	8	**6.0**	**0.78**

Table 1. Test Parameters and Dissolution Measurement Results for YMP-Sponsored UO_2 and Spent-Fuel Studies (Continued)

Run	BU[a]	LBU	T (°C)	T (K)	IT (K^{-1})	Total CO_3	pCO_3	O_2	pO_2	$[H^+](M)$	pH	DR	LDR
39	0	b	50	323	3.09E-03	0.002	2.70	0.02	1.7	1E-09	9	12.30	1.090
40	0	b	50	323	3.09E-03	0.002	2.70	0.02	1.7	1E-09	9	7.96	0.901
41	0	b	50	323	3.09E-03	0.002	2.70	0.02	1.7	1E-09	9	10.4	1.015
42	0	b	25	298	3.35E-03	0.02	1.70	0.2	0.7	1E-08	8	2.42	0.384
43	0	b	75	348	2.87E-03	0.02	1.70	0.2	0.7	1E-10	10	77.38	1.889
44	0	b	75	348	2.87E-03	0.0002	3.70	0.2	0.7	1E-08	8	10.9	1.036
45	0	b	25	298	3.35E-03	0.0002	3.70	0.2	0.7	1E-10	10	2.55	0.407
46	0	b	25	298	3.35E-03	0.02	1.70	0.002	2.7	1E-08	8	0.22	-0.666
47	0	b	75	348	2.87E-03	0.02	1.70	0.002	2.7	1E-10	10	5.61	0.749
48	0	b	75	348	2.87E-03	0.0002	3.70	0.002	2.7	1E-08	8	0.51	-0.292
49	0	b	26	299	3.34E-03	0.0002	3.70	0.002	2.7	1E-10	10	0.23	-0.633
50	0	b	26	299	3.34E-03	0.0002	3.70	0.02	1.7	1E-08	8	0.12	-0.922
51	0	b	75	348	2.87E-03	0.0002	3.70	0.02	1.7	1E-10	10	9.21	0.964
52	0	b	26	299	3.34E-03	0.02	1.70	0.02	1.7	1E-10	10	1.87	0.272
53	0	b	75	348	2.87E-03	0.02	1.70	0.02	1.7	1E-08	8	5.11	0.709
54	0	b	50	323	3.09E-03	0.02	1.70	0.002	2.7	1E-10	10	4.60	0.663
55	0	b	25	298	3.35E-03	0.02	1.70	0.2	0.7	1E-09	9	6.72	0.827
56	0	b	25	298	3.35E-03	0.002	2.70	0.2	0.7	1E-10	10	9.34	0.970
57	0	b	26	299	3.34E-03	0.002	2.70	0.002	2.7	1E-09	9	1.52	0.180
58	0	b	75	348	2.87E-03	0.0002	3.70	0.2	0.7	1E-10	10	6.48	0.812
59	0	b	75	348	2.87E-03	0.002	2.70	0.2	0.7	1E-09	9	23.3	1.367
60	0	b	75	348	2.87E-03	0.02	1.70	0.2	0.7	1E-08	8	54.0	1.700

DTN: [LL980601551021.042 (runs 1-20, 39-60); LL980704251021.045 (runs 21, 26); LL980711051021.048 (runs 22-25, 27-31); LL990707151021.075 (runs 32-38); LL990901851021.084 (runs 61-64)]

NOTES: [a] BU = burnup MWd/kgU. For discussion of burnups, see Table 2.1 of Gray and Wilson (1995, p. 2.2).
LBU = log10 (BU),
[b] log(0) is undefined, a LBU of 0 is used for modeling.
T = temperature, Total CO_3 = $[HCO_3^-]$ + $[CO_3^=]$ in molar, pCO_3 = -log10 (Total CO_3)
O_2 = oxygen pressure in atmospheres, pO_2 = -log10 (O_2)
DR = dissolution rate in mg/(m^2·d), LDR = log10(DR)
Data integrated from Stout and Leider (1998, pp. 2-220 through 2-225)

Because of this uncertainty in burnup, the newest four runs are separated in the table and were not a part of the modeling regression data set for Section 6.2. Instead, they were used for model validation.

Gray (DTN: LL990707151021.075) reports an acidic spent fuel (ATM-103) dissolution rate of 109 mg/(m^2·d) at a pH of 3. This measurement was performed at 25°C in 10^{-3}M nitric acid sparged with CO_2-free air. This is the only qualified data point at an acidic pH (Section 6.2.2.4).

Steward and Mones (1996) obtained acidic dissolution rates for UO_2 at room temperature. The UO_2 dissolution rates were 5 mg/(m^2·d) at pH = 4 and 3 mg/(m^2·d) at pH = 6. At 75°C the rate for pH = 4 was 23 mg/(m^2·d). Table 2 contains published results (Torrero et al. 1997) of changes in UO_2 dissolution rate versus pH at room temperature[1]. These data were used for confirmation purposes only in Section 6.2.2.5.

Table 2. Measured UO_2 Flow-Through Dissolution Data with Variation of Oxygen and pH

5%O_2/N_2				21%O_2/N_2			
pH	[U] mol/dm^3	*q* (dm^3/s)	*DR*	pH	[U] mol/dm^3	*q* (dm^3/s)	*DR*
3.3	4.90E-07	1.78E-06	1.59E+00	3.2	8.00E-07	2.08E-06	3.03E+00
3.6	3.40E-07	1.78E-06	1.10E+00	3.5	6.70E-07	2.08E-06	2.54E+00
4.4	1.93E-07	1.78E-06	6.25E-01	4.1	4.50E-07	2.08E-06	1.70E+00
4.8	1.50E-07	1.78E-06	4.86E-01	4.7	2.30E-07	2.07E-06	8.66E-01
5.2	1.10E-07	1.76E-06	3.52E-01	5.2	1.20E-07	2.17E-06	4.74E-01
5.6	7.90E-08	1.70E-06	2.44E-01	6.2	1.00E-07	1.67E-06	3.04E-01
6.6	4.00E-08	1.57E-06	1.14E-01	6.5	7.00E-08	1.70E-06	2.17E-01
8.6	2.70E-08	1.63E-06	8.01E-02	6.6	5.00E-08	1.71E-06	1.56E-01
9	2.00E-08	3.17E-06	1.15E-01	8.8	5.10E-08	1.68E-06	1.56E-01
9.4	2.60E-08	3.06E-06	1.45E-01				
10.6	1.10E-08	3.20E-06	6.41E-02				
11.6	4.00E-08	3.30E-06	2.40E-01				

NOTES: Surface Area = 1.13E-02 m^2/g
q = flow rate, *DR* [mg/(m^2·d)]
Torrero et al. (1997)

4.1.3 Unsaturated Drip Tests

The data in this section were acquired at ANL and reported in a transmittal of input titled *Commercial Spent Nuclear Fuel Degradation in Unsaturated Drip Tests* (CRWMS M&O 2000). They provide a basis for estimating radionuclide release and spent-fuel dissolution under a range of more prototypical test conditions for comparison with the intrinsic dissolution rate model.

The data that will be summarized here is based on the results from three sets of service conditions tests at 90°C with two commercial PWR spent nuclear fuels of different type and burnup (referred to as ATM-103 and ATM-106). These tests, which were initiated in FY1992, simulate limited water access under oxidizing conditions. The tests include a test with saturated water vapor and two drip tests in which simulated groundwater is injected at nominal rates of 0.75 and 0.075 mL every 3.5 days.

The fuel fragments that were used in the three sets of unsaturated tests were not washed or ground prior to use. They were sieved to remove all material smaller than 20 mesh (~ 840 μm, CRC 1991, p 15-33), which was 0.1% of the total fuel sample for ATM-103 and 1% for ATM-106. Because every species, except iodine, had minimal initial releases, it is highly unlikely that

[1] Room temperature was not specified in original data source. Its absolute value is not important for this document.

fines contributed significantly to the amounts of radionuclides that were released in any of the drip tests. Even though the cladding was removed from the fragments, care was taken to ensure that the fuel/clad gap inventory was not removed.

Minimally soluble radionuclides are held up in the corrosion product layers. These corrosion products, based on solids characterization, are of two types, uranyl alteration phases and inhomogeneous, amorphous, and insoluble residues that are highly enriched in fission products and are found as thin layers between the fuel and the uranyl alteration phases (Finn et. al. 1998).

In FY1999, unsaturated tests were started with ATM-109 spent fuel, which has a burnup > 65 MWd/kgU. In addition, two sets of low-drip-rate tests with UO_2 have been in progress for 14 years and for 10 years, respectively. For these UO_2 tests, the U release rates and the suite of uranyl corrosion products have been reported (Stout and Leider 1998, p. 2-228).

The terms that were derived from the results of the tests are defined as follows. The term "interval" refers to a particular sequential test period and is identified by the cumulative reaction time achieved by a fuel. For example, the 4.8-year value in the time column of Table 3 refers to the interval between 4.2 and 4.8 years of cumulative reaction for a fuel sample. The term "release" indicates elements that have left the Zircaloy-4 holder and are either dissolved in solution, suspended as colloids in solution, or sorbed onto the stainless steel test vessel. It does not include material incorporated into alteration products and adsorbed on the Zircaloy sample holder, or the spent fuel. The "interval release mass fraction" for a given radionuclide is the ratio R/T. The value R is the amount of radionuclide collected in a given interval, i.e., the total amount in the leachate and the acid-strip of the test vessel. The value T is the estimated amount of radionuclide in the fuel sample. The term "cumulative release fraction" is the sum of the interval release mass fractions. The term "interval release rate" (also called interval release mass rate, or IRMR) is defined as the mass fraction per day of a given species that is released in a specific time interval. It is the interval release mass fraction divided by the number of days in the time interval.

4.1.3.1 Definitions of Data Terms for the Unsaturated Drip Tests

A data dictionary for the variables used in the unsaturated tests is supplied.

Cumulative Reaction Time–The number of days, months, or years that a fuel sample has been under test. This is also known as reaction time and is listed as time in column 1 of Tables 3-6.

Cumulative Release Fraction, Cumulative Fraction, cum frac–The sum of the individual interval release fractions for a total time period.

Interval Release Mass Rate (IRMR)–The interval release fraction of a given radionuclide divided by the number of days in a specific time interval. The units are 1/d.

Normalized Release Rate–A normalization of the release rate–It is obtained by multiplying the radionuclide interval mass release rate by 1000 (to convert to mg) and by the total mass of the fuel sample and then dividing by the surface area, which is the product of the specific surface area and the total mass of the fuel sample. The units are $mg/(m^2 \cdot d)$.

Radionuclide Concentration–The ratio of the moles of radionuclide released divided by the liters of injected equilibrated J-13 water (EJ-13). This is the concentration as the injected water leaves the Zircaloy-4 holder and is in units of molarity (*M*). It can only be calculated for the high-drip-rate and the low-drip-rate tests.

Radionuclide Release Mass Fraction–A variable fraction that is defined as the ratio *R/T* for a given radionuclide. The value *R* is the radionuclide total in a given time interval, i.e., the total amount in the leachate and the acid-strip. The value *T* is the estimated amount of radionuclide in the fuel sample. This is a mass fraction and is equivalent to the "interval release fraction."

Specific Surface Area (SSA)–The geometric surface area of the fuel fragments estimated by using an idealized geometry of wedge-shaped pieces. The calculated value is 2.1×10^{-4} m^2/g. The surface area of the fuel in a given test at each time interval is the product of the specific surface area and the mass of the fuel in the test.

Time–The cumulative reaction time, in years, of the fuel at the end of the test period.

The sources of uncertainty for leachate characterization include uncertainties associated with weight measurement of an aliquot and of the total amount of leachate solution; counting uncertainties for gamma and alpha data; and the accumulated uncertainties associated with the measurement of analytes, control solutions, and standards for ICP-MS data. See Finn (1999) for more detailed discussion of data uncertainty.

For the unsaturated drip tests on spent fuel, the interval release fractions, cumulative release fractions, interval release rates, and the concentrations of ^{99}Tc, ^{238}U, ^{239}Pu, ^{237}Np, ^{129}I, ^{137}Cs, ^{90}Sr, ^{241}Am, and ^{97}Mo are reported (DTN: LL991001251021.090). These data are summarized from data package submissions from ANL (CRWMS M&O 2000). A table is supplied for each test: Table 3 for the ATM-103 high-drip-rate test, Table 4 for the ATM-106 high-drip-rate test, Table 5 for the ATM-103 low-drip-rate test, Table 6 for the ATM-106 low-drip-rate test, Table 7 for the ATM-103 vapor test, and Table 8 for the ATM-106 vapor test. The pH measured at room temperature for each test is in Table 9.

Table 3. ATM-103 High-Drip-Rate Test: Interval Fractions, Cumulative Fractions, Interval Release Rate, and Concentration of Isotopes

Time (y)	Tc-99 Interval Frac	U-238 Interval Frac	Pu-239 Interval Frac	Np-237 Interval Frac	I-129 Interval Frac	Cs-137 Interval Frac	Sr-90 Interval Frac	Am-241 Interval Frac	Mo-97 Interval Frac
0.2	1.94E-03	2.82E-05	4.30E-06	8.47E-04	7.62E-03	4.63E-04	1.78E-03	1.95E-03	9.76E-06
0.3	2.78E-03	2.12E-05	1.97E-06	3.19E-04	4.26E-03	7.78E-04	7.14E-04	8.95E-04	1.57E-04
0.8	1.94E-03	5.28E-06	1.04E-06	3.23E-06	6.80E-03	2.42E-04	4.99E-05	1.34E-05	9.42E-05
1.3	6.61E-03	8.50E-06	2.23E-06	1.24E-07	3.25E-04	9.33E-05	1.18E-04	7.97E-05	2.46E-04
1.6	7.83E-03	2.34E-05	8.71E-07	2.62E-06	2.81E-04	2.05E-04	3.42E-05	1.64E-05	1.40E-03
2.0	1.05E-03	2.39E-06	2.04E-08	2.13E-07	1.18E-04	1.11E-04	4.04E-06	6.43E-07	4.57E-04
2.5	1.81E-03	7.56E-07	1.57E-08	5.94E-07	2.42E-04	1.35E-04	1.84E-05	4.60E-07	2.45E-04
3.1	5.17E-03	2.81E-06	2.58E-06	2.59E-06	3.25E-03	1.64E-03	1.04E-05	7.20E-07	1.19E-02
3.7	1.26E-03	6.41E-07	1.12E-07	3.54E-06	1.85E-04	1.07E-03	1.31E-05	2.26E-06	1.44E-03
4.2	1.14E-03	8.77E-07	1.13E-06	1.30E-06	7.30E-03	1.58E-03	1.61E-05	5.20E-07	5.13E-03
4.8	1.94E-03	2.46E-06	6.27E-07	9.71E-07	7.50E-04	6.08E-05	2.31E-05	1.39E-06	6.75E-03
Time (y)	**Tc-99 Cum Frac**	**U-238 Cum Frac**	**Pu-239 Cum Frac**	**Np-237 Cum Frac**	**I-129 Cum Frac**	**Cs-137 Cum Frac**	**Sr-90 Cum Frac**	**Am-241 Cum Frac**	**Mo-97 Cum Frac**
0.2	1.94E-03	2.82E-05	4.30E-06	8.47E-04	7.62E-03	4.63E-04	1.78E-03	1.95E-03	9.76E-06
0.3	4.71E-03	4.93E-05	6.27E-06	1.17E-03	1.19E-02	1.24E-03	2.49E-03	2.84E-03	1.66E-04
0.8	6.66E-03	5.46E-05	7.31E-06	1.17E-03	1.87E-02	1.48E-03	2.54E-03	2.86E-03	2.60E-04
1.3	1.33E-02	6.31E-05	9.53E-06	1.17E-03	1.90E-02	1.58E-03	2.66E-03	2.94E-03	5.07E-04
1.6	2.11E-02	8.65E-05	1.04E-05	1.17E-03	1.93E-02	1.78E-03	2.70E-03	2.95E-03	1.90E-03
2.0	2.22E-02	8.89E-05	1.04E-05	1.17E-03	1.94E-02	1.89E-03	2.70E-03	2.95E-03	2.36E-03
2.5	2.40E-02	8.97E-05	1.04E-05	1.17E-03	1.96E-02	2.03E-03	2.72E-03	2.95E-03	2.61E-03
3.1	2.91E-02	9.25E-05	1.30E-05	1.17E-03	2.29E-02	3.67E-03	2.73E-03	2.95E-03	1.45E-02
3.7	3.04E-02	9.31E-05	1.31E-05	1.18E-03	2.31E-02	4.74E-03	2.74E-03	2.96E-03	1.59E-02
4.2	3.15E-02	9.40E-05	1.43E-05	1.18E-03	3.04E-02	6.32E-03	2.76E-03	2.96E-03	2.11E-02
4.8	3.35E-02	9.65E-05	1.49E-05	1.18E-03	3.11E-02	6.38E-03	2.78E-03	2.96E-03	2.78E-02
Time (y)	**Tc-99 Rate Frac/d**	**U-238 Rate Frac/d**	**Pu-239 Rate Frac/d**	**Np-237 Rate Frac/d**	**I-129 Rate Frac/d**	**Cs-137 Rate Frac/d**	**Sr-90 Rate Frac/d**	**Am-241 Rate Frac/d**	**Mo-97 Rate Frac/d**
0.2	3.52E-05	5.12E-07	7.83E-08	1.54E-05	1.39E-04	8.41E-06	3.24E-05	3.54E-05	1.77E-07
0.3	4.41E-05	3.36E-07	3.12E-08	5.06E-06	6.75E-05	1.24E-05	1.13E-05	1.42E-05	2.48E-06
0.8	1.25E-05	3.41E-08	6.70E-09	2.09E-08	4.39E-05	1.56E-06	3.22E-07	8.68E-08	6.08E-07
1.3	3.19E-05	4.11E-08	1.08E-08	6.01E-10	1.57E-06	4.51E-07	5.72E-07	3.85E-07	1.19E-06
1.6	7.91E-05	2.37E-07	8.80E-09	2.64E-08	2.83E-06	2.07E-06	3.45E-07	1.66E-07	1.41E-05
2.0	6.31E-06	1.43E-08	1.22E-10	1.27E-09	7.05E-07	6.63E-07	2.42E-08	3.85E-09	2.74E-06
2.5	1.03E-05	4.29E-09	8.92E-11	3.37E-09	1.37E-06	7.67E-07	1.05E-07	2.61E-09	1.39E-06
3.1	2.38E-05	1.30E-08	1.19E-08	1.19E-08	1.50E-05	7.56E-06	4.78E-08	3.32E-09	5.48E-05
3.7	6.02E-06	3.07E-09	5.35E-10	1.69E-08	8.83E-07	5.13E-06	6.28E-08	1.08E-08	6.88E-06
4.2	6.85E-06	5.25E-09	6.78E-09	7.77E-09	4.37E-05	9.48E-06	9.67E-08	3.12E-09	3.07E-05
4.8	8.15E-06	1.04E-08	2.64E-09	4.08E-09	3.15E-06	2.55E-07	9.71E-08	5.83E-09	2.84E-05

Table 3. ATM-103 High-Drip-Rate Test: Interval Fractions, Cumulative Fractions, Interval Release Rate, and Concentration of Isotopes (Continued)

Time (y)	Tc-99 Conc. (mol/L)	U-238 Conc. (mol/L)	Pu-239 Conc. (mol/L)	Np-237 Conc. (mol/L)	I-129 Conc. (mol/L)	Cs-137 Conc. (mol/L)	Sr-90 Conc. (mol/L)	Am-241 Conc. (mol/L)	Mo-97 Conc. (mol/L)
0.2	9.48E-06	7.78E-05	6.26E-08	9.77E-07	6.84E-06	1.77E-06	4.42E-06	3.68E-06	4.98E-08
0.3	1.25E-05	5.36E-05	2.62E-08	3.37E-07	3.50E-06	2.73E-06	1.62E-06	1.55E-06	7.31E-07
0.8	3.76E-06	5.76E-06	5.96E-09	1.47E-09	2.41E-06	3.65E-07	4.89E-08	1.00E-08	1.90E-07
1.3	2.40E-05	1.74E-05	2.40E-08	1.06E-10	2.17E-07	2.65E-07	2.18E-07	1.12E-07	9.33E-07
1.6	2.26E-05	3.81E-05	7.46E-09	1.78E-09	1.48E-07	4.62E-07	5.00E-08	1.82E-08	4.20E-06
2.0	2.50E-06	3.20E-06	1.43E-10	1.19E-10	5.11E-08	2.05E-07	4.85E-09	5.88E-10	1.13E-06
2.5	7.42E-06	1.75E-06	1.91E-10	5.75E-10	1.82E-07	4.33E-07	3.83E-08	7.27E-10	1.05E-06
3.1	7.13E-06	2.18E-06	1.05E-08	8.39E-10	8.18E-07	1.77E-06	7.24E-09	3.82E-10	1.71E-05
3.7	2.10E-06	6.04E-07	5.55E-10	1.39E-09	5.64E-08	1.40E-06	1.11E-08	1.46E-09	2.50E-06
4.2	2.10E-06	9.05E-07	6.15E-09	5.87E-10	2.43E-06	2.26E-06	1.50E-08	3.66E-10	9.76E-06
4.8	3.07E-06	2.20E-06	2.94E-09	4.08E-10	2.16E-07	7.51E-08	1.85E-08	8.45E-10	1.11E-05

DTN: LL991001251021.090

Table 4. ATM-106 High-Drip-Rate Test: Interval Fractions, Cumulative Fractions, Interval Release Rate, and Concentration of Isotopes

Time (y)	Tc-99 Interval Frac	U-238 Interval Frac	Pu-239 Interval Frac	Np-237 Interval Frac	I-129 Interval Frac	Cs-137 Interval Frac	Sr-90 Interval Frac	Am-241 Interval Frac	Mo-97 Interval Frac
0.2	0.00E+00	1.05E-09	3.23E-10	2.52E-08	1.65E-03	2.92E-08	9.30E-08	5.59E-09	0.00E+00
0.3	9.68E-06	1.82E-05	2.38E-05	1.69E-05	1.35E-02	4.12E-05	5.02E-05	2.67E-05	5.57E-06
0.7	1.32E-04	1.51E-04	1.08E-04	8.53E-05	2.20E-02	1.86E-03	3.65E-04	2.19E-04	5.57E-04
1.3	5.99E-05	7.77E-06	7.90E-06	6.79E-06	1.81E-04	9.64E-04	1.33E-05	7.76E-06	8.56E-06
1.6	1.43E-03	1.33E-06	3.15E-08	1.87E-07	5.63E-04	1.26E-04	2.66E-05	8.14E-07	2.77E-04
2.0	3.90E-03	1.14E-07	2.78E-08	3.31E-08	3.98E-04	2.92E-04	9.27E-06	2.82E-08	8.85E-05
2.5	4.04E-03	3.42E-07	4.47E-08	1.89E-07	7.54E-04	1.56E-04	7.72E-06	2.82E-08	9.42E-05
3.1	7.92E-03	3.15E-07	1.78E-08	5.93E-07	6.41E-03	6.03E-04	4.78E-06	6.57E-08	7.85E-04
3.7	2.90E-03	4.41E-08	7.04E-08	7.16E-07	2.83E-04	9.79E-04	1.01E-05	2.99E-06	2.76E-04
4.2	4.97E-03	6.12E-08	1.10E-08	5.33E-07	1.47E-02	9.36E-04	1.05E-05	1.23E-08	2.25E-03
4.8	4.27E-03	3.63E-07	7.37E-07	6.90E-07	1.87E-03	2.20E-05	1.16E-03	1.55E-08	3.37E-03
Time (y)	**Tc-99 Cum Frac**	**U-238 Cum Frac**	**Pu-239 Cum Frac**	**Np-237 Cum Frac**	**I-129 Cum Frac**	**Cs-137 Cum Frac**	**Sr-90 Cum Frac**	**Am-241 Cum Frac**	**Mo-97 Cum Frac**
0.2	0.00E+00	1.05E-09	3.23E-10	2.52E-08	1.65E-03	2.92E-08	9.30E-08	5.59E-09	0.00E+00
0.3	9.68E-06	1.82E-05	2.38E-05	1.69E-05	1.51E-02	4.13E-05	5.03E-05	2.67E-05	5.57E-06
0.7	1.42E-04	1.70E-04	1.32E-04	1.02E-04	3.71E-02	1.90E-03	4.16E-04	2.46E-04	5.63E-04
1.3	2.02E-04	1.77E-04	1.40E-04	1.09E-04	3.73E-02	2.87E-03	4.29E-04	2.54E-04	5.71E-04
1.6	1.63E-03	1.79E-04	1.40E-04	1.09E-04	3.79E-02	2.99E-03	4.56E-04	2.55E-04	8.49E-04
2.0	5.53E-03	1.79E-04	1.40E-04	1.09E-04	3.83E-02	3.29E-03	4.65E-04	2.55E-04	9.37E-04
2.5	9.56E-03	1.79E-04	1.40E-04	1.09E-04	3.90E-02	3.44E-03	4.73E-04	2.55E-04	1.03E-03
3.1	1.75E-02	1.80E-04	1.40E-04	1.10E-04	4.54E-02	4.05E-03	4.77E-04	2.55E-04	1.82E-03
3.7	2.04E-02	1.80E-04	1.40E-04	1.11E-04	4.57E-02	5.02E-03	4.88E-04	2.58E-04	2.09E-03
4.2	2.53E-02	1.80E-04	1.40E-04	1.11E-04	6.04E-02	5.96E-03	4.98E-04	2.58E-04	4.34E-03
4.8	2.96E-02	1.80E-04	1.41E-04	1.12E-04	6.23E-02	5.98E-03	1.66E-03	2.58E-04	7.72E-03
Time (y)	**Tc-99 Rate frac/d**	**U-238 Rate frac/d**	**Pu-239 Rate frac/d**	**Np-237 Rate frac/d**	**I-129 Rate frac/d**	**Cs-137 Rate frac/d**	**Sr-90 Rate frac/d**	**Am-241 Rate frac/d**	**Mo-97 Rate frac/d**
0.2	0.00E+00	1.92E-11	5.88E-12	4.58E-10	3.00E-05	5.30E-10	1.69E-09	1.02E-10	0.00E+00
0.3	1.67E-07	3.15E-07	4.11E-07	2.92E-07	2.33E-04	7.11E-07	8.65E-07	4.60E-07	9.60E-08
0.7	8.38E-07	9.58E-07	6.84E-07	5.40E-07	1.39E-04	1.18E-05	2.31E-06	1.39E-06	3.53E-06
1.3	2.84E-07	3.68E-08	3.75E-08	3.22E-08	8.60E-07	4.57E-06	6.32E-08	3.68E-08	4.06E-08
1.6	1.44E-05	1.34E-08	3.19E-10	1.89E-09	5.68E-06	1.27E-06	2.68E-07	8.22E-09	2.80E-06
2.0	2.35E-05	6.89E-10	1.68E-10	1.99E-10	2.40E-06	1.76E-06	5.59E-08	1.70E-10	5.33E-07
2.5	2.29E-05	1.95E-09	2.54E-10	1.07E-09	4.28E-06	8.87E-07	4.39E-08	1.60E-10	5.35E-07
3.1	3.63E-05	1.44E-09	8.18E-11	2.72E-09	2.94E-05	2.77E-06	2.19E-08	3.01E-10	3.60E-06
3.7	1.39E-05	2.12E-10	3.38E-10	3.44E-09	1.36E-06	4.71E-06	4.84E-08	1.44E-08	1.33E-06
4.2	2.98E-05	3.67E-10	6.61E-11	3.19E-09	8.81E-05	5.61E-06	6.28E-08	7.36E-11	1.35E-05
4.8	1.78E-05	1.51E-09	3.07E-09	2.87E-09	7.81E-06	9.15E-08	4.84E-06	6.46E-11	1.41E-05

Table 4. ATM-106 High-Drip-Rate Test: Interval Fractions, Cumulative Fractions, Interval Release Rate, and Concentration of Isotopes (Continued)

Time (y)	Tc-99 Conc. mol/L	U-238 Conc. mol/L	Pu-239 Conc. mol/L	Np-237 Conc. mol/L	I-129 Conc. mol/L	Cs-137 Conc. mol/L	Sr-90 Conc. mol/L	Am-241 Conc. mol/L	Mo-97 Conc. mol/L
0.2	0.00E+00	2.95E-09	4.93E-12	4.50E-11	2.34E-06	1.67E-10	2.95E-10	1.53E-11	0.00E+00
0.3	6.02E-08	4.57E-05	3.25E-07	2.71E-08	1.71E-05	2.11E-07	1.43E-07	6.55E-08	3.81E-08
0.7	5.14E-07	2.36E-04	9.18E-07	8.50E-08	1.74E-05	5.94E-06	6.47E-07	3.36E-07	2.37E-06
1.3	2.57E-07	1.34E-05	7.44E-08	7.50E-09	1.59E-07	3.41E-06	2.62E-08	1.32E-08	4.04E-08
1.6	5.94E-06	2.22E-06	2.88E-10	2.00E-10	4.78E-07	4.31E-07	5.05E-08	1.34E-09	1.27E-06
2.0	9.11E-06	1.07E-07	1.43E-10	1.99E-11	1.90E-07	5.61E-07	9.90E-09	2.60E-11	2.27E-07
2.5	1.26E-05	4.30E-07	3.06E-10	1.52E-10	4.80E-07	4.01E-07	1.10E-08	3.47E-11	3.23E-07
3.1	1.44E-05	2.30E-07	7.11E-11	2.78E-10	2.38E-06	9.05E-07	3.98E-09	4.73E-11	1.57E-06
3.7	6.18E-06	3.78E-08	3.28E-10	3.93E-10	1.23E-07	1.72E-06	9.80E-09	2.51E-09	6.47E-07
4.2	1.29E-05	6.40E-08	6.29E-11	3.57E-10	7.81E-06	2.00E-06	1.25E-08	1.26E-11	6.43E-06
4.8	8.86E-06	3.02E-07	3.35E-09	3.68E-10	7.94E-07	3.75E-08	1.10E-06	1.27E-11	7.68E-06

DTN: LL991001251021.090

Table 5. ATM-103 Low-Drip-Rate Test: Interval Fractions, Cumulative Fractions, Interval Release Rate, and Concentration of Isotopes

Time (y)	Tc-99 Interval Frac	U-238 Interval Frac	Pu-239 Interval Frac	Np-237 Interval Frac	I-129 Interval Frac	Cs-137 Interval Frac	Sr-90 Interval Frac	Am-241 Interval Frac	Mo-97 Interval Frac
0.2	4.81E-05	3.34E-06	2.11E-05	4.18E-05	2.52E-01	1.40E-05	0.00E+00	3.67E-04	3.65E-05
0.3	4.75E-06	4.49E-07	6.79E-07	4.64E-07	2.65E-04	1.60E-06	4.10E-06	9.79E-07	1.15E-05
0.8	2.46E-06	1.01E-07	1.09E-07	1.40E-07	4.81E-04	1.74E-07	6.42E-07	4.04E-07	1.77E-06
1.6	3.31E-05	1.81E-07	0.00E+00	5.66E-09	2.44E-04	3.95E-07	1.09E-06	8.64E-08	3.85E-07
2.1	2.33E-06	4.35E-09	1.78E-09	5.56E-09	1.52E-04	6.53E-08	5.14E-06	0.00E+00	4.10E-06
2.5	1.84E-05	4.80E-09	2.56E-09	1.68E-08	5.01E-05	3.39E-07	7.74E-06	1.75E-08	4.43E-07
3.1	2.37E-04	2.20E-08	3.11E-09	2.87E-08	5.23E-03	1.74E-06	2.01E-06	1.01E-07	1.03E-06
4.1	2.59E-05	1.84E-08	6.83E-09	6.10E-08	4.42E-03	2.13E-06	5.41E-06	2.11E-07	0.00E+00
4.7	5.22E-05	1.89E-06	1.61E-06	1.25E-06	3.77E-03	2.35E-06	3.78E-06	2.84E-06	3.69E-06
Time (y)	**Tc-99 Cum Frac**	**U-238 Cum Frac**	**Pu-239 Cum Frac**	**Np-237 Cum Frac**	**I-129 Cum Frac**	**Cs-137 Cum Frac**	**Sr-90 Cum Frac**	**Am-241 Cum Frac**	**Mo-97 Cum Frac**
0.2	4.81E-05	3.34E-06	2.11E-05	4.18E-05	2.52E-01	1.40E-05	0.00E+00	3.67E-04	3.65E-05
0.3	5.28E-05	3.79E-06	2.18E-05	4.22E-05	2.52E-01	1.56E-05	4.10E-06	3.68E-04	4.80E-05
0.8	5.53E-05	3.89E-06	2.19E-05	4.24E-05	2.53E-01	1.58E-05	4.75E-06	3.69E-04	4.98E-05
1.6	8.84E-05	4.07E-06	2.19E-05	4.24E-05	2.53E-01	1.62E-05	5.84E-06	3.69E-04	5.01E-05
2.1	9.08E-05	4.07E-06	2.19E-05	4.24E-05	2.53E-01	1.62E-05	1.10E-05	3.69E-04	5.42E-05
2.5	1.09E-04	4.08E-06	2.19E-05	4.24E-05	2.53E-01	1.66E-05	1.87E-05	3.69E-04	5.47E-05
3.1	3.46E-04	4.10E-06	2.19E-05	4.24E-05	2.58E-01	1.83E-05	2.07E-05	3.69E-04	5.57E-05
4.1	3.72E-04	4.12E-06	2.19E-05	4.25E-05	2.63E-01	2.04E-05	2.61E-05	3.69E-04	5.57E-05
4.7	4.24E-04	6.01E-06	2.35E-05	4.37E-05	2.67E-01	2.28E-05	2.99E-05	3.72E-04	5.94E-05
Time (y)	**Tc-99 Rate frac/d**	**U-238 Rate frac/d**	**Pu-239 Rate frac/d**	**Np-237 Rate frac/d**	**I-129 Rate frac/d**	**Cs-137 Rate frac/d**	**Sr-90 Rate frac/d**	**Am-241 Rate frac/d**	**Mo-97 Rate frac/d**
0.2	8.75E-07	6.07E-08	3.83E-07	7.59E-07	4.58E-03	2.54E-07	0.00E+00	6.68E-06	6.64E-07
0.3	9.13E-08	8.63E-09	1.31E-08	8.92E-09	5.09E-06	3.08E-08	7.89E-08	1.88E-08	2.21E-07
0.8	1.42E-08	5.83E-10	6.29E-10	8.07E-10	2.78E-06	1.00E-09	3.71E-09	2.34E-09	1.03E-08
1.6	1.22E-07	6.65E-10	0.00E+00	2.08E-11	8.99E-07	1.45E-09	4.01E-09	3.18E-10	1.42E-09
2.1	1.19E-08	2.22E-11	9.09E-12	2.83E-11	7.76E-07	3.33E-10	2.62E-08	0.00E+00	2.09E-08
2.5	1.14E-07	2.98E-11	1.59E-11	1.05E-10	3.11E-07	2.11E-09	4.81E-08	1.09E-10	2.75E-09
3.1	1.08E-06	1.01E-10	1.42E-11	1.31E-10	2.39E-05	7.95E-09	9.18E-09	4.62E-10	4.71E-09
4.1	7.15E-08	5.06E-11	1.88E-11	1.68E-10	1.22E-05	5.88E-09	1.49E-08	5.80E-10	0.00E+00
4.7	2.50E-07	9.06E-09	7.70E-09	5.97E-09	1.81E-05	1.12E-08	1.81E-08	1.36E-08	1.77E-08
Time (y)	**Tc-99 Conc. mol/L**	**U-238 Conc. mol/L**	**Pu-239 Conc. mol/L**	**Np-237 Conc. mol/L**	**I-129 Conc. mol/L**	**Cs-137 Conc. mol/L**	**Sr-90 Conc. mol/L**	**Am-241 Conc. mol/L**	**Mo-97 Conc. mol/L**
0.2	2.22E-06	8.70E-05	2.89E-06	4.55E-07	2.12E-03	5.05E-07	0.00E+00	6.53E-06	1.76E-06
0.3	2.80E-07	1.49E-05	1.19E-07	6.46E-09	2.85E-06	7.38E-08	1.23E-07	2.22E-08	7.07E-07
0.8	4.36E-08	1.01E-06	5.73E-09	5.83E-10	1.55E-06	2.40E-09	5.78E-09	2.76E-09	3.27E-08
1.6	8.42E-07	2.59E-06	0.00E+00	3.39E-11	1.13E-06	7.85E-09	1.41E-08	8.46E-10	1.02E-08
2.1	3.20E-08	3.38E-08	7.28E-11	1.80E-11	3.82E-07	7.03E-10	3.60E-08	0.00E+00	5.88E-08
2.5	6.39E-07	9.39E-08	2.64E-10	1.38E-10	3.18E-07	9.20E-09	1.37E-07	2.34E-10	1.60E-08
3.1	2.08E-06	1.09E-07	8.13E-11	5.95E-11	8.39E-06	1.20E-08	8.96E-09	6.02E-10	9.44E-09
4.1	2.15E-07	8.57E-08	1.68E-10	1.19E-10	6.68E-06	1.38E-08	2.27E-08	1.18E-09	0.00E+00
4.7	1.02E-06	2.08E-05	9.32E-08	5.72E-09	1.26E-05	3.57E-08	3.73E-08	3.75E-08	7.49E-08

DTN: LL991001251021.090

Table 6. ATM-106 Low-Drip-Rate Test: Interval Fractions, Cumulative Fractions, Interval Release Rate, and Concentration of Isotopes

Time (y)	Tc-99 Interval Frac	U-238 Interval Frac	Pu-239 Interval Frac	Np-237 Interval Frac	I-129 Interval Frac	Cs-137 Interval Frac	Sr-90 Interval Frac	Am-241 Interval Frac	Mo-97 Interval Frac
0.2	7.52E-05	1.76E-05	2.33E-05	4.89E-05	6.40E-01	7.96E-09	0.00E+00	1.07E-04	6.11E-05
0.3	8.61E-07	3.08E-07	2.77E-07	2.80E-07	1.76E-03	4.37E-07	8.88E-06	1.77E-07	4.75E-05
0.8	3.02E-07	1.38E-08	6.22E-09	1.37E-08	2.95E-03	1.70E-07	3.91E-07	3.83E-08	9.92E-06
1.6	1.43E-05	3.57E-08	0.00E+00	4.89E-08	1.20E-03	5.23E-07	1.45E-05	0.00E+00	1.36E-06
2.1	1.88E-06	2.10E-09	2.75E-09	4.34E-09	3.06E-04	3.14E-07	6.76E-06	2.94E-09	4.95E-06
2.5	9.68E-06	2.09E-09	1.32E-09	9.13E-10	2.60E-04	1.81E-06	1.53E-06	3.73E-09	2.27E-07
3.1	4.87E-03	1.37E-04	1.77E-04	1.07E-04	1.82E-02	4.86E-04	2.92E-04	2.28E-04	1.36E-04
4.1	2.62E-04	1.94E-05	2.55E-06	4.45E-06	2.75E-03	1.98E-04	9.79E-06	2.39E-06	4.98E-04
4.7	7.18E-04	3.26E-06	2.22E-06	1.62E-06	4.08E-03	1.19E-05	5.93E-06	3.21E-06	2.20E-06
Time (y)	**Tc-99 Cum Frac**	**U-238 Cum Frac**	**Pu-239 Cum Frac**	**Np-237 Cum Frac**	**I-129 Cum Frac**	**Cs-137 Cum Frac**	**Sr-90 Cum Frac**	**Am-241 Cum Frac**	**Mo-97 Cum Frac**
0.2	7.52E-05	1.76E-05	2.33E-05	4.89E-05	6.40E-01	7.96E-09	0.00E+00	1.07E-04	6.11E-05
0.3	7.61E-05	1.80E-05	2.36E-05	4.92E-05	6.42E-01	4.45E-07	8.88E-06	1.07E-04	1.09E-04
0.8	7.64E-05	1.80E-05	2.36E-05	4.92E-05	6.45E-01	6.15E-07	9.27E-06	1.07E-04	1.19E-04
1.6	9.07E-05	1.80E-05	2.36E-05	4.93E-05	6.46E-01	1.14E-06	2.38E-05	1.07E-04	1.20E-04
2.1	9.26E-05	1.80E-05	2.36E-05	4.93E-05	6.46E-01	1.45E-06	3.05E-05	1.07E-04	1.25E-04
2.5	1.02E-04	1.80E-05	2.36E-05	4.93E-05	6.47E-01	3.26E-06	3.21E-05	1.07E-04	1.25E-04
3.1	4.97E-03	1.55E-04	2.01E-04	1.57E-04	6.65E-01	4.89E-04	3.24E-04	3.36E-04	2.61E-04
4.1	5.24E-03	1.75E-04	2.04E-04	1.61E-04	6.68E-01	6.87E-04	3.34E-04	3.38E-04	7.59E-04
4.7	5.95E-03	1.78E-04	2.06E-04	1.63E-04	6.72E-01	6.99E-04	3.40E-04	3.41E-04	7.61E-04
Time (y)	**Tc-99 Rate frac/d**	**U-238 Rate frac/d**	**Pu-239 Rate frac/d**	**Np-237 Rate frac/d**	**I-129 Rate frac/d**	**Cs-137 Rate frac/d**	**Sr-90 Rate frac/d**	**Am-241 Rate frac/d**	**Mo-97 Rate frac/d**
0.2	1.37E-06	3.21E-07	4.24E-07	8.90E-07	1.16E-02	1.45E-10	0.00E+00	1.94E-06	1.11E-06
0.3	1.62E-08	5.82E-09	5.22E-09	5.29E-09	3.32E-05	8.25E-09	1.68E-07	3.33E-09	8.95E-07
0.8	1.79E-09	8.19E-11	3.68E-11	8.09E-11	1.75E-05	1.00E-09	2.31E-09	2.27E-10	5.87E-08
1.6	5.25E-08	1.31E-10	0.00E+00	1.79E-10	4.41E-06	1.92E-09	5.31E-08	0.00E+00	4.98E-09
2.1	9.52E-09	1.07E-11	1.40E-11	2.20E-11	1.55E-06	1.60E-09	3.43E-08	1.49E-11	2.52E-08
2.5	6.05E-08	1.31E-11	8.24E-12	5.71E-12	1.62E-06	1.13E-08	9.58E-09	2.33E-11	1.42E-09
3.1	2.25E-05	6.33E-07	8.17E-07	4.95E-07	8.38E-05	2.24E-06	1.35E-06	1.05E-06	6.27E-07
4.1	7.17E-07	5.32E-08	6.98E-09	1.22E-08	7.53E-06	5.43E-07	2.68E-08	6.56E-09	1.36E-06
4.7	3.47E-06	1.57E-08	1.07E-08	7.81E-09	1.97E-05	5.76E-08	2.86E-08	1.55E-08	1.06E-08
Time (y)	**Tc-99 Conc. mol/L**	**U-238 Conc. mol/L**	**Pu-239 Conc. mol/L**	**Np-237 Conc. mol/L**	**I-129 Conc. mol/L**	**Cs-137 Conc. mol/L**	**Sr-90 Conc. mol/L**	**Am-241 Conc. mol/L**	**Mo-97 Conc. mol/L**
0.2	3.66E-06	3.45E-04	2.49E-06	6.13E-07	6.36E-03	3.19E-10	0.00E+00	2.05E-06	3.27E-06
0.3	7.06E-08	1.01E-05	4.97E-08	5.91E-09	2.95E-05	2.95E-08	3.32E-07	5.71E-09	4.27E-06
0.8	1.25E-08	2.29E-07	5.62E-10	1.45E-10	2.49E-05	5.75E-09	7.36E-09	6.24E-10	4.50E-07
1.6	3.85E-07	3.85E-07	0.00E+00	3.38E-10	6.59E-06	1.16E-08	1.78E-07	0.00E+00	4.01E-08
2.1	3.04E-08	1.37E-08	9.74E-11	1.81E-11	1.01E-06	4.18E-09	4.99E-08	1.88E-11	8.81E-08
2.5	3.08E-07	2.67E-08	9.18E-11	7.47E-12	1.69E-06	4.74E-08	2.22E-08	4.67E-11	7.94E-09
3.1	5.35E-05	6.05E-04	4.27E-06	3.03E-07	4.06E-05	4.38E-06	1.46E-06	9.87E-07	1.64E-06
4.1	2.50E-06	7.45E-05	5.33E-08	1.10E-08	5.34E-06	1.56E-06	4.27E-08	9.02E-09	5.23E-06
4.7	1.03E-05	1.87E-05	6.98E-08	5.96E-09	1.19E-05	1.40E-07	3.87E-08	1.81E-08	3.46E-08

DTN: LL991001251021.090

Table 7. ATM-103 Vapor Test: Interval Fractions, Cumulative Fractions, and Interval Release Rate of Isotopes

Time (y)	Tc-99 Interval Frac	U-238 Interval Frac	Pu-239 Interval Frac	Np-237 Interval Frac	I-129 Interval Frac	Cs-137 Interval Frac	Sr-90 Interval Frac	Am-241 Interval Frac	Mo-97 Interval Frac
0.2	1.84E-08	1.50E-09	2.43E-09	1.08E-08	5.03E-04	5.80E-10	6.24E-08	2.28E-08	6.51E-07
0.4	1.09E-06	4.15E-08	1.99E-07	6.93E-07	4.83E-04	2.42E-08	8.36E-06	2.48E-06	1.03E-05
0.8	1.83E-07	4.55E-09	1.97E-08	1.33E-08	6.98E-05	5.00E-09	9.04E-09	7.90E-08	4.83E-07
1.6	1.14E-06	9.40E-09	0.00E+00	2.09E-09	1.28E-04	6.60E-08	2.12E-06	0.00E+00	1.42E-06
2.1	9.63E-06	1.26E-09	1.05E-09	0.00E+00	1.04E-04	2.80E-09	7.92E-07	7.09E-09	6.08E-06
2.6	5.04E-05	4.18E-07	6.46E-07	3.84E-07	7.83E-05	9.99E-07	2.17E-05	9.05E-07	3.16E-07
3.2	4.46E-05	1.56E-09	1.37E-09	2.94E-08	2.54E-03	7.42E-08	1.67E-06	1.41E-07	4.12E-06
4.1	2.11E-06	1.21E-09	7.26E-09	6.34E-08	4.56E-03	1.25E-09	1.75E-06	1.55E-08	2.11E-06
4.7	5.28E-06	1.15E-07	2.45E-08	3.05E-08	1.13E-03	1.71E-07	6.13E-07	6.57E-08	0.00E+00
Time (y)	**Tc-99 Cum Frac**	**U-238 Cum Frac**	**Pu-239 Cum Frac**	**Np-237 Cum Frac**	**I-129 Cum Frac**	**Cs-137 Cum Frac**	**Sr-90 Cum Frac**	**Am-241 Cum Frac**	**Mo-97 Cum Frac**
0.2	1.84E-08	1.50E-09	2.43E-09	1.08E-08	5.03E-04	5.80E-10	6.24E-08	2.28E-08	6.51E-07
0.4	1.11E-06	4.30E-08	2.02E-07	7.03E-07	9.86E-04	2.48E-08	8.42E-06	2.51E-06	1.10E-05
0.8	1.29E-06	4.75E-08	2.21E-07	7.17E-07	1.06E-03	2.98E-08	8.43E-06	2.59E-06	1.14E-05
1.6	2.43E-06	5.69E-08	2.21E-07	7.19E-07	1.18E-03	9.58E-08	1.05E-05	2.59E-06	1.29E-05
2.1	1.21E-05	5.82E-08	2.22E-07	7.19E-07	1.29E-03	9.86E-08	1.13E-05	2.59E-06	1.89E-05
2.6	6.25E-05	4.76E-07	8.68E-07	1.10E-06	1.37E-03	1.10E-06	3.30E-05	3.50E-06	1.93E-05
3.2	1.07E-04	4.77E-07	8.70E-07	1.13E-06	3.90E-03	1.17E-06	3.47E-05	3.64E-06	2.34E-05
4.1	1.09E-04	4.78E-07	8.77E-07	1.20E-06	8.46E-03	1.17E-06	3.64E-05	3.65E-06	2.55E-05
4.7	1.14E-04	5.93E-07	9.01E-07	1.23E-06	9.59E-03	1.34E-06	3.71E-05	3.72E-06	2.55E-05
Time (y)	**Tc-99 Rate frac/d**	**U-238 Rate frac/d**	**Pu-239 Rate frac/d**	**Np-237 Rate frac/d**	**I-129 Rate frac/d**	**Cs-137 Rate frac/d**	**Sr-90 Rate frac/d**	**Am-241 Rate frac/d**	**Mo-97 Rate frac/d**
0.2	3.34E-10	2.72E-11	4.41E-11	1.96E-10	9.15E-06	1.05E-11	1.13E-09	4.15E-10	1.18E-08
0.4	2.09E-08	7.97E-10	3.83E-09	1.33E-08	9.29E-06	4.66E-10	1.61E-07	4.78E-08	1.98E-07
0.8	1.27E-09	3.16E-11	1.37E-10	9.22E-11	4.84E-07	3.47E-11	6.28E-11	5.48E-10	3.35E-09
1.6	3.79E-09	3.11E-11	0.00E+00	6.93E-12	4.23E-07	2.19E-10	7.01E-09	0.00E+00	4.71E-09
2.1	5.10E-08	6.68E-12	5.56E-12	0.00E+00	5.50E-07	1.48E-11	4.19E-09	3.75E-11	3.22E-08
2.6	2.98E-07	2.47E-09	3.82E-09	2.27E-09	4.63E-07	5.91E-09	1.28E-07	5.35E-09	1.87E-09
3.2	1.94E-07	6.77E-12	5.94E-12	1.28E-10	1.10E-05	3.22E-10	7.25E-09	6.13E-10	1.79E-08
4.1	6.20E-09	3.55E-12	2.13E-11	1.86E-10	1.34E-05	3.66E-12	5.14E-09	4.55E-11	6.19E-09
4.7	2.59E-08	5.64E-10	1.20E-10	1.50E-10	5.54E-06	8.39E-10	3.00E-09	3.22E-10	0.00E+00

DTN: LL991001251021.090

Table 8. ATM-106 Vapor Test: Interval Fractions, Cumulative Fractions, and Interval Release Rate of Isotopes

Time (y)	Tc-99 Interval Frac	U-238 Interval Frac	Pu-239 Interval Frac	Np-237 Interval Frac	I-129 Interval Frac	Cs-137 Interval Frac	Sr-90 Interval Frac	Am-241 Interval Frac	Mo-97 Interval Frac
0.2	3.80E-08	6.95E-09	1.29E-08	1.04E-07	8.02E-03	0.00E+00	0.00E+00	4.54E-08	1.49E-07
0.4	5.05E-07	3.30E-07	2.33E-07	3.95E-07	1.34E-03	1.83E-06	6.09E-06	4.73E-07	8.79E-06
0.8	1.61E-08	5.59E-09	2.15E-10	9.03E-09	2.24E-03	3.95E-08	6.51E-06	5.14E-10	7.33E-07
1.6	1.91E-07	8.08E-08	5.03E-08	6.11E-09	1.04E-03	1.74E-06	9.48E-06	6.73E-08	1.57E-06
2.1	3.55E-07	9.16E-10	4.75E-09	1.17E-08	2.38E-04	1.57E-08	3.94E-07	4.44E-09	1.92E-06
2.6	1.36E-06	3.71E-09	6.80E-10	5.83E-09	8.76E-04	1.71E-08	4.93E-07	3.43E-09	4.60E-07
3.2	8.56E-08	5.85E-09	1.46E-09	0.00E+00	1.19E-02	3.77E-09	1.01E-06	4.78E-08	3.60E-06
4.1	2.19E-07	1.91E-09	4.63E-09	4.03E-08	1.32E-02	5.22E-08	2.87E-06	1.32E-08	3.30E-06
4.7	7.72E-08	1.90E-09	2.22E-09	2.02E-08	4.53E-03	2.19E-08	1.12E-06	1.24E-08	2.28E-06
Time (y)	**Tc-99 Cum Frac**	**U-238 Cum Frac**	**Pu-239 Cum Frac**	**Np-237 Cum Frac**	**I-129 Cum Frac**	**Cs-137 Cum Frac**	**Sr-90 Cum Frac**	**Am-241 Cum Frac**	**Mo-97 Cum Frac**
0.2	3.80E-08	6.95E-09	1.29E-08	1.04E-07	8.02E-03	0.00E+00	0.00E+00	4.54E-08	1.49E-07
0.4	5.43E-07	3.37E-07	2.46E-07	4.99E-07	9.36E-03	1.83E-06	6.09E-06	5.19E-07	8.94E-06
0.8	5.59E-07	3.43E-07	2.46E-07	5.08E-07	1.16E-02	1.87E-06	1.26E-05	5.19E-07	9.67E-06
1.6	7.50E-07	4.24E-07	2.96E-07	5.14E-07	1.26E-02	3.62E-06	2.21E-05	5.86E-07	1.12E-05
2.1	1.10E-06	4.25E-07	3.01E-07	5.26E-07	1.29E-02	3.63E-06	2.25E-05	5.91E-07	1.32E-05
2.6	2.46E-06	4.28E-07	3.02E-07	5.32E-07	1.38E-02	3.65E-06	2.30E-05	5.94E-07	1.36E-05
3.2	2.55E-06	4.34E-07	3.03E-07	5.32E-07	2.57E-02	3.65E-06	2.40E-05	6.42E-07	1.72E-05
4.1	2.77E-06	4.36E-07	3.08E-07	5.72E-07	3.89E-02	3.71E-06	2.69E-05	6.55E-07	2.05E-05
4.7	2.84E-06	4.38E-07	3.10E-07	5.92E-07	4.34E-02	3.73E-06	2.80E-05	6.68E-07	2.28E-05
Time (y)	**Tc-99 Rate frac/d**	**U-238 Rate frac/d**	**Pu-239 Rate frac/d**	**Np-237 Rate frac/d**	**I-129 Rate frac/d**	**Cs-137 Rate frac/d**	**Sr-90 Rate frac/d**	**Am-241 Rate frac/d**	**Mo-97 Rate frac/d**
0.2	6.90E-10	1.26E-10	2.34E-10	1.89E-09	1.46E-04	0.00E+00	0.00E+00	8.26E-10	2.71E-09
0.4	9.90E-09	6.48E-09	4.57E-09	7.75E-09	2.63E-05	3.59E-08	1.19E-07	9.28E-09	1.72E-07
0.8	9.62E-11	3.35E-11	1.29E-12	5.41E-11	1.34E-05	2.36E-10	3.90E-08	3.08E-12	4.39E-09
1.6	6.99E-10	2.96E-10	1.84E-10	2.24E-11	3.80E-06	6.39E-09	3.47E-08	2.47E-10	5.76E-09
2.1	1.82E-09	4.70E-12	2.44E-11	5.98E-11	1.22E-06	8.04E-11	2.02E-09	2.28E-11	9.85E-09
2.6	8.07E-09	2.21E-11	4.04E-12	3.47E-11	5.21E-06	1.02E-10	2.93E-09	2.04E-11	2.74E-09
3.2	3.72E-10	2.54E-11	6.33E-12	0.00E+00	5.19E-05	1.64E-11	4.41E-09	2.08E-10	1.57E-08
4.1	6.38E-10	5.57E-12	1.35E-11	1.17E-10	3.85E-05	1.52E-10	8.37E-09	3.84E-11	9.62E-09
4.7	3.78E-10	9.31E-12	1.09E-11	9.90E-11	2.22E-05	1.07E-10	5.51E-09	6.10E-11	1.12E-08

DTN: LL991001251021.090

Table 9. Unsaturated Tests: pH at Each Time Interval

Time (y)	ATM-103			ATM-106		
	pH			pH		
	High-drip	Low-drip	Vapor	High-drip	Low-drip	Vapor
0.2	6.0	5.4	7.4	6.2	5.6	7.1
0.3	6.3	6.5	7.2	4.7	7.4	dry[a]
0.8	6.4	4.8	5.3	6.2	4.2	3.7
1.3	4.7	b	b	5.1	b	b
1.6	6.8	6.6	7.2	6.8	6.4	6.9
2.0	7.1	6.5	8.8	6.9	6.4	7.5
2.5	7.1	6.8	7.4	7.0	7.1	8.2
3.1	6.9	6.4	8.6	7.0	6.5	8.5
3.7	7.3	b	b	7.2	b	b
4.2	7.2	6.7	7.5	7.2	7.1	7.4
4.8	7.1	6.7	7.0	6.4	6.8	7.3

NOTES: [a] The test vessel was dry at the end of the time interval.
[b] Not measured
Finn (1999)

4.1.4 Batch (Semi-Static) Tests

Data from the Series 3 semi-static leaching tests of Wilson (1990) are included to provide the basis for estimating spent-fuel dissolution rates from that type of test.

The Series 3 semi-static tests (Wilson 1990) were the third of several tests planned at PNNL to characterize potential radionuclide release from and behavior of spent fuel stored under YMP-proposed conditions. See Stout and Leider (1998, pp. 2-214 - 2-216). The Series 3 tests were run in sealed stainless steel vessels and used the same four-specimen configurations used in Series 1 and Series 2 Cycles 1 and 2. Five specimens–one each of the four configurations using H. B. Robinson (HBR) reactor fuel (plus an additional bare fuel specimen using Turkey Point [TP] reactor fuel)–were tested at 85°C, and a sixth specimen (HBR bare fuel) was run at 25°C. In the Series 1 tests, specimens prepared from TP Reactor Unit 3 fuel were tested in deionized distilled water in unsealed fused silica vessels under ambient hot cell air and temperature conditions. The Series 2 tests were similar to the Series 1 tests except that (1) the Series 2 tests were run in YMP reference J-13 well water, (2) each of the four specimen configurations was duplicated using both the TP Reactor and HBR Reactor pressurized-water reactor (PWR) spent fuels, and (3) a vessel and specimen rinse procedure was added to the cycle termination procedures. The Series 1 and 2 tests were originally entitled "Cladding Containment Credit Tests." All of the test series were later referred to as "Spent Fuel Dissolution Tests."

Because the amount of data used from Wilson (1990) is small, to provide clarity, the data are not presented in this input section but are in the analysis section Tables 28-30.

4.1.5 Gap and Grain Boundary Radionuclide Inventories of Light-Water Reactor (LWR) Spent Fuels

Figure 1 (DTN: LL990200151021.071) is based on the data in Table 10 (DTN: LL000107951021.107). The figure shows the measured gap inventories (1a), grain-boundary inventories (1b), and the sum of the averages of the gap- and grain-boundary inventories for each spent fuel (1c)[2]. Data that are plotted for a given fission gas release (FGR) percentage in Figures 1a and 1b correspond to measurements that were performed on separate specimens from the same spent-fuel rod.

According to Gray, much of the data scatter in Figure 1 is likely due to actual differences between specimens. He believes this scatter is not unexpected because several different specimens came from different regions of a given spent-fuel rod. Also, although the specimens were selected from regions with nearly equal burnups, there may have been temperature gradients that would produce differences in the amounts of cesium and iodine migrating to the grain boundaries and gap regions.

[2] Note: Gray (1999) states in the text that Figure 1c is the sum of the averages but labels Figure 1c as the average sum. The sum of the averages is correct.

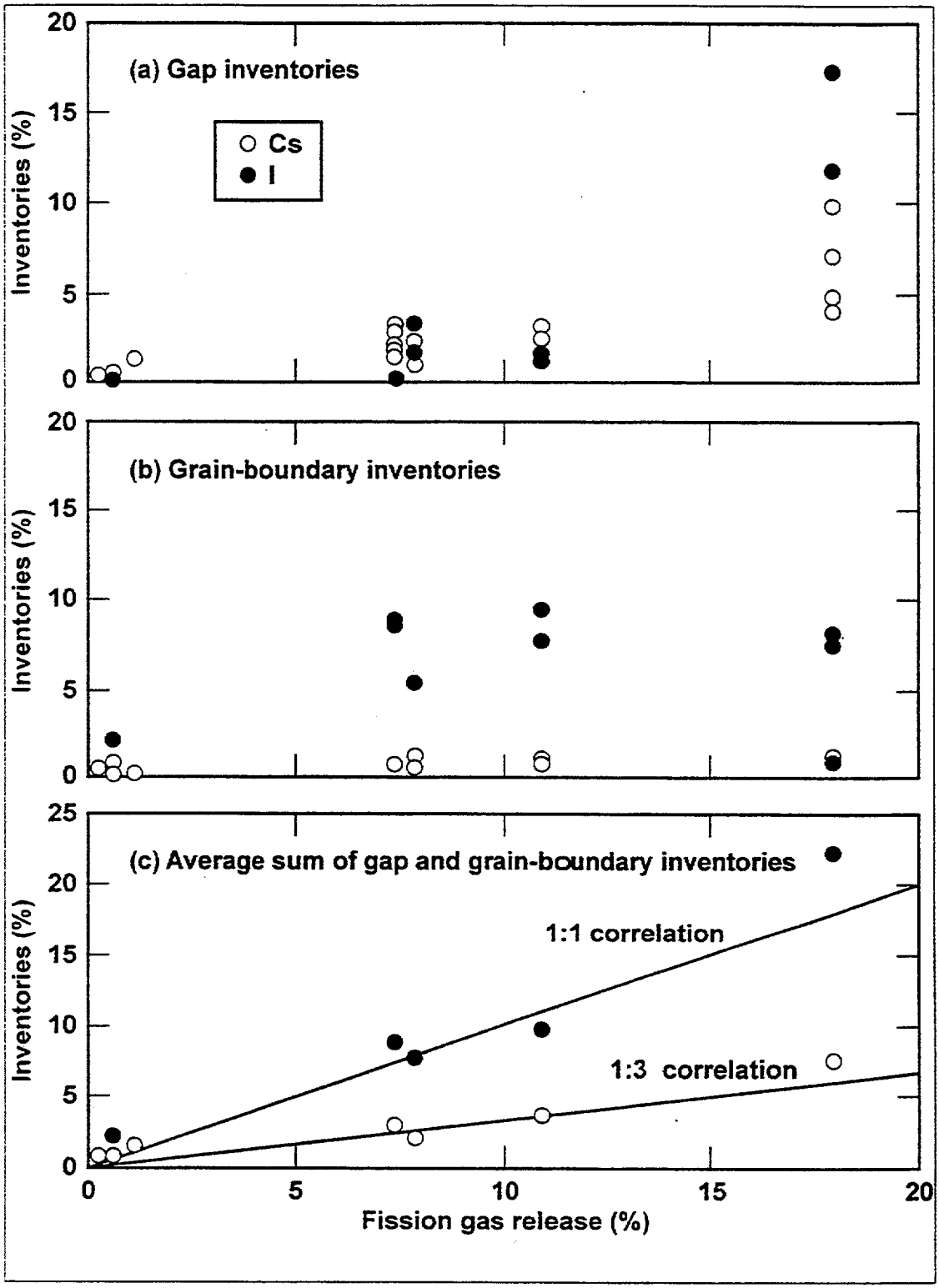

Note: Data for a given fission gas release represent different specimens from the same fuel rod (DTN: LL990200151021.071; Gray 1999).

Figure 1. Inventories as a Percentage of Total Inventories versus Fission-Gas Release

Table 10. LWR Spent-Fuel Gap and Grain-Boundary Inventories Used in Figure 1

FGR (%)	Cs-GI (%)	Cs-GBI (%)	Tc-GI (%)	Tc-GBI (%)	Sr-GI (%)	Sr-GBI (%)	I-GI (%)	I-GBI (%)
1.10	1.20	0.20	-2.30E-04	5.00E-02	4.10E-04	2.00E-02		
7.85	0.72	1.16	0.00E+00	7.70E-02	8.70E-05	2.00E-02		
7.85	0.85	0.39	-1.90E-04	5.40E-02	3.90E-04	6.30E-02		
7.85	2.23						1.55	5.30
7.85	1.55						3.34	
7.85		0.62						
0.59	0.21	0.18		6.60E-02	2.00E-04	7.80E-02	0.03	
0.59	0.28						0.12	
0.59		0.74						2.01
7.40	1.92						0.10	8.50
7.40	3.25	0.56	1.39E-01	-1.90E-01	1.16E-01	3.50E-02		
7.40		0.74						
7.40		0.72						8.87
11.00	2.49	1.00	1.50E-02	1.10E-02	2.29E-02	1.30E-01		
11.00	2.32		8.20E-03		1.22E-02			
11.00	3.25						1.48	7.65
11.00	3.04						1.10	
11.00		0.77						
11.00		0.83						9.35
18.00	4.11	0.88	5.27E-02	1.15E-01	9.39E-02	6.90E-02		
18.00	4.84		2.45E-02		3.91E-02			
18.00	7.11						17.40	7.35
18.00	9.90						11.80	
18.00		1.05						
18.00		1.15						8.10

NOTES: GI = Gap Inventory
GBI = Grain Boundary Inventory
DTN: LL000107951021.107
Blank table cells indicate no data

4.1.6 Natural Analogs

The data in this section provide the basis for comparing the mineral phases and paragenesis seen at Nopal I, the natural geologic site, and the chronological progression of spent fuel and UO_2 corrosion products seen in the unsaturated drip tests at ANL. The data in Table 11 are a combination of Table 2 and Figure 8 of Pearcy et al. (1994).

Table 11. Paragenesis of Uranium Minerals at Nopal I

Mineral	Time	Nominal Chemical Formula
Oxide Uraninite	· · · · · · · ·	UO_{2+x}
Oxyhydroxides Ianthinite	—	$U^{4+}(U^{6+}O_2)_5(OH)_{14}\cdot 3H_20$
Schoepite/ Dehydrated Schoepite	—· · · · ·	$UO_3\cdot 2H_20$ $UO_3\cdot nH_2O(n< 2)$
Becquerelite	—· ·	$Ca(UO_2)_6O_4(OH)_6\cdot 8H_2O$
Billietite(?)/ Abernathyite(?)	· · · · · · ·	$Ba(UO_2)_6O_4(OH)_6\cdot nH_2O(n=4\text{-}8)$ $K(UO_2)(AsO_4)\cdot 4H_2O$
Silicates Soddyite	—	$(UO_2)_2SiO_4\cdot 2H_2O$
Weeksite Boltwoodite	· · · · · · · · · ·	$K_2(UO_2)_2Si_6O_{15}\cdot 4H_2O$ $KH(UO_2)SiO_4\cdot 1.5H_2O$
Uranophane β-Uranophane	═══	$Ca(UO_2)_2Si_2O_7\cdot 6H_2O$

NOTES: · · · · · · · minor
—· · · · · abundant, then minor
——— abundant
═══ very abundant

? indicates tentative identification
Pearcy et al. (1994)

Reported results for the UO_2 and spent-fuel corrosion products seen in the unsaturated drip tests at ANL are given in Tables 12 and 13. Only a tiny fraction of the total volume of corrosion products that have formed on the surfaces of UO_2 and spent-fuel fragments have been removed and analyzed. The extent to which a sample is representative of an entire fragment is uncertain. Repeated observations of similar features from a variety of samples obtained at different time intervals, however, have increased the investigators' confidence that observed features in analyzed samples are representative of most solids in the unsaturated tests.

Table 12. Summary of UO_2 Alteration Phases

Uranyl Oxide Hydrates	Formula
Schoepite (meta-schoepite)	$UO_3 \cdot 2H_2O$
Dehydrated Schoepite	$UO_3 \cdot (0.8\text{-}1.0H_2O)$
Compreignacite	$(Na,K)_2[(UO_2)_6O_4(OH)_6] \cdot 8H_2O$
Becquerelite	$Ca[(UO_2)_6O_4(OH)_6] \cdot 8H_2O$
Uranyl Silicate Hydrate	
Soddyite	$(UO_2)_2SiO_4 \cdot 2H_2O$
Uranyl Alkaline Silicate Hydrates	
β-Uranophane	$Ca(UO_2)_2(SiO_3OH)_2(H_2O)_5$
Boltwoodite	$K_2(UO_2)(SiO_3OH)(H_2O)$
Na-Boltwoodite	$(Na,K)(UO_2)(SiO_3OH)(H_2O)$
Sklodowskite	$Mg(UO_2)_2(SiO_3OH)(H_2O)_4$
Non-Uranyl Phases	
Palygorskite	$(Mg,Al_{0.12\text{-}0.66})_5(Si,Al_{0.12\text{-}0.66})_8O_{20}(OH)_5 \cdot 4H_2O$
Fe-Oxides	$FeO_x(OH)_y$
Ti-Oxides	TiO_x
Amorphous Silica	SiO_2

NOTE: Stout and Leider (1998, Table 2.1.3.5-10, p. 2-237)

Table 13. Identification of Alteration Phases in Unsaturated Tests from Electron and X-ray Diffraction and Crystal Morphology

Test Type	Reaction (y)	Compound Identified	Technique		
			Electron Diffraction	XRD[a]	Morphology/ EDS
ATM-103					
High-Drip	3.7	Na-Boltwoodite	√	80-90%	√
		β-Uranophane	√	10%	—
Low-Drip	4.1	Dehy. Schoepite	—	—	√
		Metaschoepite	—	—	√
		Cs-Mo-UO_x	√	—	—
		Na-UOH	—	—	√
		Soddyite	—	—	√
		Na-Boltwoodite	—	—	√
	5.2	Na-UOH	—	—	√
		Soddyite	—	—	√
		Na-Boltwoodite	—	—	√
Vapor	4.1	Cs-Mo-UO_x	√	—	—
		Dehy. Schoepite	√	—	√
		Metaschoepite	—	—	√
ATM-106					
High-Drip	0.8	Cs-Mo-UO_x	√	√	√
		Dehy. Schoepite	—	√	√
	3.7	Na-Boltwoodite	—	—	√
		β-Uranophane	√	—	—
	4.1	Na-Boltwoodite	—	80-90%	√
		β-Uranophane	—	√[b]	√
	5.2	Na-Boltwoodite	—	√	√
		β-Uranophane	—	√[b]	—
Low-Drip	4.1	Metaschoepite	—	—	√
		Na-UOH	—	—	√
		Soddyite	—	—	√
Vapor	4.1	Cs-Mo-UO_x	√	—	—
		Dehy. Schoepite	—	—	√
		Metaschoepite	—	—	√

NOTES: [a] Listed as vol%
[b] XRD data lack one diffraction peak that is characteristic of β-uranophane.
XRD = x-ray diffraction; EDS = energy-dispersive x-ray spectroscopy
√ = phase identified using the analysis technique indicated; — = phase not identified
(CRWMS M&O 2000, Table 11)

4.2 CRITERIA

The model validation criterion is that the available relevant data fall within or below the stated model uncertainty range.

4.3 CODES AND STANDARDS

ASTM C 1174-97 applies to the prediction of the long-term behavior of materials, including waste forms.

INTENTIONALLY LEFT BLANK

5. ASSUMPTIONS

It is assumed that predictions of long term CSNF dissolution rates may be made based on semi-empirical models based on short-term tests per ASTM C 1174-97.

It is assumed that an oxygen pressure of 0.2 atmospheres will result in bounding predicted dissolution rates for the proposed repository based on the work of Shoesmith (1999) (see Section 6.1).

It was assumed that the temperature and oxygen pressure coefficients, a_1 and a_3 respectively (Eq. 11, Section 6.2.2.2), from the alkaline model could be used for the acid model (Section 6.2.2.4). The basis of this assumption is the relative insensitivity of the wet dissolution rate to the small range of temperature and assumed constant O_2 pressure in the repository. This assumption is justified because the resulting dissolution model (see Figure 2) gives reasonable or overestimated dissolution rates (see Section 6.2.2.5 Model Validation).

INTENTIONALLY LEFT BLANK

6. ANALYSIS/MODEL

There is a subsection for each of the six topics in the technical product development plan (CRWMS M&O 1999c). Section 6.2, 6.3, and 6.4 discuss the three types of dissolution study sponsored by YMP as described in Section 4.1.

6.1 CHEMICAL BASIS OF SPENT FUEL DISSOLUTION

The purpose of this section is to provide a summary of the chemical processes that occur when spent nuclear fuel reacts with groundwater in order to provide a mechanistic framework for dissolution modeling. The information in this section is not directly used in the model or Process Model Report. Commercial nuclear fuel is composed of mostly uranium dioxide. Its reactions potentially initiate the release of radionuclides into the environment. Much of the following is abstracted from a recent review of spent-fuel corrosion processes (Shoesmith 1999). This reference should be consulted for details of electrochemical studies on UO_2. Uranium(IV) minerals, primarily uraninite (UO_2) in the mined uranium-bearing ores, are relatively insoluble in nonoxidizing aqueous solutions. Uranium(VI) forms much more soluble species. Uranium is extracted from natural ores by oxidative dissolution with acidic iron(III) sulphate solutions or in alkaline carbonate solutions with oxygen under pressure. Electrochemical studies by Nicol and Needes (see Shoesmith 1999) of the oxidative dissolution of uranium in both acidic and basic carbonate media demonstrated that this U(IV) to U(VI) dissolution process is indeed electrochemical, involving the oxidation of U(IV) and reduction of oxidants. The overall reaction can be considered a sum of the oxidation and reduction electrochemical half-reactions:

$$UO_2 \Rightarrow UO_2^{2+} + 2e^- \qquad \text{(Eq. 1)}$$

$$\text{oxidant} + 2e^- \Rightarrow \text{reduced species} \qquad \text{(Eq. 2)}$$

The two half-reactions are affected by the solid, and particularly surface, properties of the fuel.

Studies of the effects of groundwater constituents on fuel corrosion and dissolution indicate that surface complexation occurs, leading to partial reaction orders (Shoesmith 1999, p. 3). This has been seen with pH, total carbonate, and dissolved oxygen. In natural systems, unlike electrochemical studies, reaction orders are also affected by the forward and reverse reactions simultaneously (Shoesmith 1999, Sec. 3.1).

Carbonate present in groundwaters, including those at Yucca Mountain, is a strong complexing agent for the uranyl species, UO_2^{2+} (Grenthe et al. 1992; Shoesmith 1999). At the alkaline conditions of groundwater, uranyl carbonate complexes predominate. The most important are:

$$UO_2^{2+} + CO_3^{2-} \Leftrightarrow UO_2CO_3(aq) \qquad \text{(Eq. 3)}$$

$$UO_2^{2+} + 2\,CO_3^{2-} \Leftrightarrow UO_2(CO_3)_2^{2-} \qquad \text{(Eq. 4)}$$

$$UO_2^{2+} + 3\,CO_3^{2-} \Leftrightarrow UO_2(CO_3)_3^{4-} \qquad \text{(Eq. 5)}$$

According to Shoesmith the most appropriate dissolution mechanism involving uranyl carbonate follows:

$$UO_2 + HCO_3^- \Rightarrow (UO_2HCO_3)_{ads} + e \qquad \text{(Eq. 6)}$$

$$(UO_2HCO_3)_{ads} + OH^- \Rightarrow (UO_2CO_3)_{ads} + H_2O + e \qquad \text{(Eq. 7)}$$

$$(UO_2CO_3)_{ads} + HCO_3^- \Rightarrow UO_2(CO_3)_2^{2-} + H^+ \qquad \text{(Eq. 8)}$$

$$UO_2(CO_3)_2^{2-} + HCO_3^- \Rightarrow UO_2(CO_3)_3^{4-} + H^+ \qquad \text{(Eq. 9)}$$

The influence of carbonate is described as a function of concentration (Shoesmith 1999, Sec. 3.1.3). (1) With no carbonate, corrosion products are more likely to deposit and suppress dissolution rate. (2) At less than 10^{-3} molar total carbonate, the predominant influence of carbonate is to complex UO_2^{2+}, thus reducing alteration product buildup. (3) Between 0.001 and 0.1 molar, carbonate is kinetically involved in the dissolution process via carbonate surface intermediates. (4) At higher carbonate concentrations, formation of UO_2CO_3 on the surface may inhibit dissolution, and carbonate dependency may lessen. A surface adsorption mechanism was proposed in 1976 by Grandstaff (Stout and Leider 1998, p. 3-128).

Orders of magnitude differences in aqueous dissolution rates are characteristic of metal oxides (Shoesmith 1999, Sec. 3.1), even for the same oxide, depending on water chemistry. For the slowly dissolving semiconductor oxides, which include UO_2, the dissolution-rate-controlling process can either be (1) charge-transfer to the surface or (2) surface alterations. The solution redox potential is the critical variable because U(VI) is much more soluble than U(IV). This sensitivity to uranium oxidation state makes spent UO_2 fuel dissolution sensitive to the redox conditions within the repository and Engineered Barrier System (EBS).

For dissolution rate purposes, the redox conditions in the proposed repository are assumed to be bounded by an oxygen pressure of 0.2 atmospheres. Oxidants such as H_2O_2 will be supplied by radiolysis of water. However, in an open system, the rapid decomposition of H_2O_2 to O_2 will prevent the redox potential to rise above that achievable in aerated solutions (Shoesmith 1999, Sec. 5.7.2). This argument forms the basis for the assumption that 0.2 atmosphere O_2 is bounding. This assumption is conservative, in that it maximizes the dissolution rate and thus the release rate from the package. The resulting redox potential from dissolved oxygen and radiolytically produced oxidants is sufficiently high at Yucca Mountain to allow oxidative dissolution of commercial spent UO_2 fuel. This is also true for all of the higher oxides seen in oxidation studies of UO_2 or spent fuel. Shoesmith compared the importance of β/γ radiolysis to α radiolysis and found β/γ to be much more aggressive. Since the β/γ fields of spent fuel decay within hundreds of years, he concludes that corrosion tests on fresh spent fuel (<30 years out of reactor) may over estimate the corrosion of spent fuel in the long term. The reaction order for dissolved oxygen is different for spent fuel and UO_2 in both the Canadian (Tait and Luht 1997) and U.S. studies (Stout and Leider 1998, p. 2-225) and is probably due to radiolysis, but unknown effects can also contribute to a suppressed spent-fuel reaction order for oxygen.

Radiolysis of a moist air environment has been shown to increase acidity via production of HNO_3 (Reed and Bowers 1990). When pure water is irradiated, either by alpha particles or by

beta particles or gamma rays, there is no pH change. When a water/air system is irradiated, this results in the fixation of nitrogen from the gas phase, the formation of nitric acid (probably also in the gas phase), and its condensation into the liquid water phase (Reed and Bowers 1990). They showed that very little of the nitric acid that is formed results from irradiation of the nitrogen gas that is dissolved in the water. Shoesmith (1999, Sec. 5.7.1) discusses pH suppression during the irradiation of liquid water in contact with uranium oxide with and without air.

Other important groundwater species are calcium and silicon ions, which can form stable corrosion products with low solubilities. Electrochemical studies have shown fast reduction in dissolution currents when thin layers of corrosion products form, as measured by XPS. Other electrochemical studies have shown an increase of UO_2 reactivity as the applied potential is increased (Shoesmith 1999). At very low applied potentials (< -400 mV vs. saturated calomel electrode [SCE]) oxidation begins, possibly concentrating at grain boundaries; up to -100 mV irreversible UO_2 lattice oxidation occurs, seemingly preferentially at grain boundaries. Noticeable dissolution begins. As the applied potential increases to +300 mV oxidation, dissolution and corrosion product formation are significant; above +300 mV dissolution is rapid leading to local acidity and grain boundary etching. The dissolution rate increases because corrosion products are not formed on the solid surface. The likely electrochemically determined UO_2 reaction sequence is shown in Figure 15 of Shoesmith (1999). That sequence is as follows:

$$UO_2 \Rightarrow UO_{2+x} \Rightarrow UO_{2.33} \Rightarrow \overset{\text{surface oxidation}}{\{UO_2^{2+}\}_{surface}} \Rightarrow \overset{\text{bulk oxidation}}{[UO_2^{2+}]_{bulk}} \Rightarrow \overset{\text{dissolution}}{[UO_2^{2+}]_{soln}} \Rightarrow \text{Secondary Phases}$$

The current mechanistic understanding of the aqueous corrosion and dissolution of UO_2 does not provide for an *a priori* reaction model.

6.2 FLOW-THROUGH DISSOLUTION TESTS AND MODELS

The purpose of the flow-through dissolution studies was to examine the systematic effects of temperature and important water chemistry variables on the intrinsic dissolution rates of the UO_2 matrix in both unirradiated UO_2 and spent fuel. These variables control the long-term dissolution of spent fuel. The intrinsic dissolution rate is the forward reaction rate, which includes UO_2 corrosion/oxidation steps and a dissolution step. The term "dissolution" is chosen because the release of radionuclides from the spent fuel into the contacting water is a major problem of repository design and lifetime. The intrinsic dissolution rates of UO_{2+x} and spent fuel were determined by using a single-pass flow-through method (Stout and Leider 1998, p. 220). The advantage of the single pass flow-through technique, compared to batch and unsaturated drip tests, is that flow-rates and specimen size can be controlled so that the UO_2 dissolves under conditions that are far from solution saturation (no precipitation of dissolved products). Under such conditions, the steady-state dissolution rates are directly proportional to the effective surface area of the specimen.

The intrinsic dissolution rate controls and bounds the release rate. The release rate is the material loss rate from the fuel. Any material incorporated in alteration phases on the fuel represents the difference between the dissolution rate and the release rate. The available spent-

fuel surface area exposed for aqueous dissolution is addressed in another analysis report: Clad Degradation Wet Unzipping (DI: ANL-EBS-MD-000014) by William O'Connell.

The dissolution rates of the higher oxides of uranium, U_4O_{9+x}, U_3O_8, and $UO_3 \cdot xH_2O$ are also mentioned because of their likely presence in spent fuel placed in a repository. Unirradiated UO_{2+x} represents reactor fuel with no burnup or loss of radioactivity from long-term decay. Flow-through dissolution data sets for UO_2, the higher uranium oxides, and spent fuel obtained at equivalent conditions (1) allow a direct comparison of UO_{2+x} and spent-fuel dissolution rates and (2) provide insight into the effect of the measured variables.

The exact chemistry of groundwater in an underground repository is not certain, but groundwater has typical constituents, such as carbonates, sulfates, chlorides, silicates, and calcium. Water taken from well J-13 near Yucca Mountain contains all of these ions and has a pH near 8 (Stout and Leider 1998, pp. 2-263). Acid and carbonate media are used for uranium ore processing because they are aggressive in dissolving UO_2. For this reason, of the anions commonly found in groundwater, carbonate is considered to be the most aggressive towards UO_2 and, as such, is a conservative surrogate for all anions in groundwater (Grenthe 1992, p. 308; Grambow 1989, p. 2) (see Section 6.1).

There have been many investigations of the dissolution of UO_2, spent fuel, and uraninite in aqueous solutions, under both reducing and oxidizing conditions, and as a function of various other environmental variables, all under a wide range of conditions (Grambow 1989; McKenzie 1992). Important variables considered in the investigations included pH, temperature, oxygen fugacity, carbonate/bicarbonate concentrations, and fuel attributes (fuel burnup). These same variables were used in the flow-through tests supported by YMP and elsewhere.

The data obtained from the flow-through tests identify the important parameters that control the dissolution rates of the UO_2 matrix phase of spent fuel. They are also the basis for estimating bounding values for UO_2 and spent-fuel matrix dissolution rates. A dissolution rate model can be used to develop a release model for radionuclides from spent fuel that can be used in repository performance assessment.

To determine nonlinear effects of the above variables, tests at three different values of each variable were performed. A statistical test design approach was used to select the tests to be performed and to reduce the number of required tests. Because carbonate solutions are natural pH buffers, total carbonate concentration and pH could be tested independently by varying the carbonate/bicarbonate and CO_2 gas ratios. Similar sets of tests at atmospheric-oxygen partial pressure were conducted on U_3O_8 and $UO_3 \cdot xH_2O$ to measure the effect of higher oxidation states on dissolution. The carbonate concentrations bracketed the typical groundwater concentration of about 1-2 millimol/L. The oxygen pressure represented the atmospheric value down two orders of magnitude to a minimally oxidizing atmosphere. The pH covered a value typical of groundwaters (pH = 8) to very alkaline conditions. In the basic region, carbon dioxide dissolved in water, CO_2 (aq), occurs mostly as carbonate/bicarbonate species.

6.2.1 Flow-Through Test Results

Details of the flow-through tests are in Stout and Leider (1998). Tests were selected to examine systematically the effects of temperature (25-75°C), dissolved oxygen (0.002-0.2 atm overpressure), pH (8-10), and carbonate concentrations (2×10^{-4} - 2×10^{-2} molar on UO_2 and spent-fuel dissolution (Stout and Leider 1998, p. 221). The results of the combined uranium dioxide and spent-fuel test matrices are given in Table 1 (Stout and Leider 1998; DTNs: LL990707151021.075; LL990901851021.084). The data show the temperature has the strongest effect on alkaline spent-fuel dissolution rates, followed by dissolved oxygen concentration. The carbonate effect is a distant third. As Shoesmith (1999) points out, this low carbonate effect can be due to changing mechanisms at different concentrations or temperatures. Additional very high burnup spent-fuel data are available now for specific fuels and conditions and are included as runs 61-64 in Table 1.

Because UO_2 will likely oxidize in the repository environment, the dissolution of the higher oxides was also studied. The dependence of UO_{2+x} dissolution kinetics on pH, temperature, time, and carbon dioxide/carbonate/bicarbonate concentrations was also investigated (Stout and Leider 1998, p. 223). All tests in this higher oxide test series were run at 20% oxygen buffer solution overpressure or 8 ppm dissolved oxygen. The flow-through tests were carried out in basic buffer solutions (pH of 8-10). The chemical composition of the solutions provides concentrations and dissolution rate data useful in developing kinetic models for UO_2 matrix dissolution of spent fuel. The intrinsic dissolution rate obtained from these data is expected to be an upper-bound dissolution response for high-pH water chemistries. Tests were done at three temperatures (25, 50, and 75°C), three carbonate/bicarbonate concentrations (2×10^{-4} - 2×10^{-2} mol/L), and three pHs (8, 9, 10) for the two compounds U_3O_8 and $UO_3 \cdot xH_2O$.

Table 2.1.3.5-5, Part 1 of Stout and Leider (1998, p. 224) lists the uranium dissolution rates for the three oxides—UO_2, U_3O_8, and $UO_3 \cdot xH_2O$—that were measured at LLNL under atmospheric oxygen conditions. As shown in Table 2.1.3.5-5, Part 1 of Stout and Leider (1998, p. 224) the oxide state has by far the strongest effect on the uranium dissolution rate. The rate increases significantly from UO_2 to U_3O_8 and dramatically from U_3O_8 to $UO_3 \cdot xH_2O$. Increasing carbonate concentrations increase the dissolution rates of U_3O_8 and $UO_3 \cdot xH_2O$, as shown previously (Section 6.1) with UO_2. An increase in U_3O_8 dissolution rate with increasing temperature was seen as well. A similar temperature effect on $UO_3 \cdot xH_2O$ is not apparent, which may be due to the rapid $UO_3 \cdot xH_2O$ dissolution. Raising the temperature to 75°C from room temperature increases the dissolution rate by a factor of two to four for the two higher oxides. Similar to the UO_2 results, alkaline pH does not have a significant role in changing the dissolution rate of the higher oxides.

The data in Stout and Leider (1998, p. 224) indicate that with the higher oxides, unlike UO_2, carbonate seems to affect the dissolution rate to a greater extent than does temperature. The enhancement is particularly strong at the highest carbonate concentration. Shoesmith (1999, Sec. 5.2) states that this is consistent with the results seen in a dissolution study of soddyite, another fully-oxidized uranium oxide. This strong dependence of U(VI) uranium-oxide dissolution on carbonate indicates that concentrated carbonate might prevent deposition of corrosion products during spent-fuel dissolution.

Because U_3O_8 has both U(V) and U(VI) valence states, its dissolution rates might be expected to be between that of UO_2 and $UO_3 \cdot xH_2O$, particularly as carbonate concentrations increase. That does not seem to be the case with the present data. As Shoesmith (1999) describes in more detail, the data indicate that alkaline pH is the least significant factor in dissolution of spent fuel or any of the uranium oxides under the alkaline conditions of these tests.

6.2.2 Modeling of Flow-Through Dissolution Data

This section discusses modeling of the aqueous dissolution of uranium-oxide spent-fuel waste forms. Section 6.2.2.1 summarizes the development of dissolution rate function forms. Section 6.2.2.2 presents the regression analysis of several forms of the model, which have different levels of complexity. Section 6.2.2.3 presents the recommended abstracted alkaline model. Section 6.2.2.4 presents the acid dissolution model. Model validation is discussed in Section 6.2.2.5.

6.2.2.1 Development of the Flow-Through Dissolution Model

The approach for spent-fuel dissolution rate model development used concepts from nonequilibrium thermodynamics. The final function form embeds thermodynamic chemical potentials of both the solid (spent fuels) and the solution (water chemistries) along with a set of coefficients and parameters that can be evaluated by numerical regression of dissolution test data. As discussed in Section 6.1, detailed knowledge is not available for the atomic (mechanistic) steps or the sequence of chemical/electrochemical reaction steps to describe the dissolution process over the range of spent-fuel inventory, potential water chemistries, and temperatures. The existing approach has been to obtain an experimental data base of flow-through dissolution rates for a set of specific spent fuels (approved testing materials, or ATMs) over a range of controlled, aggressive water chemistries and temperatures. With a numerical regression algorithm, these data are used to evaluate empirical parameters in a rate law (Stout and Leider 1998, p. 3-119) that is the product polynomial of the bulk water chemistry concentrations and temperature. This function form has been extended to have an explicit dependence on the thermodynamic properties of the uranium-oxide waste form by using fuel reaction burnup as an aggregate variable for fission product and actinide concentrations. The use of water chemistry concentrations and spent-fuel burnup in the regression function form of the dissolution data does not explicitly account for a dependence from possible surface to bulk concentration differences due to radiolysis and surface effects such as adsorption. However, the some of these shortcomings were addressed by including surface chemisorption.

The dissolution model development in Stout and Leider (1998, p. 3-120) provides a plausible explanation for the additional interaction terms in the model. These terms improve the fit and have a physical basis. That these terms are important to explain the data re-emphasizes the conclusions of others (Shoesmith 1999) that the dissolution process is complex and cannot be explained well by simple models that ignore the complexity.

If the dissolution model development were left at this point, it could be considered semi-empirical in that cross-terms were included without addressing their physical significance. In addressing this point, it is important to realize that dissolution model development for a multicomponent solid (spent fuel) in a multicomponent water chemistry environment will be more complex than for a single-component solid in a single- or dual-component water chemistry.

Certainly, if a simple physical model with some purported mechanistic basis "fits" the range of data sets available (has a large R-squared value, where R-squared is the correlation-coefficient), then that simple model should be acceptable. However, if the simple model has a low R-squared value for the available data set, then irrespective of the purported physical significance, the simple model is normally rejected by statisticians as unsuitable for predicting response. Put concisely, a simple regression model that does not "explain" the available data sets (has small R-squared values) is not generally accepted as a predictive model, any more than a regression model without some physical basis. Thus, in the ideal situation, model development must address both physical basis issues and predictive issues. The developed model (Stout and Leider 1998, p. 3-120) has a strong physical basis from nonequilibrium thermodynamics and is similar to function forms proposed in the literature for chemical reactions. Physical basis issues can be addressed by identifying chemical processes or mechanisms that are functionally described by exponent function forms. One such chemical process or mechanism exists in the form of chemical adsorption on the solid-liquid interface. The surface adsorption mechanism was identified in uraninite dissolution tests performed by Grandstaff (Stout and Leider 1998, p. 3-127). Grandstaff proposed that the uraninite dissolution rate dependence on aqueous carbonate concentrations could be explained by using a Langmuir adsorption isotherm. According to Grandstaff, the Langmuir isotherm described the surface coverage as a function of carbonate solution concentration. At low carbonate concentrations, Grandstaff linearized the Langmuir isotherm and proposed a linear relationship between surface coverage and concentration. However, at intermediate aqueous concentrations, the Tempkin adsorption isotherm is considered more descriptive of surface adsorption because it is expressed in terms of the thermodynamic chemical potential function (also see Section 6.1).

Aagaard and Helgeson (Stout and Leider 1998, p. 3-129) showed that stoichiometric coefficients are not expected in proposed chemical reaction rate laws derived from regression analysis of data. Shoesmith (1999) confirms this. Also in the case of spent fuel, since the UO_2 solid has fission products and actinides, both the number of active sites on the solid and the concentrations of radiolytic aqueous species are functionally dependent on an aggregate variable such as spent-fuel burnup.

6.2.2.2 Regression Fit of Alkaline Data to Models

The developed intrinsic spent-fuel dissolution model has several characteristics. The tests that provide the data set for the model were undertaken at aggressive conditions to provide the basis for a bounding dissolution model. These aggressive conditions included alkaline pHs up to 10; total carbonate concentrations ten times that found in typical groundwaters, including J-13; and high water-flow rates that eliminated precipitation or reverse reactions.

Equation 3.4.2-18 of Stout and Leider (1998, p. 3-125) provides a classical Butler-Volmer relationship for the dissolution rate that is exponentially related to the energy change of the solid dissolving into a liquid. Equations 3.4.2-12 and 3.4.2-18 provide a consistent thermodynamic basis for the function forms of dissolution rate models. Function forms based on both Equations 3.4.2-12 and 3.4.2-18 were used for multilinear regression analyses over subsets of unirradiated UO_2 and spent-fuel UO_2 dissolution rate data. Several forms of these models have been

examined, and some were included in previous updates and revisions of the *Waste Form Characteristics Report* (WFCR) (Stout and Leider 1998).

The current model has the Butler-Volmer form, as discussed in Section 3.4.2.3 of Stout and Leider (1998) and reduces to the classic chemical kinetic rate law:

$$\text{Rate} = k[A]^a[B]^b[C]^c \ldots \exp(-E_a/RT) \qquad \text{(Eq. 10)}$$

Where k is the reaction rate constant, [A] stands for concentration of reactant A, E_a is the activation energy, R is the gas constant and T is the temperature in Kelvin.

Burnup is represented as a concentration term as well because it is proportional to the aggregated production and concentration of fission products and represents the chemical potential of the solid state. For regression purposes, Equation 10 was transformed by taking logarithms of each term, fitting that equation, and allowing interaction and quadratic terms indicated by the data to improve the fit. The negative logarithms of the water chemistry variables were used to be consistent with the standard definition of pH, $-\log_{10}[H^+]$.

This model form includes a linear term of all variables. The linear portion of the model is equivalent to the classic chemical rate law (Eq. 10). Equation 10 has the same form as used in Stout and Leider (1998). Equation 11 (note base-10 logarithms) represents this current model:

$$\begin{aligned}\log_{10}(\text{Rate } UO_2 \text{ or CSNF}) = {} & a_0 \cdot 1 + a_1 \cdot \text{IT} + a_2 \cdot PCO_3 + a_3 \cdot PO_2 + a_4 \cdot \text{PH} \\ & + a_5 \cdot \text{LBU} + a_6 \cdot PO_2 \cdot \text{IT} + a_7 \cdot \text{LBU} \cdot \text{IT} + a_8 \cdot \text{LBU} \cdot PCO_3 \\ & + a_9 \cdot \text{LBU} \cdot PO_2 + a_{10} \cdot \text{LBU} \cdot \text{PH} + a_{11} \cdot PCO_3^2 \qquad \text{(Eq. 11)}\end{aligned}$$

The term definitions, coefficients, and fitting statistics are in Table 14.[3] They are slightly different than those given for the WFCR Ver.1.3 (Stout and Leider 1998, p. 3-130) because the additional seven spent-fuel dissolution data at high and low burnup (runs 32-38) are included.

The standard error given in Tables 14-20 provides a measure of the uncertainty of the coefficient estimate in the same units as the estimate. The fourth and fifth columns provide statistics related to the test of the hypothesis that the coefficient being estimated is zero. A high significance value indicates there is reason to believe that the coefficient is zero, so the term can be dropped from the model. Conversely, the closer the significance value in column five is to zero, the more important the term.

The notes of the tables provide some statistics to help assess the fit. First, the number of cases or runs are given. Second, the residual degrees of freedom (cases less the number of terms in the model) are enumerated. The correlation coefficients R-squared (R^2) and adjusted R-squared are

[3]Because unirradiated UO_2 represents zero or no burnup, logarithmic values of zero UO_2 burnup used in this model would produce infinitely negative values for the terms in the regression fit of such data. For this reason, a value of 1 MWd/kgU [$\log_{10}(1) = 0$] was substituted for the burnup of UO_2 in the regression data set for this model and is a typical normalization used in thermodynamic standard states.

numbers that indicate how well the fitted values produced by the model are correlated with the measured values. An R^2 value is always between zero and one. An adjusted R^2 value (which is adjusted for the number of terms in the model) is less than R^2, but is the better of the two for selecting the model with the most significant terms. The closer a value is to one, the better the fit. The best model is usually the one that maximizes both the R-squared (R^2) and adjusted R-squared value. The root mean square (RMS) error is a measure of the response variability that is not explained by the fit in units of the fit.

Table 14. Coefficients and Statistics for the Best Fit Alkaline Spent-Fuel Dissolution Model (Eq. 11)

Term	Coefficient (a_i)	Standard Error	*T*-value	Significance	Term Description
1	5.479057	1.176914	4.66	0.0001	Regression constant
IT	-2457.050662	308.646873	-7.96	0.0001	Inverse temperature (K^{-1})
PCO_3	1.510878	0.411485	3.67	0.0006	[–Log10] of total carbonate conc. $HCO_3^- + CO_3^=$, (mol/L)
PO_2	-1.729906	0.480710	-3.60	0.0000	[–Log10] of oxygen partial pressure (atm)
PH	0.234718	0.055684	4.22	0.0001	[–Log10] of hydrogen ion conc. (mol/L)
LBU	-0.799526	0.693062	-1.15	0.2544	[+Log10] of burnup (MWd/kgM)
PO_2·IT	400.755947	152.630586	2.63	0.0116	2nd-order interactions
LBU·IT	780.806133	176.287174	4.43	0.0001	
LBU·PCO_3	0.172305	0.044787	3.85	0.0004	
LBU·PO_2	0.174428	0.047220	3.69	0.0006	
LBU·PH	-0.271203	0.046748	-5.80	0.0001	
PCO_3^2	-0.339535	0.075978	-4.47	0.0001	Quadratic

NOTES: No. cases = 60
R-sq. = 0.8515
RMS Error = 0.2222
Resid. *DF* = 48
R-sq-adj. = 0.8174

The model described by Equation 11 has the best fit to the qualified data. It has a relatively high correlation coefficient; it is based on chemical and physical principles. Because the model is a simple polynomial, it is stable when used to extrapolate to variable values outside the original data space. This model, like the others, should be used only at alkaline conditions and should not be used at acidic conditions, i.e., less than pH = 7, which is a chemically different regime. The regression of the data with no interaction terms, produced the model in Table 15. The removed interaction terms approximate important information about the interaction of the spent fuel, represented by burnup, *with* temperature and the water chemistry variables (see Section 6.1). Removal of those terms reduces the fit significantly. Those interactions are where the burnup, surface complexes, and changing mechanisms express their effect on dissolution rate. Once the interaction terms are removed, the high significance value for log10(burnup) (LBU) and pH in Table 15, indicates that the terms are not as important by themselves. As discussed in Section 6.2.1, the pH is not a big contributor to dissolution rate changes and was removed along with LBU in the regression to produce Table 16. Further removal of the least significant term pCO3 yields the model in Tables 17 with lessened R-squared. Oxygen concentration has a big influence on the dissolution rate, but since it is assumed constant (Section 5), it was removed

from Table 17. The resulting Table 18 has drastically reduced R-squared. Temperature has the strongest effect on dissolution, but by itself is inadequate to satisfactorily explain variations in dissolution. The final simplification would be to remove all variables from the equation and use only the average of the data from Table 1. This arithmetic average is 7 mg/(m^2·d). Averaging provides less predictive capability and has no sensitivity to environmental conditions

Table 15. Coefficients and Statistics for the Alkaline Spent-Fuel Dissolution Model in Table 14 without Interaction Terms

Term	Coefficient	Standard Error	*T*-value	Significance
1	4.720241	0.845013		
IT	–1061.397862	208.937799	–5.08	0.0001
PCO_3	–0.117233	0.053660	–2.18	0.0333
PO_2	–0.333428	0.058070	–5.74	0.0001
PH	–0.001008	0.056802	–0.02	0.9859
LBU	–0.091288	0.067372	–1.35	0.1811

NOTES: No. cases = 60
R-sq. = 0.5435
RMS Error = 0.3672
Resid. *DF* = 54
R-sq-adj. = 0.5013

Table 16. Coefficients and Statistics for the Alkaline Spent-Fuel Dissolution Model in Table 15 after Removing Less Important Terms

Term	Coefficient	Standard Error	*T*-value	Significance
1	4.698852	0.678473		
IT	–1085.469491	208.200811	–5.21	0.0001
PCO_3	–0.115065	0.053631	–2.15	0.0363
PO_2	–0.324434	0.057436	–5.65	0.0001

NOTES: No. cases = 60
R-sq. = 0.5267
RMS Error = 0.3672
Resid. *DF* = 56
R-sq-adj. = 0.5014

Table 17. Coefficients and Statistics for the Alkaline Spent-Fuel Dissolution Model in Table 16 after Removing Least-Important Carbonate Term

Term	Coefficient	Standard Error	*T*-value	Significance
1	4.368724	0.681360		
IT	–1073.251014	214.600187	–5.00	0.0001
PO_2	–0.326909	0.059211	–5.52	0.0001

NOTES: No. cases = 60
R-sq. = 0.4878
RMS Error = 0.3786
Resid. *DF* = 57
R-sq-adj. = 0.4699

Table 18. Coefficients and Statistics for the Alkaline Spent-Fuel Dissolution Model in Table 17 with Temperature as the Only Variable

Term	Coefficient	Standard Error	*T*-value	Significance
1	3.824295	0.827990		
IT	–1046.960206	263.492557	–3.97	0.0002

NOTES: No. cases = 60
R-sq. = 0.2140
RMS Error = 0.465
Resid. *DF* = 58
R-sq-adj. = 0.2004

An alternate approach is one in which the unirradiated UO_2 and spent-fuel dissolution data are modeled separately not including cross-terms. Those fits are included in Tables 19 and 20. The UO_2 model has an R-squared of 0.8. The spent-fuel model in Table 20 has an R^2 of only 0.6.

Table 19. Coefficients and Statistics for the Alkaline UO_2 Dissolution Model

Term	Coefficient	Standard Error	*T*-value	Significance
1	5.612993	1.345481		
IT	–1821.008694	353.161180	–5.16	0.0001
PCO_3	–0.303113	0.089489	–3.39	0.0035
PO_2	–0.475644	0.093283	–5.10	0.0001
PH	0.241005	0.089458	2.69	0.0154

NOTES: No. cases = 22
R-sq. = 0.8089
RMS Error = 0.3541
Resid. *DF* = 17
R-sq-adj. = 0.7639

Table 20. Coefficients and Statistics for the Alkaline Spent-Fuel-Only Dissolution Model

Term	Coefficient	Standard Error	*T*-value	Significance
1	4.444920	0.878684		
IT	–702.182559	168.339695	–4.17	0.0002
PCO_3	–0.044638	0.043371	–1.03	0.3111
PO_2	–0.222600	0.049589	–4.49	0.0001
PH	–0.136076	0.047954	–2.84	0.0078
LBU	–0.096252	0.302149	–0.32	0.7521

NOTES: No. cases = 38
R-sq. = 0.6067
RMS Error = 0.2393
Resid. *DF* = 32
R-sq-adj. = 0.5452

Shoesmith (1999, Sec. 5.8) states that the corrosion of spent fuel is inherently the same process as that of unirradiated UO_2. This viewpoint depends on the chemical environment as well as what is considered to be significantly different. Table 1 shows dissolution rate differences

between UO_2 and spent fuel, which are significant by traditional analysis-of-variance measures. Sensitivity studies in repository performance assessment are the best guide to determining the importance of differences in dissolution behavior of UO_2 and spent fuel. Shoesmith (1999, Sec. 6.1) points out that it is becoming clearer that no single fuel corrosion mechanism applies over the full range of parameters studied. At this time, modeling of these parameters can only approximate the real mechanisms, but it is sufficient for predictive purposes in repository design.

An alkaline dissolution model is also available for unirradiated U_3O_8. It is discussed in Stout and Leider (1998, p. 3-134). As with the earlier UO_2 and spent-fuel dissolution data, the pH did not have much effect on the model. However, carbonate concentration, not temperature, had the strongest effect on the U_3O_8 dissolution rate (see Section 6.1). Shoesmith (1999) indicates that the dependence of dissolution rate on pH may indicate surface complexes. All three variables, temperature, pH, and carbonate concentration show significant interaction.

During the first series of expert panel elicitation meetings, an alternative spent-fuel intrinsic dissolution model was proposed by CRWMS M&O (1998b):

$$\text{Rate} = k\cdot[O_2]^{0.7}\cdot[CO_3]^{0.45}\cdot\exp(-Q/RT) \qquad \text{(Eq. 12)}$$

where k is a rate constant with appropriate units and Q is an Arrhenius activation energy. The exponents of the oxygen and carbonate concentrations were fixed and based on a compilation (Tait and Luht 1997) of single-variable tests by authors at several laboratories. Spent fuel and UO_2 were considered to have similar dissolution rates; that is, burnup is not a factor.

This model was fit to the points used in earlier models with T as the only variable, and Q and k were derived from the fit (Stout and Leider 1998, Sec. 3.4.2, Appendix A). The results follow:

$$\text{Rate } [\text{mg}/(\text{m}^2\cdot\text{d})] = 4.3172\cdot10^6\cdot[O_2]^{0.7}\cdot[CO_3]^{0.45}\cdot\exp(-5760.9/RT) \qquad R^2 = 0.23 \qquad \text{(Eq. 13)}$$

This is a poor regression fit, and the correlation coefficient is very similar to using only the most significant variable, temperature, in the fit:

$$\text{Rate } [\text{mg}/(\text{m}^2\cdot\text{d})] = 2.0497\cdot10^4\cdot\exp(-5541.3/RT) \qquad R^2 = 0.24 \qquad \text{(Eq. 14)}$$

By determining the coefficient and exponents directly from a regression fit of the data with the same terms as in Equation 12, the following equation was obtained:

$$\text{Rate } [\text{mg}/(\text{m}^2\cdot\text{d})] = 1.928\cdot10^5\cdot[O_2]^{0.35}\cdot[CO_3]^{0.15}\cdot\exp(-5627/RT) \qquad R^2 = 0.57 \qquad \text{(Eq. 15)}$$

This equation provides a much better fit but has a different rate constant and different exponents on the oxygen and carbonate terms. The correlation coefficient of Equation 15 is similar to the full simple rate law in Equation 10 (Table 15). This is due to the small effect of pH and the fact that burnup exhibits its importance not by itself but only with the interaction or cross-terms. Equations 13-15 were taken from Stout and Leider (1998) using a smaller data set.

6.2.2.3 Abstraction Model at Alkaline Conditions

As discussed in Section 6.2.2, the 12-term model for alkaline conditions yields the best fit of the data for UO_2 and spent fuel. However, a simpler model may be abstracted and used by performance assessment. Equation 15 was regressed using the full the 60 runs from Table 1, yielding Equation 16:

For pH > 7,

$$\text{Log}_{10}\, DR = a_0 \cdot 1 + a_1 \cdot IT + a_2 \cdot PCO_3 + a_3 \cdot O_2 \qquad \text{(Eq. 16)}$$

where $a_0 = 4.69$, $a_1 = -1085$, $a_2 = -0.12$, and $a_3 = -0.32$. (Table 16) $R^2 = 0.53$

The R-squared value is not as good a fit as the best fit, 12-term model, but it is well behaved, and is adequate for performance assessment. The standard error of each of the four terms, ($a_0 \cdot 1$, $a_1 \cdot IT$, $a_2 \cdot PCO_3$, and $a_3 \cdot O_2$), in Equation 16, were evaluated at nominal conditions (50°C, 10^{-3} atmospheres CO_2, 0.2 atmospheres O_2).

Table 21. Standard Error of Terms in Equation 16

Term	Term Evaluated at Nominal Conditions	Standard Error from Table 16	Terms from Equation 16	Standard Error of Terms in Eq. 16 (col. 2 x col. 3)
1	1	0.68	$a_0 \cdot 1$	0.68
IT	0.00275	208	$a_1 \cdot IT$	0.64
PCO_3	3	0.054	$a_2 \cdot PCO_3$	0.16
PO_3	0.7	0.057	$a_3 \cdot O_2$	0.04

To estimate the range of model validity, the standard errors at nominal conditions (last column in Table 21) were summed to yield 1.5 for log10(DR), or ±1.5 orders of magnitude for DR. A full analysis of the errors would yield an effective standard error for the model that would be lower than ±1.5 orders of magnitude. Such an analysis was performed for the TSPA-VA 12-term model (CRWMS M&O 1998a, Figure 6-26, p. 6-63). This analysis showed an effective standard error of about 0.33 in log space (CRWMS M&O 1998a, Figure 6-26). Since 99.7% of data in a normal distribution falls within 3 standard errors, this analysis shows the model to be valid to about 1 order (3 x 0.33) of magnitude. However, this 12-term model fit the data better than the recommended abstracted model (Equation 16). In addition, there is some uncertainty in the application of fresh spent fuel (<30 years out of reactor) and UO_2 dissolution UO_2 and rates to fuel that has aged in a repository for hundreds to thousands of years. Therefore, the larger range of ±1.5 orders of magnitude was chosen to represent the valid range for this model.

6.2.2.4 Intrinsic Dissolution Model at Acidic Conditions

There are limited data for UO_2 or spent-fuel dissolution at acidic conditions. Grambow (1989) calculated room-temperature acidic dissolution rates for boiling-water reactor (BWR) spent fuels with data reported by Forsyth et al. (1986). Steward and Mones (1996) reported UO_2 dissolution rates in nitric acid at 25 and 75°C and pHs of 4 and 6. Bruno reported UO_2 dissolution at reducing conditions and room temperature over an acidic and basic dissolution range (Stout and Leider 1998, p. 2-228).

Grambow (1989, p. 11) in his Figure 2 plot of the converted Forsyth et al. (1986) acidic spent-fuel dissolution rate data, gives a slope of about -0.5. An estimate of the intercept of the data line in Figure 2 is about 0.4 in log [g/(m^2·d)]. Converting to log [mg/(m^2·d)] gives an intercept of 3.4. This yields the following room-temperature acidic dissolution rate model for spent fuel:

$$\text{Log } DR[\text{mg}/(\text{m}^2\cdot\text{d})] = 3.4 - 0.5\cdot(\text{PH}) \qquad \text{(Eq. 17)}$$

Steward and Mones (1996) obtained similar or lower acidic dissolution rates for UO_2 than those for spent fuel from Equation 17. At room temperature, the UO_2 dissolution rates were 5 mg/(m^2·d) at pH = 4 and 3 mg/(m^2·d) at pH = 6. At 75°C the rate for pH = 4 was 23 mg/(m^2·d).

Gray (DTN: LL990707151021.075) reports an acidic spent fuel (ATM-103) dissolution rate of 109 mg/(m^2·d) at a pH of 3. This measurement was performed at 25°C in 10^{-3}M nitric acid sparged with CO_2-free air.

The abstracted acid dissolution model for spent fuel was constructed using qualified data, the alkaline abstracted model and an assumption (Equation 18).

For pH ≤ 7,

$$\text{Log}_{10}\, DR = a_0 \cdot 1 + a_1 \cdot \text{IT} + a_3 \cdot \text{PO}_2 + a_4 \cdot \text{PH} \qquad \text{(Eq. 18)}$$

where a_0= 7.13, a_1 = -1085, a_3 = -0.32, and a_4 = -0.41.

First, it was assumed (Section 5) that the temperature and oxygen pressure coefficients, a_1 and a_3 respectively, from the alkaline model could be used for the acid model. The basis of this assumption is the relative insensitivity of the wet dissolution rate to the relatively small range of temperature and assumed constant O_2 pressure in the repository. Next, the dissolution rate at pH = 7 was evaluated using the alkaline model (Eq. 16), at 25°C, atmospheric oxygen pressure, and CO_2 pressure of 10^{-3} atmospheres. This calculated point was combined with the qualified data point at pH = 3 to obtain the slope and intercept terms, a_4 and a_0, respectively. The resulting abstracted model is shown in Figure 2, along with several unqualified data points and the Grambow model. The resulting dissolution model (see Figure 2) gives reasonable or overestimated dissolution rates (see model validation, Section 6.2.2.5). Therefore, it is concluded that the uncertainty in the acid model is comparable to that in the alkaline model.

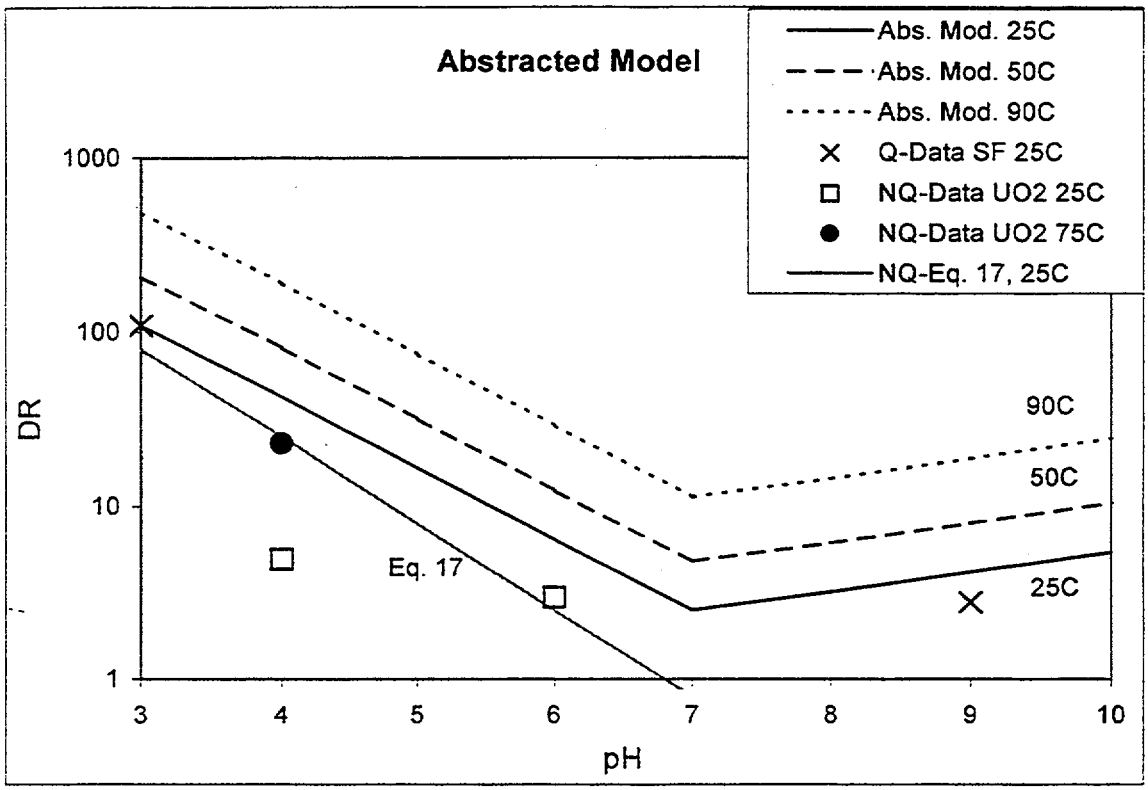

NOTE: Abstracted CSNF dissolution model evaluated at 10^{-3} atm. CO_2, 0.2 atm. O_2, and at 25°C, 50°C and 90°C.
DR in mg/(m^2·d)
Other data and Eq. 17 included for comparison.
Qualified (Q) data by Gray, DTN:LL990707151021.075 and run 8, Table 1, DTN:LL980601551021.042
Non-qualified (NQ) data by Steward and Mones (1996).

Figure 2. Abstracted Dissolution Model

6.2.2.5 Model Validation

For any semi-empirical model, the scatter in the data sets a limit on how accurately the equation can make a prediction. Per ASTM C 1174, Section 20.4.3.1, a model is considered valid if it accounts for all of the available data. If the validation and understanding is insufficient, bounding models may be used. Therefore, the following criterion was used for model validation; the model will be said to be valid if it either overestimates dissolution rates or predicts them within the specified uncertainty, in this case 1.5 orders of magnitude (Section 6.2.2.3). That is, the model is valid if the error metric (EM) is greater than or equal to -1.5 for all data, where EM = $\log_{10}(DR_c / DR_m)$, DR_c is the calculated dissolution rate and DR_m is the measured dissolution rate. The criterion that EM ≥ -1.5 must be met for all 64 qualified measured dissolution rates for alkaline conditions and the qualified measured dissolution rate for acidic conditions. In addition, comparison with relevant literature data should also yield error metrics that meet the criterion.

The Grambow model (Eq. 17) and the three NQ data points by Steward and Mones (1996) corroborate that the dissolution model in acid pH, Equation 18 is bounding (see Figure 2). The three data points by Steward and Mones (1996) were 5 mg/(m^2·d) at pH = 4, T = 25°C, 3

$mg/(m^2 \cdot d)$ at pH = 6, T = 25°C, and 23 $mg/(m^2 \cdot d)$ at pH = 4, T = 75°C. The error metrics for these three points are +0.93, +0.33, and +0.79 respectively.

Table 22 and 23 show DR_m, DR_c, and EM for the qualified alkaline dissolution data in Table 1 and the models presented in Tables 14-20. The maximum and minimum EM for each data set is listed at the bottom of each table, and the maximum and minimum EM for the full data set is listed at the bottom of Table 23. All 7 models meet the validation criteria for the full qualified data set. In addition, the newest runs at high burn-up, 61-64, were not included in the production of the model and thus serve as validation runs. The EMs of the abstraction model, Equation 16, and Table 16 are quite good (+0.05, +0.5, -.32 and +0.15 for runs 61-64, respectively).

Table 22. Comparison of Model Fitting to Alkaline CSNF dissolution data

Run	DR_m	Calculated DR (DR_c) Model							Error Metric (EM), Model						
		14	15	16	17	18	19	20	14	15	16	17	18	19	20
1	**6.34**	8.01	5.58	6.41	6.66	3.88	10.1	4.28	0.10	-0.06	0.00	0.02	-0.21	0.20	-0.17
2	**7.05**	8.01	5.58	6.41	6.66	3.88	10.1	4.28	0.06	-0.10	-0.04	-0.02	-0.26	0.16	-0.22
3	**5.07**	8.01	5.58	6.41	6.66	3.88	10.1	4.28	0.20	0.04	0.10	0.12	-0.12	0.30	-0.07
4	**3.45**	3.10	3.52	3.95	3.17	1.88	3.31	4.00	-0.05	0.01	0.06	-0.04	-0.26	-0.02	0.06
5	**14.2**	4.78	12.2	14.1	11.2	6.44	85.2	4.87	-0.47	-0.07	0.00	-0.10	-0.34	0.78	-0.46
6	**8.60**	7.54	7.13	8.31	11.2	6.44	6.95	7.42	-0.06	-0.08	-0.01	0.11	-0.13	-0.09	-0.06
7	**0.63**	1.03	1.99	2.27	3.10	1.84	2.38	1.71	0.21	0.50	0.56	0.69	0.47	0.58	0.43
8	**2.83**	2.11	3.51	3.95	3.17	1.88	5.76	2.92	-0.13	0.09	0.14	0.05	-0.18	0.31	0.01
9	**2.04**	2.69	2.67	3.03	3.17	1.88	4.99	1.93	0.12	0.12	0.17	0.19	-0.03	0.39	-0.02
10	**1.79**	1.91	1.10	1.28	1.73	2.18	0.35	2.15	0.03	-0.21	-0.15	-0.01	0.09	-0.71	0.08
11	**1.49**	1.76	3.54	4.25	5.68	6.93	8.00	2.49	0.07	0.38	0.45	0.58	0.67	0.73	0.22
12	**2.05**	1.18	1.79	2.07	1.65	2.07	3.97	1.36	-0.24	-0.06	0.00	-0.09	0.01	0.29	-0.18
13	**2.89**	5.10	5.96	7.03	5.54	6.76	10.2	5.64	0.25	0.31	0.39	0.28	0.37	0.55	0.29
14	**2.83**	1.95	0.91	1.06	0.84	1.93	0.48	1.61	-0.16	-0.50	-0.43	-0.53	-0.17	-0.77	-0.24
15	**0.69**	1.28	3.06	3.68	2.89	6.44	11.9	1.94	0.27	0.65	0.73	0.62	0.97	1.24	0.45
16	**1.98**	2.06	1.93	2.34	3.11	6.93	1.10	3.10	0.02	-0.01	0.07	0.20	0.54	-0.26	0.19
17	**0.51**	0.65	0.48	0.56	0.76	1.75	0.31	0.66	0.10	-0.03	0.04	0.17	0.54	-0.22	0.11
18	**1.04**	1.11	1.83	2.18	1.72	3.88	4.92	1.38	0.03	0.25	0.32	0.22	0.57	0.67	0.12
19	**1.87**	2.46	0.66	0.77	0.80	1.84	0.38	1.03	0.12	-0.45	-0.39	-0.37	-0.01	-0.69	-0.26
20	**4.75**	2.30	5.65	6.69	5.27	6.44	28.5	2.92	-0.32	0.08	0.15	0.05	0.13	0.78	-0.21
21	**6.60**	7.78	5.43	6.25	6.50	3.79	9.67	4.20	0.07	-0.08	-0.02	-0.01	-0.24	0.17	-0.20
22	**1.50**	3.25	3.36	3.95	3.17	1.88	3.31	3.81	0.34	0.35	0.42	0.33	0.10	0.34	0.40
23	**4.00**	3.34	3.78	4.26	3.42	2.03	3.75	4.19	-0.08	-0.02	0.03	-0.07	-0.30	-0.03	0.02
24	**9.10**	10.5	12.5	14.5	11.5	6.60	29.3	9.25	0.06	0.14	0.20	0.10	-0.14	0.51	0.01
25	**2.60**	2.46	2.20	2.51	3.42	2.03	0.93	3.41	-0.02	-0.07	-0.02	0.12	-0.11	-0.45	0.12
26	**11.0**	7.72	7.29	8.53	11.5	6.60	7.25	7.53	-0.15	-0.18	-0.11	0.02	-0.22	-0.18	-0.16
27	**3.50**	3.42	3.66	4.26	3.42	2.03	3.75	4.05	-0.01	0.02	0.08	-0.01	-0.24	0.03	0.06
28	**3.80**	3.45	3.61	4.26	3.42	2.03	3.75	4.00	-0.04	-0.02	0.05	-0.05	-0.27	-0.01	0.02
29	**6.90**	8.99	12.0	14.5	11.5	6.60	29.3	8.83	0.11	0.24	0.32	0.22	-0.02	0.63	0.11
30	**2.90**	3.01	2.11	2.51	3.42	2.03	0.93	3.25	0.02	-0.14	-0.06	0.07	-0.16	-0.49	0.05
31	**9.50**	7.84	6.98	8.53	11.5	6.60	7.25	7.19	-0.08	-0.13	-0.05	0.08	-0.16	-0.12	-0.12
32	**4.10**	2.31	0.78	0.96	0.76	2.03	0.42	1.43	-0.25	-0.72	-0.63	-0.73	-0.31	-0.99	-0.46
33	**1.40**	2.44	2.58	3.25	2.55	6.60	3.27	3.17	0.24	0.27	0.37	0.26	0.67	0.37	0.35
34	**1.90**	2.02	0.45	0.56	0.76	2.03	0.10	1.17	0.03	-0.62	-0.53	-0.40	0.03	-1.26	-0.21
35	**3.50**	2.13	1.50	1.91	2.55	6.60	0.81	2.58	-0.22	-0.37	-0.26	-0.14	0.28	-0.64	-0.13
36	**3.20**	3.17	4.03	4.26	3.42	2.03	3.75	4.48	0.00	0.10	0.12	0.03	-0.20	0.07	0.15
37	**11.9**	13.1	13.4	14.5	11.5	6.60	29.3	9.90	0.04	0.05	0.09	-0.02	-0.26	0.39	-0.08
38	**3.70**	1.83	2.35	2.51	3.42	2.03	0.93	3.65	-0.31	-0.20	-0.17	-0.03	-0.26	-0.60	-0.01
61	**3.80**	3.53	3.50	4.26	3.42	2.03	3.75	3.87	-0.03	-0.04	0.05	-0.05	-0.27	-0.01	0.01
62	**4.60**	8.07	11.6	14.5	11.5	6.60	29.3	8.54	0.24	0.40	0.50	0.40	0.16	0.80	0.27
63	**2.90**	2.32	1.14	1.38	1.89	1.14	0.34	2.14	-0.10	-0.41	-0.32	-0.19	-0.41	-0.93	-0.13
64	**6.00**	7.93	6.76	8.53	11.5	6.60	7.25	6.95	0.12	0.05	0.15	0.28	0.04	0.08	0.06
						Maximum SF EM			0.34	0.65	0.73	0.69	0.97	1.24	0.45
						Minimum SF EM			-0.47	-0.72	-0.63	-0.73	-0.41	-1.26	-0.46

Table 23. Comparison of Model Fitting to Alkaline UO_2 Data

Run	DR_m	Calculated DR (DR_c) Model							Error Metric (EM), Model						
		14	15	16	17	18	19	20	14	15	16	17	18	19	20
39	12.3	5.86	3.53	3.04	3.14	3.88	3.37	3.56	-0.32	-0.54	-0.61	-0.59	-0.50	-0.56	-0.54
40	7.96	5.86	3.53	3.04	3.14	3.88	3.37	3.56	-0.13	-0.35	-0.42	-0.40	-0.31	-0.37	-0.35
41	10.4	5.86	3.53	3.04	3.14	3.88	3.37	3.56	-0.25	-0.47	-0.53	-0.52	-0.43	-0.49	-0.47
42	2.4	2.77	5.29	4.36	3.50	2.07	3.91	5.92	0.06	0.34	0.26	0.16	-0.07	0.21	0.39
43	77.4	90.4	17.0	14.5	11.5	6.60	88.8	6.87	0.07	-0.66	-0.73	-0.83	-1.07	0.06	-1.05
44	10.9	6.94	9.97	8.53	11.5	6.60	7.25	10.5	-0.20	-0.04	-0.11	0.02	-0.22	-0.18	-0.02
45	2.55	1.84	3.07	2.57	3.50	2.07	2.94	2.58	-0.14	0.08	0.00	0.14	-0.09	0.06	0.00
46	0.22	0.46	1.14	0.98	0.78	2.07	0.44	2.12	0.32	0.71	0.65	0.55	0.97	0.30	0.98
47	5.61	6.26	3.67	3.25	2.55	6.60	9.94	2.47	0.05	-0.18	-0.24	-0.34	0.07	0.25	-0.36
48	0.51	0.48	2.15	1.91	2.55	6.60	0.81	3.76	-0.03	0.62	0.57	0.70	1.11	0.20	0.87
49	0.23	0.32	0.68	0.59	0.80	2.13	0.34	0.94	0.14	0.47	0.41	0.54	0.97	0.17	0.61
50	0.12	0.27	1.47	1.25	1.69	2.13	0.34	2.93	0.35	1.09	1.02	1.15	1.25	0.45	1.39
51	9.21	5.38	4.61	4.04	5.40	6.60	7.36	3.35	-0.23	-0.30	-0.36	-0.23	-0.14	-0.10	-0.44
52	1.87	3.48	2.51	2.12	1.69	2.13	4.14	1.93	0.27	0.13	0.05	-0.04	0.06	0.35	0.01
53	5.11	8.07	7.94	6.86	5.40	6.60	9.79	7.70	0.20	0.19	0.13	0.02	0.11	0.28	0.18
54	4.60	3.12	2.14	1.88	1.48	3.88	3.95	1.73	-0.17	-0.33	-0.39	-0.49	-0.07	-0.07	-0.43
55	6.72	4.75	5.28	4.36	3.50	2.07	6.81	4.33	-0.15	-0.10	-0.19	-0.28	-0.51	0.01	-0.19
56	9.34	8.47	4.02	3.35	3.50	2.07	5.91	2.85	-0.04	-0.37	-0.45	-0.43	-0.65	-0.20	-0.51
57	1.52	0.86	0.89	0.77	0.80	2.13	0.40	1.42	-0.25	-0.23	-0.30	-0.28	0.15	-0.58	-0.03
58	6.48	20.5	9.93	8.53	11.5	6.60	22.0	5.60	0.50	0.19	0.12	0.25	0.01	0.53	-0.06
59	23.3	54.7	13.0	11.1	11.5	6.60	25.4	8.48	0.37	-0.25	-0.32	-0.31	-0.55	0.04	-0.44
60	54.0	30.7	17.1	14.5	11.5	6.60	29.3	12.9	-0.25	-0.50	-0.57	-0.67	-0.91	-0.27	-0.62
					Maximum UO_2 EM				0.50	1.09	1.02	1.15	1.25	0.53	1.39
					Minimum UO_2 EM				-0.32	-0.66	-0.73	-0.83	-1.07	-0.58	-1.05
					Maximum SF/UO_2 EM				0.50	1.09	1.02	1.15	1.25	1.24	1.39
					Minimum SF/UO_2 EM				-0.47	-0.72	-0.73	-0.83	-1.07	-1.26	-1.05

Under YMP sponsorship, some additional UO_2 and spent-fuel dissolution rates were measured under oxidizing conditions using the flow-through test method (Stout and Leider 1998, p. 225). Water compositions included synthetic J-13 well water, deionized distilled water (DIW), and variations on the J-13 water composition selected to measure the effects of various J-13 water components on UO_2 dissolution rates. These data are summarized in Table 24. Flow-through dissolution rates in the synthetic J-13 groundwater were about 0.2 mg/(m^2·d). This compares to about 3 mg/(m^2·d) in Figure A.43 in Gray and Wilson (1995). Dissolution rates at 25°C in air-equilibrated DIW were 0.5 - 1 mg/(m^2·d). Calcium (15 µg/mL as $CaCl_2$ and $CaNO_3$) and silicon (30 µg/mL as silicic acid) were sequentially added to the DIW, resulting in an order of magnitude decrease in uranium dissolution rate.

The single measurement data in Table 24 fall into two groups, (1) "J-13-like" conditions with calcium, silicates, and carbonate present and (2) measurements similar to "aggressive groundwater" conditions that have no calcium or silicates. The Forsyth (1997) and Gray and Wilson (1995) groundwater (J-13 like) numbers are similar at 6 and 3 mg/(m^2·d), respectively. But they are also similar to the "aggressive groundwater conditions" (120 mg/L HCO_3) given by Gray and Wilson. Gray and Wilson also report values for very low J-13 or Ca/Si-containing

waters. The omission of explicit consideration of these effects in the model will make the model err on the conservative side.

Table 24. Single-Measurement Dissolution Data

Dissolution Rate [mg/(m2·d)]	Sample	Water	Test Method	Datum Source	Reference
0.2	UO_2	J-13	Flow	Figure 4[a]	Wilson and Gray (1990)
6	UO_2	120 mg/L HCO_3	Flow	Figure 4	Wilson and Gray (1990)
0.03	UO_2	HCO_3+Ca+Si	Flow	Figure 4	Wilson and Gray (1990)
0.6	UO_2	DIW	Flow	Figure 4	Wilson and Gray (1990)
3	UO_2	120 mg/L HCO_3	Flow	Figure A.71	Gray and Wilson (1995)
0.05	UO_2	HCO_3+Ca+Si	Flow	Figure A.71	Gray and Wilson (1995)
3	SF	J-13	Flow	Figure A.43	Gray and Wilson (1995)
6	SF (BWR Fragments)	J-13 (similar)	Batch	Table 7-2	Forsyth (1997)

NOTE: [a] Dissolution rate calculations from Figure 4 of Wilson and Gray (1990) use the reported flow rate of 0.2 mL/min, a sample mass of 7 g, and a specific surface area of 7.2 cm^2/g. The equation used for the calculations is the same as Equation 3.2 of Gray and Wilson (1995).
BWR = boiling-water reactor

Results from flow-through dissolution tests with oxidized specimens of spent fuel and unirradiated U_3O_7 and U_3O_8 were also reported (Stout and Leider 1998, p. 225). Dissolution rates of spent fuels oxidized to U_4O_{9+x} were measured for three spent fuels, ATM-104, ATM-105, and ATM-106. The surface area normalized dissolution rate of oxidized fuel grains was little or no higher than unoxidized (UO_2) grains for ATM-105. Oxidized ATM-106 fuel grains dissolved faster than unoxidized grains, but still the difference was a factor of only about five.

Oxidation has the potential to change spent-fuel intrinsic dissolution rates by increasing the effective surface area. The intrinsic dissolution rates of ATM-104, ATM-105, and ATM-106 (data obtained using grain specimens) (Stout and Leider 1998, p. 226) were not significantly affected by oxidation to U_4O_{9+x}.

The data suggest that oxidation up to the U_4O_{9+x} stage does not have a large effect on intrinsic dissolution rates (the largest increase was a factor of < 6). However, data for some of the particle specimens suggest that this degree of oxidation may markedly increase dissolution rates of relatively intact fuel rods by opening the grain boundaries, thereby increasing the effective surface area that is available for contact by water. From a disposal viewpoint, this is the more important consideration (Stout and Leider 1998).

When ATM-106 fuel was oxidized to U_3O_8, its surface area normalized dissolution rate was about 10 times faster than unoxidized ATM-106 fuel grains and about twice as fast as ATM-106 fuel grains oxidized to U_4O_{9+x} (Gray and Wilson 1995). A more important effect of oxidation to U_3O_8 was the very large increase in surface area compared to the particles used to prepare the U_3O_8. This resulted in a fractional dissolution rate (rate per unit specimen weight) of U_3O_8 equal to 150 times that of the unoxidized particles.

At atmospheric O_2 overpressure, the intrinsic dissolution rate of unirradiated U_3O_7 [~3 mgU/(m^2·d)] was similar to UO_2 [~2.5 mgU/(m^2·d)], and the intrinsic dissolution rate of unirradiated U_3O_8 [~10-15 mgU/(m^2·d)] was about four to six times that of UO_2. At an O_2 overpressure of 0.003 atm, the intrinsic dissolution rate of the U_3O_7 was two to three times that of UO_2 [0.5-1 mgU/(m^2·d)]. These estimates are based on a single test on each oxide at each condition.

In summary, for each supplemental test conducted with oxidized spent fuel or unirradiated U_3O_7 or U_3O_8, the intrinsic dissolution rate of the oxidized material was only moderately higher than the unoxidized (UO_2) material. The largest difference was a factor of 10 with spent fuel U_3O_8. This difference is relatively small given that the surface of UO_2 must first oxidize to a stoichiometry equivalency of approximately $UO_{2.33}$ before significant dissolution of U, as U(VI) species, can occur. These observations are similar to Shoesmith (1999, Sec. 5.2).

Model Comparison to Nonproject Data–There are a number of uranium oxide and spent-fuel dissolution studies in the literature. Grambow (1989) and McKenzie (1992) provide reviews of the literature prior to 1992. There are three more recent reports of particular interest for flow-through dissolution data. De Pablo et al. (1997) performed flow-through studies of UO_2 dissolution in brine solutions as a function of both temperature and carbonate concentration at atmospheric oxygen (Table 25). Torrero et al. (1997) measured uranium dioxide dissolution at various dissolved oxygen concentrations and pH at room temperature (Table 2). Tait and Luht (1997) published a report summarizing UO_2 and spent-fuel flow-through dissolution studies performed over an extended period of time at Atomic Energy of Canada Limited, Whiteshell Laboratories (Table 26). Acidic and alkaline dissolution of UO_2 under reducing conditions at room temperature were reported by Bruno (Stout and Leider 1998, p. 2-228). These were used for comparison with dissolution models developed for performance assessment.

Table 25. Measured UO_2 Flow-Through Dissolution Data in Brines with Variation of Temperature and Carbonate Concentration

Temp (°C)	Carbonate (mol/L)	PH*	Measured *DR* [mg/(m^2·d)]	Calculated *DR* [mg/(m^2·d)] Table 14	Calculated *DR* [mg/(m^2·d)] Table 16	EM for Eq. 11 Table 14	EM for EQ. 16 Table 16
25	0.05	10	8.64	5.23	4.81	-0.22	-0.25
40	0.05	10	116	11.7	7.18	-1.00	-1.21
60	0.05	10	221	31.7	11.6	-0.84	-1.28
25	0.01	9.3	2.2	6.64	3.99	0.48	0.26
40	0.01	9.3	17	14.9	5.97	-0.06	-0.45
60	0.01	9.3	59.9	39.0	9.63	-0.19	-0.79
25	0.001	8.3	0.84	2.51	3.06	0.48	0.56
40	0.001	8.3	1.73	5.63	4.58	0.51	0.42
60	0.001	8.3	2.4	14.7	7.39	0.79	0.49
25	0.0001	7.3	0.19	0.20	2.35	0.02	1.09
40	0.0001	7.3	0.3	0.45	3.51	0.18	1.07
60	0.0001	7.3	0.53	1.18	5.67	0.35	1.03
					Maximum	0.79	1.09
					Minimum	-1.00	-1.28

NOTES: *pH estimated using Figure 4.3, p. 181, of Stumm and Morgan (1981)
de Pablo et al. (1997)

The comparisons between Equation 11 and 16 models (Tables 14 and 16) and the carbonate- and temperature-varying study in Table 25 show that models 11 and 16 do not have as strong a dependency on carbonate as that seen in de Pablo et al.'s (1997) study, although the trends are in the same direction. The models underpredict the highest carbonate dissolution rates and overpredict the lowest. This may be due to the multiple mechanisms that de Pablo attributes to the nonlinear effect of carbonate data that our model does not account for completely. With de Pablo's data at only three temperatures and carbonate concentrations, it is statistically impossible to determine whether there is really a change in mechanism or a larger error at one temperature. The data corroborates the models with EMs greater than -1.5.

The alkaline model calculations gave dissolution rates that were consistently higher than Torrero et al.'s (1997) oxygen and alkaline pH variation data in Table 2 (see Section 4). Some effect could be explained by the use of 0.0002 *M* total carbonate concentration in the model, which would increase solubility, where Torrero's measurements were carbonate-free. The large differences come with the acidic comparisons, where the calculated dissolution rates were up to 20 times higher. Torrero dissolution rates values under acidic conditions were low in general when compared to other work (see Grambow 1989), but also corroborate the bounding nature of the acid model (Eq. 18).

Table 26. Comparison of Data from Tait and Luht (1997) with the Alkaline Models Equations 11 and 16

Sample	Water (Aerated Unless Noted)	T (°C)	From Tait (1997)	DR_m	DR_c Eq. 11 Table 14	DR_c Eq. 16 Table 16	EM for EQ. 16 Table 16
UO_2	SC[b]	25	Figure 4	1.37	6.6	4.0	0.46
UO_2	SC[b]	25	Figure 9	1.4	6.6	4.0	0.46
UO_2	SC (pO_2=4.4)[b]	25	Figure 10	0.03	0.24	0.3	0.92
UO_2	SC (pO_2=0.7)[b]	25	Figure 10	11	6.5	4.0	-0.44
UO_2 (CANDU)	SC[b]	35	Figure 13	10.2	12 (pH=9.3)	5.2	-0.29
UO_2 (CANDU)	SC[b]	50	Figure 13	22	25 (pH=9.3)	7.6	-0.46
UO_2 (CANDU)	SC[b]	50	Figure 13	25.6	25 (pH=9.3)	7.6	-0.53
UO_2 (CANDU)	SC[b]	75	Figure 13	102	75 (pH=9.3)	13.3	-0.88
UO_2 (CANDU)	HCO_3 5E-4 M	25	Figure 12	2	1.4 (pH=8)	2.8	0.15
UO_2 (CANDU)	HCO_3 1E-3 M	25	Figure 12	3.1	2.5 (pH=8.3)	3.1	-0.01
UO_2 (CANDU)	HCO_3 5E-3 M	25	Figure 12	5.7	5.8 (pH=9)	3.7	-0.19
UO_2 (CANDU)	HCO_3 1E-2 M	25	Figure 12	11.6	5.6 (pH=9.3)	4.0	-0.46
UO_2 (CANDU)	HCO_3 5E-2 M	25	Figure 12	11	5.2 (pH=10)	4.8	-0.36
UO_2 (CANDU)	HCO_3 0.1 M	25	Figure 12	15.1	3.7 (pH=10.3)	5.2	-0.46
Used Fuel[a]	SC (pO_2=4.4)[b]	25	Figure 10	0.2	0.6	0.3	0.10
Used Fuel[a]	SC (pO_2=4.4)[b]	25	Figure 10	0.6	0.6	0.3	-0.38
Used Fuel[a]	SC (pO_2=0.7)[b]	25	Figure 10	10	3.8	4.0	-0.40
Used Fuel[a]	SC[b]	25	Figure 17	13	3.8 (pH=9.3)	4.0	-0.51
Used Fuel[a]	SC (Deaerated)[b]	25	Figure 18	0.2	0.9 (pO_2=2E-4)	0.4	0.33
Used Fuel[a]	SC[b]	25	Figure 19	4	3.8 (pH=9.3)	4.0	0.00
Used Fuel[a]	SC[b]	35	Figure 21	20	5.5	5.2	-0.58
Used Fuel[a]	SC[b]	75	Figure 21	45	18	13.3	-0.53
					Maximum Minimum	EM EM	0.92 -0.88

NOTE: [a]Used Fuel Burnup =10 MWd/kgU
[b]SC = Aerated 0.01*M* $NaHCO_3$/0.1 *M* NaCl (pH≅9.3)
CANDU = Canada Deuterium Uranium
DR in mg/(m^2·d), m for measured, c for calculated

Table 26, from Tait and Luht (1997), lists dissolution rates from flow-through dissolution tests. These tests from outside literature are the closest in configuration and conditions to the YMP data in Table 1. In general, the models predict the various Tait results well at the various sample, temperature, oxygen, and water-chemistry conditions, providing a good confirmation of the model. For deaerated conditions, an oxygen pressure of 0.0002 atm was used for modeling. The pHs were estimated from bicarbonate concentrations as in Table 25. Unirradiated UO_2 and Canada Deuterium Uranium (CANDU) fuel were treated the same (burnup = 1 in modeling). The in-reactor irradiated CANDU fuel has a burnup of roughly 10 MWd/kgU (Gray 1999) so a nominal value of 10 was used for modeling. The trends in the model and data with temperature, carbonate, and oxygen are the same. The models underpredict Tait's data at bounding conditions, such as 75°C, and 0.1 *M* bicarbonate, where the error is largest. Tait's Figures 7 and 8 show dissolution results from adding calcium and silicon to the leaching solution. The resulting room temperature dissolution rates are between 0.01 and 0.1 mg/(m^2·d) in the same range as the calcium and silicate data from many of those of reports by Gray and Wilson (1995) in Table 24. These data corroborate the alkaline models (Eq. 11 and 16).

6.3 UNSATURATED DRIP TESTS

Long-term testing of CSNF, in conditions that mimic geologically unsaturated, i.e., limited water and oxidizing conditions, has been in progress for over six years (since FY1992) at ANL. These tests are called unsaturated drip tests (UDTs). The purpose of these tests is to determine the relationship between the rate of CSNF alteration, i.e., dissolution and secondary phase formation, and the release rate of radionuclides in conditions that are likely to occur when water contacts spent fuel after the protective waste package is breached. These tests provide dissolution rate model confirmation. There are three sets of so-called "service test" conditions: vapor, low-drip-rate, and high-drip-rate with two commercial PWR spent nuclear fuels, ATM-103 and ATM-106 (CRWMS M&O 2000). All six ongoing tests are performed in experimental cells containing some water, which constantly exposes the fuel samples to water vapor. In these cells, a thin film of water continuously contacts and reacts with the fuel.

In some tests, water also drips on the fuel to imitate the cooler longer-term conditions when water can fall on the fuel from small corroded holes in the waste package. This water contact mode also provides additional liquid for transport of reacted material away from the fuel. The experimental configuration, the test procedures, and the composition of the leachant, EJ-13, have been described previously (Stout and Leider 1998, p. 2-238). All tests were done at 90°C. The nominal drip rate is 0.75 mL every 3.5 days in the high-drip-rate tests and 0.075 mL every 3.5 days in the low-drip-rate-tests. A water drop covers about 1 cm^2 of fuel surface after contact, thus the low-drip-rate test is equivalent to $(0.075cm^3 \cdot 365d/y)/(1cm^2 \cdot 3.5d)$ or approximately 8 cm of rainfall per year, similar to the annual rainfall at the semi-arid Yucca Mountain. The 10× higher drip rate can mimic water intrusion rates channeled onto the exposed spent fuel from rock fractures. In the vapor tests, minimum water is available for transport, and the absence of added cations and anions limits the type of alteration products (secondary phases) that may form.

The primary purpose of analyzing the UDT release data is to calculate an estimated CSNF intrinsic dissolution/corrosion rate based on the concentrations of the highly soluble radionuclides, ^{99}Tc and ^{90}Sr. These two radionuclides should be more homogeneously distributed in the spent-fuel matrix than ^{129}I and ^{139}Cs, which are more highly segregated at the fuel grain boundaries and fuel-clad gap. Because uranium may precipitate in alteration phases, it is not a good dissolution marker in these tests.

6.3.1 High-Drip-Rate Tests

Iodine and technetium in the high-drip-rate tests exhibit large interval release rates for later time intervals. For iodine, the interval release rates in both high-drip-rate tests decrease about an order of magnitude after 1.3 years of reaction (Tables 3 and 4).

Technetium exhibits different dissolution responses in the ATM-103 and ATM-106 tests. The Tc interval release rates in the ATM-106 test remained relatively constant and were about two times larger than those in the ATM-103 test for the last three time intervals at 3.7, 4.2, and 4.8 years (Tables 3 and 4). The factor of two difference between the Tc release rates for the two fuels is comparable to the 1.5 factor between the two fuels' burnups (45 MWd/kgU for ATM-106 and 30 MWd/kgU for ATM-103).

Most of the measured uranium, neptunium and plutonium release occurred in the first year of reaction, and thereafter nearly all of these elements were retained. Based on the Tc release as a marker for dissolution, about 99.7% of ^{238}U, 96.5% of ^{237}Np, and 99.96% of ^{239}Pu were retained for ATM-103 and 99.4% of ^{238}U, 99.6% of ^{237}Np, and 99.5% of ^{239}Pu were retained for ATM-106.

The ^{237}Np concentrations in the 3.7, 4.2, and 4.8-year time intervals were in the range 4×10^{-10} to 1×10^{-9} *M* for ATM-103 and 4×10^{-10} *M* for ATM-106 (Tables 3 and 4, respectively). These concentrations are similar to those reported in three sets of batch tests with LWR fuels (Wilson 1990).

Transmission-electron microscope examination (Finn et al. 1998) shows the Pu retained at the fuel surface in a residue. Of the 0.01% of the Pu that is released into the leachate, greater than 50% is sorbed on the walls of the stainless steel vessel. The other 50% of the Pu is colloidal. For both fuels, after 4.8 years of reaction the ^{129}I interval release rate and the cumulative release fraction is comparable to that of ^{99}Tc.

Through 4.2 years of reaction, the ^{90}Sr interval release rates for both fuels are an order of magnitude larger than those of ^{238}U but smaller than the ^{99}Tc release rates. After 4.8 years of reaction, the ^{90}Sr interval release rate in the ATM-106 test increased to 10^{-5} fraction/d, which is comparable to the Tc interval release rate.

6.3.2 Low-Drip-Rate Tests

In the low-drip-rate tests, the ^{99}Tc interval release rates for both fuels were comparable after 2.5 years of reaction (see Tables 5 and 6). The ATM-106 fuel was immersed in the EJ-13 leachate for 10 minutes at the 3.1-year time interval. The measured ^{99}Tc release rate increased by 2.5 orders of magnitude and the cumulative ^{99}Tc release fraction was 0.005. Prior to immersion, it was 0.0001. A 0.005 cumulative release fraction is 28% of the high-drip-rate cumulative release fraction (0.0175) at the 3.1-year-time interval (see Table 4). The increase in the Tc cumulative release fraction indicates that ^{99}Tc had reacted prior to immersion and was readily released during immersion because it was loosely bound to the corrosion products or dissolved at high concentrations in the water filling the corrosion product pores.

The concentration of Tc as it leaves the Zircaloy holder is $< 1 \times 10^{-5}$ *M* in either of the low-drip-rate tests at any time interval, as listed in Tables 5 and 6. (Note that the value at the 3.1-year-time interval in the ATM-106 test includes the amount released after immersion.) The concentration of Tc in this liquid should be at steady state with the liquid in the pores in the corrosion layer. The Tc concentration in the pores that would correspond to the amount of Tc released during immersion, 2.9×10^{-5} g, is 0.13 or 0.07 *M* depending on whether the 15-μm-thick corrosion layer had a porosity of 10 or 20%, respectively. (The corresponding pore volume is 0.002-0.004 cm^3 if one approximates the fuel particle as spheres whose radius is 10.85 mm. This estimation was based on the geometric surface area of the fuel in the ATM-103 low-drip-rate test at the 3.1-year time interval.)

There is a 10^5-10^6 difference between the Tc concentration that leaves the Zircaloy holder (3×10^{-7} *M*) at the 2.5-year-time interval and the concentration in the pores (0.13-0.07 *M*) that

accounts for the Tc released during immersion at the 3.1-year-time interval. Because of this large difference, it is more likely that the pertechnetate, TcO_4^-, precipitates as a soluble salt as the liquid in the low-drip-rate test becomes concentrated. When excess water is introduced as in an immersion test, the salts dissolve and Tc, Cs, and Sr are released.

For the ratios of low-drip- to high-drip-rate cumulative fractions, the Sr ratio is 68% and the Cs ratio is 12%. The solubility of the Cs-Mo-U phase may be low. For the ATM-103 low-drip rate tests, ratios are ~1%, i.e., 99% of the Tc, Cs, and Sr that arose from reacted fuel is being retained.

6.3.3 Vapor Tests

Thin-film flow may be the major means of transport of reacted material in the vapor tests. Spallation of unwashed fuel fines is an alternative explanation for radionuclide transport from the vapor-exposed fuel into the catch basin. At the 4.7-year time interval, the interval release rates in the ATM-103 test for all of the elements reported, except for I, Sr, and Np are 5-200 times larger than those in the ATM-106 test. For Sr and Np, the interval release rates are comparable. For I, the ATM-106 interval release rate is four times that in the ATM-103 test. The cause of the large differences between most of the ATM-103 and ATM-106 interval release rates is uncertain. It may result from less liquid flowing in the ATM-106 test, which contains a fuel that has 50% higher decay heat.

It is difficult to compare the interval release rates for the vapor tests to their respective low-drip tests to determine if the species introduced in the groundwater have a significant effect. These differences could reflect the different modes of water transport dominating in each test: thin-film flow, advection, and spallation.

6.3.4 Estimation of Dissolution Rates from the ANL Unsaturated Drip Tests

The geometric surface area of the fuels at the start of the UDT tests were estimated as follows. Fuel fragments were taken from pellets that had a known diameter and density. An 8-g sample, which contained about 20 fragments and ranged in weight from 0.3-0.5 g, was assumed to be representative of the fuel samples. Since some of the fragments were wedge-shaped under visual examination, the geometry of the fuel fragments was modeled by as a pellet that had split into four layers with each layer containing eight pie-shaped fragments. The specific surface area that corresponded to this geometry was 2.1×10^{-4} m^2/g. The same specific surface area, 2.1×10^{-4} m^2/g, was calculated by Gray and Wilson (1995) for the same fuels by weighing each fragment and using a cubic fragment geometry. The consistency in the two calculations indicates that the uncertainty for an external geometric surface area is not large. However, the geometric surface area is not the effective surface area of the reacting fuel since it does not take into account open porosity in the fuel fragments nor roughness on the outside surface of the fragments at the start of the tests.

Also, the geometric surface area at the start of the tests does not account for the change in surface area as the fuel reacts. Visual observations over 4.8 years indicate that yellow corrosion products, which are needle shaped, have formed on the surface of the fragments. The fuel fragments become friable with increasing reaction time, as observed in the ATM-103 high-drip-

rate test at the 3.7-year time interval. Both of these effects should increase the effective surface area of the fuel fragments. Because the effective surface area during reaction was not measured or estimated, the initial geometric surface area was used to normalize the radionuclide release rates.

Estimates of the CSNF intrinsic dissolution rates are performed in the following manner. The intrinsic dissolution rate (DR or "normalized release rate"), is obtained by dividing the product of the interval mass fraction release rate and the mass of fuel by the fuel sample surface area, which is the product of the specific surface area of the fuel and the mass of fuel. This calculation is shown in Equation 19:

$$\text{Dissolution rate } [DR, \text{mg}/(\text{m}^2\cdot\text{d})] =$$

$$\{(\text{IRMR in interval } t_i)\ [X(\text{g})\ UO_2 \text{ fuel in interval } t_I \text{ (sampling time)}] \times (1000 \text{ mg/g})\}/$$

$$\{[\text{SSA} = 2.1 \times 10^{-4}\ \text{m}^2/(\text{g } UO_2)]\ [X(\text{g}) \text{ of } UO_2 \text{ fuel in interval } t_I]\} \qquad \text{(Eq. 19)}$$

which simplifies to

$$DR\ [\text{mg}/(\text{m}^2\cdot\text{d})] = [(\text{IRMR}) \times (1000 \text{ mg/g})]/\text{SSA} \qquad \text{(Eq. 20)}$$

SSA = specific surface area

This is the normalized release rate or estimated dissolution rate for a sampling interval, based on the specific geometric surface area.

The estimated CSNF dissolution rates based on ^{99}Tc release in the unsaturated drip tests and the geometric surface area are in Table 27. If a roughness factor of three (Gray and Wilson 1995) is applied to make the surface areas similar to the results in Table 1, the high drip rate estimates from Table 27 are 17 and 38 mg/(m^2·d). The intrinsic dissolution model in Equation 11 (Table 14) predicts a value of 22 mg/(m^2·d) at a pH of 8, 0.001 *M* carbonate, and 90°C for a fuel with a burnup of 30 MWd/kgU. This agreement between the model and ^{99}Tc release rates is good (EM 0.11 and –0.24). The calculations for the other isotopes show reduced release rates because the isotopes are retained in corrosion products.

Table 27. Estimates of Dissolution Rates Based on Unsaturated Drip-Test Cumulative Release Fractions

	Time (year)	Tc-99 Cum Frac	U-238 Cum Frac	Pu-239 Cum Frac	Np-237 Cum Frac	I-129 Cum Frac	Cs-137 Cum Frac	Sr-90 Cum Frac
ATM-103 High Drip	1.6	2.11E-02	8.65E-05	1.04E-05	1.17E-03	1.93E-02	1.78E-03	2.70E-03
	4.8	3.35E-02	9.65E-05	1.49E-05	1.18E-03	3.11E-02	6.38E-03	2.78E-03
Time to complete dissoln (TCD)(y)		143	49741	322148	4068	154	752	1727
TCD (Using last 3 years)		258	320000	820513	320000	271	696	40000
Estimated DR [mg/(m^2·d)], Eq. 20		**51**	0	0	5	48	19	0
ATM-106 High Drip	1.6	1.63E-03	1.79E-04	1.40E-04	1.09E-04	3.79E-02	2.99E-03	4.56E-04
	4.8	2.96E-02	1.80E-04	1.41E-04	1.12E-04	6.23E-02	5.98E-03	1.66E-03
Time to complete dissoln (TCD)(y)		162	26667	34043	42857	77	803	2892
TCD (Using last 3 years)		114	3200000	3200000	1066667	131	1070	2658
Estimated DR [mg/(m^2·d)]		**114**	0	0	0	99	12	5
ATM-103 Low Drip	1.6	8.84E-05	4.07E-06	2.19E-05	4.24E-05	2.53E-01	1.62E-05	5.84E-06
	4.7	4.24E-04	6.01E-06	2.35E-05	4.37E-05	2.67E-01	2.28E-05	2.99E-05
Time to complete dissoln (TCD)(y)		11085	782030	200000	107551	18	206140	157191
TCD (Using last 3 years)		9237	1597938	1937500	2384615	221	469697	128845
Estimated DR [mg/(m^2·d)]		**1**	0	0	0	59	0	0
ATM-106 Low Drip	1.6	9.07E-05	1.8E-06	2.36E-05	4.93E-05	6.41E-01	1.14E-05	2.38E-05
	4.7	5.95E-03	1.78E-04	2.06E-04	1.63E-04	6.72E-01	6.99E-04	3.40E-04
Time to complete dissoln (TCD)(y)		790	26404	22816	28834	7	6724	13824
TCD (Using last 3 years)		529	19375	16996	27265	119	4442	9804
Estimated DR [mg/(m^2·d)]		**25**	1	1	1	109	3	1

6.4 BATCH (SEMI-STATIC) TESTS

The Series 1 tests described (Stout and Leider 1998, p. 2-213) were the first of several batch or semi-static tests planned at PNNL to characterize potential radionuclide release from and behavior of spent fuel stored under YMP-proposed conditions. In the Series 1 tests, specimens prepared from TP Reactor Unit 3 fuel were tested in deionized distilled water in unsealed fused silica vessels under ambient hot cell air and temperature conditions. Four specimen configurations were tested: (1) intact fuel rod segments with water-tight end fittings, (2) fuel rod segments containing small (~200-μm-diameter) laser-drilled holes through the cladding and with water-tight end fittings, (3) fuel rod segments with a machined slit through the cladding and water-tight end fittings, and (4) bare fuel particles removed from the cladding plus the cladding hulls. A "semi-static" test procedure was developed in which periodic solution samples were taken with the sample volume replenished with fresh DIW. Cycle 1 of the Series 1 tests was started during July 1983 and was 240 days in duration. At the end of the first cycle, samples were taken, the vessels were stripped in HNO_3, and the specimens were restarted in fresh DIW for a second cycle. Cycle 2 of the Series 1 tests was terminated at 128 days in July 1984. A cycle is a testing period, where samples are taken at its conclusion, and the test vessels are stripped and cleaned or replaced.

The Series 2 tests (Wilson 1990) were similar to the Series 1 tests except that: (1) the Series 2 tests were run in reference J-13 well water, (2) each of the four specimen configurations was duplicated using both the TP Reactor and HBR Reactor PWR spent fuels, and (3) a vessel and specimen rinse procedure was added to the cycle termination procedures. Filtration of the collected rinse solution provided solid residues that were later examined for secondary-phase formation. Cycle 1 of the Series 2 tests was started in June 1984. All eight Series 2 specimens were run for a second cycle. The two bare fuel specimens were continued for Cycles 3, 4, and 5. Cycle 5 of the Series 2 bare fuel tests was terminated in June 1987 for a total five-cycle testing time of ~34 months.

The Series 3 tests (Wilson and Gray 1990) were run for three cycles during the same approximate time period as Cycles 3, 4, and 5 of the Series 2 tests. The Series 3 tests were run in sealed 304 and 304L stainless steel vessels and used the same four-specimen configurations used in Series 1 and Series 2 Cycles 1 and 2. Stainless steel (304L) was the chosen waste package material in that time frame. The current design, EDA II, has a 316NG inner layer to the waste package. Five specimens (one each of the four configurations using HBR reactor fuel, plus an additional bare fuel specimen using TP reactor fuel) were tested at 85°C, and a sixth specimen (HBR bare fuel) was run at 25°C.

For this report, the primary interest in these batch tests is as a comparative measure of estimated bare fuel dissolution rates from Series 3 with the measured flow-through dissolution rates that form the basis for the dissolution model. Also, the radionuclide concentrations of the early cycles of these batch tests can be compared with the accepted aqueous solubilities of some of the less-soluble radionuclides.

The Series 3 tests were chosen for this analysis because they were performed in stainless steel containers and with J-13 water. The previous Series 1 and 2 tests were conducted in silica vessels from which leached silica components could affect the results. The bare fuel tests were

chosen because they offered full exposure of the fuel to water as with the flow-through and unsaturated drip tests. The final test period, Cycle 3, was selected because the originally unwashed fuel samples had been exposed to two separate batches of J-13 water for almost a year. Easily removed radionuclides that had segregated to the surface or left in unremoved fines would have likely dissolved by the time Cycle 3 had started. Cycle 3, therefore, would most likely represent bulk fuel matrix dissolution. The unfiltered sample-concentration data for the very-soluble radionuclides, ^{90}Sr, ^{99}Tc, ^{129}I, and ^{137}Cs, in the bare fuel tests were used and taken respectively from Tables A.2 through A.4 of Wilson (1990, Series 3) for the HBR/BF-25, TP/BF-85, and HBR/BF-85 samples.

Sample-specific data in the analysis Tables 28, 29, and 30 are at the top. These data include experimental vessel volume, fuel specific area and isotope inventories, and sample weight, as well as referenced tables in Wilson (1990). Isotope specific data in the analysis tables are organized by isotope at the bottom. For each isotope, the sample time and volume and sample isotope concentration are listed. The fraction released, fraction released per day, and equivalent dissolution rates are calculated values using the following definitions and equations:

Vessel volume (V_V)	mL
Sample specific surface area (A_S)	m^2/g
Sampling time (t_s)	days
Sample isotope concentration (C_i)	pCi/mL
Fraction-released (F_r)	#
Fraction released/day (F_{rd})	d^{-1}
Radionuclide inventory (I_i)	μCi/g
Sample mass (m_s)	g
Equivalent UO_2 Dissolution rate (R_d)	$mgU/(m^2 \cdot d)$
Chemical Formula Weight (FW_i)	g

$$F_r = (C_i \cdot V_V)/(I_i \cdot m_s \cdot 1000000) \quad \text{(Eq. 21)}$$

$$F_{rd} = F_r/t_s \quad \text{(Eq. 22)}$$

$$R_d = [F_{rd} \cdot 1000]/A_S \quad \text{(Eq. 23)}$$

The following is a detail of a calculation using the above equations. The calculation is taken from Table 28 for test HBR/BF-25 with ^{137}Cs at a sampling time of 97 days.

$$F_r = (1.92E+06 \cdot 250)/(6.37E+04 \cdot 83.66 \cdot 1000000) = 9.01E-05 \qquad \text{(Eq. 24)}$$

The factor of 1,000,000 accounts for microcurie to picocurie conversion.

$$F_{rd} = 9.01E-05/97 = 9.29E-07\ d^{-1} \qquad \text{(Eq. 25)}$$

$$R_d = [9.29E-07 \quad 1000]/(2.4E-04 \cdot 3) \qquad \text{(Eq. 26)}$$

The factor of 1000 accounts for gram-to-milligram conversion. The factor of three in the surface area is the roughness factor from Gray and Wilson (1995, p. 2.7).

Estimates of spent-fuel dissolution rate using late-time data from Wilson's (1990) Series 3 tests are generally close to (within a factor of 6), but less than, those predicted by the model in Eq. 11, Table 14. The Wilson test fuels are like ATM-103 in that their burnup is 30 MWd/kgU. The dissolution model predicts a rate of 20 mg/(m^2·d) at 85°C and 6 mg/(m^2·d) at 25°C. These estimates from Wilson's work (1990, Series 3) are less than those predicted by the model can easily be explained by examining the water chemistry in each estimate. Wilson's tests were carried out in calcium and silicate-containing J-13 well water. As previously emphasized, the tests on which the model is based do not have those mineral-forming components.

Table 28. Calculations of Equivalent Intrinsic Dissolution Rates of H. B. Robinson Fuel at 25°C

Table A.2 (Table references are from Wilson 1990):
Vessel volume (mL) [Fig. 2.1] = 250 mL
Specific Surface Area (Geometric) = 2.40E-04 m^2/g [Table E.3, Col. 2]
Specific Surface Area (x3 Roughness) = 7.20E-04 m^2/g

Table 2.1:
Cycle 3 Sample Weight (g) = 83.66

Table 2.3:
RN Inventories (µCi/g) [a] (HBR Measured)

137 Cs	6.37E+04
99 Tc	10.5
90 Sr	4.17E+04
129 I	0.0265

		137 Cs					99 Tc				
Time (Days)	Sampling Volume (mL)	pCi/mL	Fraction Released	FracRel/d	Dissolution Rate (Cs) Geo. SA mgU/(m²·d)	Dissolution Rate (Cs) Rough SA mgU/(m²·d)	pCi/mL	Fraction Released	FracRel/d	Dissolution Rate (Tc) Geo. SA mgU/(m²·d)	Dissolution Rate (Tc) Rough SA mgU/(m²·d)
0											
20	25	1.19E+06	5.58E-05	2.79E-06	1.16E+01	3.88E+00	6.76E+01	1.92E-05	9.62E-07	4.01E+00	1.34E+00
55	25	1.58E+06	7.41E-05	1.35E-06	5.62E+00	1.87E+00	1.26E+02	3.59E-05	6.52E-07	2.72E+00	9.06E-01
97	250	1.92E+06	9.01E-05	9.29E-07	3.87E+00	1.29E+00	2.34E+02	6.66E-05	6.87E-07	2.86E+00	9.54E-01

		90 Sr					129 I				
Time (Days)	Sampling Volume (mL)	pCi/mL	Fraction Released	FracRel/d	Dissolution Rate (Sr) Geo. SA mgU/(m²·d)	Dissolution Rate (Sr) Rough SA mgU/(m²·d)	pCi/mL	Fraction Released	FracRel/d	Dissolution Rate (I) Geo. SA mgU/(m²·d)	Dissolution Rate (I) Rough SA mgU/(m²·d)
0											
20	25	4.73E+05	3.39E-05	1.69E-06	7.06E+00	2.35E+00					
55	25	6.53E+05	4.68E-05	8.51E-07	3.55E+00	1.18E+00	6.04E-02	6.81E-06	1.24E-07	5.16E-01	1.72E-01
97	250	7.84E+05	5.62E-05	5.79E-07	2.41E+00	8.04E-01	8.26E-02	9.31E-06	9.60E-08	4.00E-01	1.33E-01

NOTE: [a] 1000000 pCi = 1 microCi
Wilson (1990)

Table 29. Calculations of Equivalent Intrinsic Dissolution Rates of H. B. Robinson Fuel at 85°C

Table A.4 (Table references are from Wilson 1990).

Vessel volume (mL) [Fig. 2.1]=	250	mL
Specific Surface Area (Geometric) =	2.40E-04	m^2/g [Table E.3, Col. 2]
Specific Surface Area (x3 Roughness) =	7.20E-04	m^2/g

Table 2.1:
Cycle 3 Sample Weight (g)
HBR/BF-85 78.67

Table 2.3
RN Inventories (μCi/g)[a] (HBR Measured)

137 Cs	6.37E+04
99 Tc	10.5
90 Sr	4.17E+04
129 I	0.0265

		137 Cs					99 Tc				
					Dissolution Rate					Dissolution Rate	
Time (Days)	**Sampling Volume (mL)**	pCi/mL	**Fraction Released**	**FracReal/ day**	**Geo. SA mgU/(m^2·d)**	**Rough SA mgU/(m^2·d)**	pCi/mL	**Fraction Released**	**FracReal/ day**	**Geo. SA mgU/(m^2·d)**	**Rough SA mgU/(m^2·d)**
0											
20	25	5.86E+05	2.92E-05	1.46E-06	6.09E+00	2.03E+00	2.34E+02	7.08E-05	3.54E-06	1.48E+01	4.92E+00
55	25	1.25E+06	6.24E-05	1.13E-06	4.72E+00	1.57E+00	5.41E+02	1.64E-04	2.98E-06	1.24E+01	4.13E+00
97	250	2.09E+06	1.04E-04	1.07E-06	4.48E+00	1.49E+00	9.91E+02	3.00E-04	3.09E-06	1.29E+01	4.29E+00

		90 Sr					129 I				
					Dissolution Rate					Dissolution Rate	
Time (Days)	**Sampling Volume (mL)**	pCi/mL	**Fraction Released**	**FracReal/ day**	**Geo. SA mgU/(m^2·d)**	**Rough SA mgU/(m^2·d)**	pCi/mL	**Fraction Released**	**FracReal/d**	**Geo. SA mgU/(m^2·d)**	**Rough SA mgU/(m^2·d)**
0											
20	25	5.59E+05	4.26E-05	2.13E-06	8.87E+00	2.96E+00					
55	25	5.72E+05	4.36E-05	7.93E-07	3.30E+00	1.10E+00	8.15E-01	9.77E-05	1.78E-06	7.40E+00	2.47E+00
97	250	6.13E+05	4.67E-05	4.82E-07	2.01E+00	6.69E-01	1.24E+00	1.49E-04	1.53E-06	6.39E+00	2.13E+00

NOTE: [a] 1000000pCi = 1 μCi
Wilson (1990)

Table 30. Calculations of Equivalent Intrinsic Dissolution Rates of Turkey Point Fuel at 85°C

Table A.3 (Table references are from Wilson 1990).

Vessel volume (mL) [Fig. 2.1]= 250 mL

Specific Surface Area (Geometric) = 2.21E-04 m^2/g [Table E.3, Col. 2]
Specific Surface Area (x3 Roughness) = 6.63E-04 m^2/g

Table 2.1

Cycle 3 Sample Weight (g)
TP/BF-85 83.64

Table 2.3

	RN Inventories ($\mu Ci/g$)[a] TP Origen-2
137 Cs	6.04E+04
99 Tc	9.74
90 Sr	4.03E+04
129 I	0.0242

		137 Cs					**99 Tc**				
					Dissolution Rate					Dissolution Rate	
Time (Days)	**Sampling Volume (mL)**	pCi/mL	**Fraction Released**	**FracReal/ day**	**Geo. SA mgU/(m^2·d)**	**Rough SA mgU/(m^2·d)**	pCi/mL	**Fraction Released**	**FracReal/ day**	**Geo. SA mgU/(m^2·d)**	**Rough SA mgU/(m^2·d)**
0											
20	25	5.36E+05	2.65E-05	1.33E-06	6.00E+00	2.00E+00	1.49E+02	4.57E-05	2.29E-06	1.03E+01	3.45E+00
55	25	1.16E+06	5.74E-05	1.04E-06	4.72E+00	1.57E+00	3.24E+02	9.94E-05	1.81E-06	8.18E+00	2.73E+00
97	250	1.70E+06	8.41E-05	8.67E-07	3.92E+00	1.31E+00	5.41E+02	1.66E-04	1.71E-06	7.74E+00	2.58E+00

		90 Sr					**129 I**				
					Dissolution Rate					Dissolution Rate	
Time (Days)	**Sampling Volume (mL)**	pCi/mL	**Fraction Released**	**FracReal/ day**	**Geo. SA mgU/(m^2·d)**	**Rough SA mgU/(m^2·d)**	pCi/mL	**Fraction Released**	**FracReal/ day**	**Geo. SA mgU/(m^2·d)**	**Rough SA mgU/(m^2·d)**
0											
20	25	4.41E+05	3.27E-05	1.64E-06	7.40E+00	2.47E+00					
55	25	5.63E+05	4.18E-05	7.59E-07	3.44E+00	1.15E+00	5.95E-01	7.35E-05	1.34E-06	6.05E+00	2.02E+00
97	250	6.26E+05	4.64E-05	4.79E-07	2.17E+00	7.22E-01	9.15E-01	1.13E-04	1.17E-06	5.27E+00	1.76E+00

NOTE: [a] 1000000pCi = 1 μCi
Wilson (1990)

6.5 GAP AND GRAIN BOUNDARY RADIONUCLIDE INVENTORIES OF LWR SPENT FUELS

Some fission-produced radionuclides, ^{14}C, ^{135}Cs, ^{137}Cs, ^{129}I, ^{99}Tc, and ^{79}Se, migrate from the UO_2 matrix of LWR spent fuels at the high fuel temperatures of reactor operation and deposit onto the cooler grain boundaries and fuel/cladding gap surfaces (Gray 1999). In a repository, when water passes through damaged spent-fuel cladding, these soluble radionuclides can quickly dissolve. Volatile cesium and iodine, in addition to the fission gases, are the most conspicuous elements in this category. Recent performance assessments (TSPA-VA) (CRWMS M&O 1998a) of the proposed repository at Yucca Mountain used gap and grain-boundary fractions of 2% of the total inventories of ^{135}Cs, ^{137}Cs, ^{129}I, and ^{99}Tc. The gap fraction was modeled to dissolve rapidly if the spent fuel were to be contacted by groundwater (CRWMS M&O 1998a, p. 6-60). Laboratory measurements of a few LWR spent fuels show that both the GIs and GBIs of ^{99}Tc and ^{90}Sr were near the detection limits of the methods used, less than 0.2% of the total inventories of these elements (Gray 1999). However, some of the ^{99}Tc may reside at the grain boundaries in the form of relatively insoluble metallic particles and not be detected by these tests (Gray 1999). Measured combined GIs and GBIs of ^{129}I approximately equal the FGR fractions. For ^{137}Cs, the combined gap and grain-boundary inventories were approximately one third of the FGR fractions (Gray 1999). For the same spent fuels, the earlier data (Gray 1999, Fig. 1) indicate that the GBIs of ^{135}Cs and ^{137}Cs[4] are generally less than about 1% of the total inventories of these nuclides and that the GIs are equal to roughly one fourth of the percentage of FGR for a given spent fuel. These measured values may be used to replace the conservative 2% estimate and, thus, reduce the uncertainties in the calculations.

Stroes-Gascoyne (1996) measured GIs and GBIs of ^{137}Cs, ^{129}I, ^{90}Sr, ^{99}Tc and ^{14}C in 15 used (spent) CANDU fuel elements. There was a good correlation (see Figure 1c) between the combined GIs and GBIs of ^{137}Cs and ^{129}I, indicating that these fission products exhibit similar behavior in CANDU fuel and LWR fuel. Results were divided into groups consisting of ten low-power (< 42 kW/m) and five high-power (> 42 kW/m) CANDU used fuels. This partition was needed because of wide differences in the ^{129}I and ^{137}Cs GIs and GBIs of these two fuel groups. The Canadian studies allow a comparison of the gap and grain-boundary inventory results for CANDU and LWR spent fuels to see whether their characteristics can be explained by differences in power levels and burnups.

U.S. LWR spent fuel generally operates at lower power but is irradiated to higher burnups. The linear power of U.S. LWR fuels is typically 20-30 kW/m (Gray 1999), which is a little lower than even the low power CANDU fuels. Lower power levels generally mean lower fuel temperatures. The resulting smaller temperature gradient reduces the flux of ^{129}I, ^{137}Cs, and fission gases diffusing out of the matrix into the grain boundaries and gap. However, CANDU spent fuels have burnups of generally 10 MWd/kgU, which is considerably lower than the LWR spent-fuel burnups. Lower burnup means that less ^{129}I, ^{137}Cs, and fission gases were generated in

[4]Although ^{135}Cs is the isotope of interest for long-term geologic disposal because of its very long half-life (2,300,000 years), ^{137}Cs, with a half-life of 30 years, would be of interest in the event of early breach of a waste package. Also, ^{137}Cs is the isotope commonly measured in GI and GBI studies because it is also representative of the ^{135}Cs inventories and because it is much easier to measure due to its much higher activity in the spent fuels being tested.

the first place (Gray 1999). For CANDU fuels, the radionuclide migration to the gap and grain boundaries is lessened by a smaller concentration gradient rather than the smaller temperature gradient of the LWR spent fuel.

The expected correlation between combined GIs and GBIs of ^{137}Cs and ^{129}I with calculated FGR of CANDU fuels could be confirmed only for lower-power fuels (< 42 kW/m). Combined GIs and GBIs of ^{90}Sr were higher than expected and showed no correlation with calculated fission-gas release. No values for the combined GIs and GBIs of ^{99}Tc were obtained because ^{99}Tc in spent-fuel samples is very insoluble and requires oxidation prior to dissolution. Combined GIs and GBIs of ^{14}C were independent of fuel power or burnup.

LWR spent fuel is considerably more friable than CANDU spent fuel. Greater friability is indicative of a greater volume and/or a difference in the distribution of fission-gas bubbles in the grain boundaries. Fission-gas bubbles in grain boundaries provide pathways for gas mobility along the grain boundaries because the bubbles reduce the length of the diffusion path. For eight out of the nine low-power CANDU fuels, almost all of the combined GIs and GBIs of both ^{129}I and ^{137}Cs remained in the grain boundaries (Stroes-Gascoyne 1996). In contrast, a much greater proportion of the ^{129}I and ^{137}Cs migrated out of the grain boundaries into the gap in LWR spent fuels (Gray 1999). This difference between the CANDU and LWR spent fuels suggests that the grain boundaries in the CANDU fuels are tighter, consistent with the CANDU fuels being less friable. However, this conclusion is inconsistent with the higher temperatures in the low-power CANDU spent fuels compared with the U.S. LWR spent fuels. The higher temperatures would be expected to drive more of the ^{129}I and ^{137}Cs out of the grain boundaries and into the gaps. The fact that higher temperatures in the CANDU spent fuels obviously did not drive a greater proportion of the ^{129}I and ^{137}Cs out of the grain boundaries may be because the amount and distribution of fission gas bubbles in the grain boundaries did not provide the necessary pathways.

Besides the difference in the combined GIs and GBIs of ^{129}I and ^{137}Cs, these two radionuclides also differed in how they were distributed between the gaps and the grain boundaries. This contrasts with the rather similar behavior that has been reported for ^{129}I and ^{137}Cs in CANDU spent fuels.

Gray (1999) measured combined GIs and GBIs of ^{129}I that were approximately equal to the FGR fractions. For ^{137}Cs, the combined GIs and GBIs were approximately one-third of the FGR fractions (Figure 1). The FGRs of LWR fuels are listed in Table 10. In some of the fuels listed, the FGRs are between 7 and 18%. Recent performance assessments (TSPA-VA) (CRWMS M&O 1998a) of the proposed repository at Yucca Mountain used gap and grain-boundary fractions of 2% of the total inventories for ^{135}Cs, ^{137}Cs, ^{129}I, and ^{99}Tc. Using Gray's measurements, the 2% inventory estimate underestimates the GIs and GBIs in some fuels. These newly measured values should be used to replace the 2% estimate for ^{129}I and ^{137}Cs. Thus, it is recommended that the 1:1 ratio of ^{129}I to fission gas percentage and the 1:3 ratio of ^{137}Cs to fission gas percentage be used to replace the constant 2% of radionuclides in the grain boundary/gap region for these isotopes.

6.6 NATURAL ANALOGS

6.6.1 Studies of Natural Analog Sites

This section on natural analogs has been included to provide a qualitative overview of the uranium mineral phases seen at natural uranium-bearing sites around the world and to provide a comparison with spent-fuel corrosion products seen in the laboratory. Long-term stability of the geologic and geochemical systems at Yucca Mountain supports the concept that the spent fuel can be isolated safely in the repository for thousands of years–studies of natural ore bodies of uranium-containing sites provide substantial evidence for their geologic stability over millions of years. Confidence may be gained for the success of Yucca Mountain proposed geologic repository if secondary phase development in multi-year laboratory tests is similar to the alteration phase paragenesis determined at the uranium-bearing natural analog sites.

Commercial spent nuclear fuel consists of uranium dioxide (UO_2) having a cubic fluorite crystalline structure. Uranium dioxide occurs in nature as the mineral uraninite, also exhibiting a fluorite structure. Numerous geologic sites contain uraninite, and studies of natural uraninite alteration cover a wide range of geologic conditions. Of the several extensively studied sites, only Nopal I, the uranium mining site at Pena Blanca, Mexico, has geologic, geochemical, and hydrogeologic characteristics similar to those at Yucca Mountain (Murphy 1995). The volcanic (tuffaceous) host rock at Nopal I, the youngest of the studied sites, has been exposed to oxygen for tens of thousands of year. Uraninite, containing U^{4+}, was originally formed several million years ago. The other sites are either somewhat reducing or hydrologically saturated or the mineralogy of the uraninite alteration is significantly affected by the presence of chemical elements, e.g., lead, phosphorus, or vanadium, not found in underground spent fuel repositories or their environs.

A major difference in the characteristics of these two sites (Nopal I and Yucca Mountain) is that natural processes produced uranium deposits at the Nopal I mining site in Pena Blanca. The process of uranium mineral formation and subsequent uranium transport at Nopal I have been extensively studied. Because the sites are geologically similar, it is anticipated that the uranium compound alteration and transport processes will be comparable to those that would occur at the proposed repository at Yucca Mountain.

Pearcy and Murphy (1991) discuss in some detail other natural analog sites around the world. The oxidizing sites discussed are Koongarra in Australia, Pocos de Caldas in Brazil, Shinkolobwe mine in the Congo, and the Krunkelbach mine in Germany.

Spent fuel degradation via oxidation and dissolution are precursors to the formation of alteration products (secondary phases). These phases affect radionuclide solubilities and colloid formation. In turn, these characteristics affect radionuclide release and transport.

The uranium minerals found at Nopal I are listed in Table 11 (Pearcy et al. 1994). The compounds found are limited compared to other sites because of the simple chemistry of the Pena Blanca system.

6.6.2 Spent-Fuel Corrosion Products in Laboratory Tests

Combined optical, scanning-electron microscope (SEM), energy-dispersive x-ray spectroscope (EDS), and x-ray diffraction (XRD) examinations of samples taken from tests being performed on the two spent fuels (ATM-103 and -106) being studied at ANL indicate that the time-dependent evolution of the alteration-phases is strongly dependent on the rate at which the equilibrated J-13 water (EJ-13) contacts the spent UO_2 (Stout and Leider 1998, p. 2-250). The three tests (high-drip-rate, low-drip-rate, and vapor) show several similarities, including corroded grain boundaries, dissolution of fuel grains, and precipitation of U^{6+}-phases. The composition of corrosion layers depend strongly on water flux and its composition, with uranyl oxy-hydroxides predominating in vapor tests and alkali and alkaline earth uranyl silicates predominating in high-drip-rate tests. Low-drip-rate tests exhibit a complex assemblage of corrosion products, including phases identified in vapor and high-drip-rate tests. A summary of the corrosion products present and the techniques used to characterize them is found in Table 13.

The vapor tests display the simplest assemblage of alteration products. Only uranium and the radionuclides in the fuel dissolve into the thin film of water in contact with the fuel surfaces. Samples from vapor tests display a relatively simple combination of uranyl oxy-hydroxide alteration phases dominated by dehydrated schoepite $(UO_2)O_{0.25-x}(OH)_{1.5+2x}$ ($0 \leq x \leq 0.15$) and metaschoepite. This assemblage is readily explained by the lack of added cations in the vapor and condensate that contacts the fuel surface. The only cations (except H^+) available for the precipitation of solids come from the dissolution of fuel. A minor phase is Cs-Ba-Mo-uranate, which incorporates two fission products, cesium and molybdenum (Table 13). The precipitation of dehydrated schoepite and metaschoepite in these tests indicates that the film of water that forms on the fuel surface is sufficiently corrosive to dissolve the fuel and form a thin corrosion rind of alteration products. Such a water film is likely present in the drip tests, as well as during those intervals that EJ-13 water is not being dripped onto the fuel. It seems likely that the corrosion processes important in the vapor tests remain important in the drip tests. Dehydrated schoepite and/or metaschoepite may continue to form in the drip tests between water injections. If these phases are present when contacted by EJ-13 water, they may be at least as susceptible to dissolution and/or replacement as the unoxidized fuel. The degree to which this may be important is unknown at this time.

The drip tests display more chemically complex alteration phases, owing to the interaction of the fuel with EJ-13 water (rather than water vapor and condensate only). The most abundant elements in EJ-13 water are Na and Si, and, not surprisingly, the most abundant alteration products in the high-drip rate tests are Na- and Si-bearing U^{6+} phases. Other U^{6+} phases are also present, including metaschoepite and β-uranophane, indicating the importance of additional minor phases and elements to the overall corrosion process.

Fuel samples exposed to the higher drip-rates also display a comparatively simple phase assemblage, consisting of two uranophane-group silicates, β-uranophane $[Ca(UO_2)_2(SiO_3OH)_2(H_2O)_5]$ and Na-boltwoodite $(Na,K)(UO_2)(SiO_3OH)(H_2O)$, compared to the complex alteration-phase assemblage seen in the low drip-rate tests. The simpler phase assemblage in the high drip-rate tests may reflect higher overall reaction progress for the spent fuel in these tests. Also, samples

from the first sampling periods were not taken, and it is possible that the early phases formed but were not detected.

For ATM-103, the U concentrations in the high drip-rate tests are consistent with Na-boltwoodite being the solid phase controlling the U solubility. For the ATM-106 test, the U concentrations range from 4×10^{-8} to 3×10^{-7} *M*, which are consistent with β-uranophane being the solid phase controlling the U solubility (CRWMS M&O 2000, p 15).

The fuel in the ATM-103 high drip-rate test seems to have reacted along a uniform front at the outer surface of the spent-fuel fragments. This dissolution has proceeded without regard to existing grain boundaries. The data show no increase with time in the rate of radionuclide release. Of course, the dissolution of the fuel along grain boundaries is also important in the high drip-rate tests. This is especially evident from the extent to which the grain boundaries in one fragment of ATM-103 had been opened, resulting in a friable fragment that decomposed during sample handling (Stout and Leider 1998, p. 2-250).

Samples from low-drip-rate tests possess a much more complex assemblage of U^{6+} phases than observed in samples from either vapor or high-drip-rate tests. This complexity may reflect the limited influx of EJ-13 groundwater, which contributes Si, Na, Ca, and other cations. Common corrosion products from low-drip-rate tests include metaschoepite, an unidentified Na-uranyl oxy-hydroxide tentatively identified as "Na-compreignacite," and soddyite. A minor constituent is the Cs-Ba-Mo-uranate phase that commonly occurs adjacent to dissolving fuel grains. In one sample from the ATM-103 low-drip-rate test at the 5.2-year time interval, soddyite appears to replace Na-compreignacite. Also, a few isolated crystals of Na-boltwoodite were first detected in the ATM-103 low-drip-rate test at the 4.1-year time interval. They were later abundant at the 5.2-year time interval but less abundant than soddyite. These observations provide limited direct evidence for the replacement of uranyl oxy-hydroxides by uranyl silicates.

In Wilson's (1990) Series 3 tests using J-13 the uranium silicate, soddyite, and calcium uranium silicates, β-uranophane (haiweeite, minor) were found using XRD and SEM (Stout and Leider 1998, p. 2-261).

6.6.3 Comparison of Mineral Formation Between Laboratory Tests and Nopal I Studies

The sequence of uraninite alteration at Nopal I is similar to that of CSNF and UO_2 in the laboratory tests. Uraninite is already partially oxidized (Pearcy et al. 1994). Spent fuel and UO_2 must first undergo that first surface oxidation to approach uraninite. The corrosion products observed in laboratory CSNF and UO_2 tests conform to the mineral phases seen at Nopal I. The general sequence is oxidation of the solid surface followed by hydration, forming uranyl-oxide hydrates. Silicate in the groundwater is incorporated as soddyite. The silicate in combination with alkali ions, e.g., calcium and sodium, form various alkaline uranyl silicate hydrates, such as Na-boltwoodite and β-uranophane. The exact sequence and timing of formation depends significantly on local chemical environment, water flows, and time both in the laboratory tests and at the Nopal I site. Simultaneous precipitation is indicated in both laboratory and field tests. Some alteration phases, such as sklodowskite and compreignacite, are found in the laboratory tests but not at Nopal I. This may simply be a result of the small number of samples in all studies.

The groundwater at Nopal I is richer in calcium than J-13 (Pearcy et al. 1994) but poorer in sodium and potassium. This could explain the dominance of β-uranophane at the natural site as well as the limited soddyite and weeksite occurrence. There is substantial calcite at Yucca Mountain. In time this may make repository alteration products conform more to the Nopal I sequence than that seen in the laboratory, which produces β-uranophane at long times.

INTENTIONALLY LEFT BLANK

7. CONCLUSIONS

The overall spent-fuel oxidation reaction can be considered a sum of the oxidation and reduction electrochemical half-reactions (Shoesmith 1999):

$$UO_2 \Rightarrow UO_2^{2+} + 2e^- \qquad \text{(Eq. 1)}$$

$$\text{oxidant} + 2e^- \Rightarrow \text{reduced species} \qquad \text{(Eq. 2)}$$

The likely electrochemically determined UO_2 reaction sequence is

$$UO_2 \Rightarrow UO_{2+x} \Rightarrow UO_{2.33} \Rightarrow \{UO_2^{2+}\}_{surface} \xRightarrow{\text{surface oxidation}} [UO_2^{2+}]_{bulk} \xRightarrow{\text{bulk oxidation}} [UO_2^{2+}]_{soln} \xRightarrow{\text{dissolution}} \text{Secondary Phases}$$

Carbonate present in groundwaters, including those at Yucca Mountain, is a strong complexing agent for the uranyl species. At the alkaline conditions of groundwater, uranyl carbonate complexes predominate. These complexes are formed at the corroding surface and are highly soluble. Their fast dissolution is the primary mechanism of aqueous uranium dissolution from spent fuel. The most important uranium carbonate reactions are given in Section 6.1.

The developed dissolution model provides a classical Butler-Volmer relationship for the dissolution rate that is exponentially related to the energy change of the solid dissolving into a liquid. The model and its predecessors have a consistent thermodynamic basis. The general model function form was used for multilinear regression analyses over subsets of unirradiated UO_2 and spent-fuel UO_2 dissolution rate data. The model reduces to the classic chemical kinetic rate law:

$$\text{Rate} = k[A]^a[B]^b[C]^c \ldots \exp(-E_a/RT) \qquad \text{(Eq. 10)}$$

Burnup is represented as a concentration term as well because it is proportional to the aggregated production and concentration of fission products. For regression purposes, Equation 10 was transformed by taking logarithms of each term, fitting that equation, and allowing interaction and quadratic terms indicated by the data to improve the fit. The negative logarithms of the water chemistry variables were consistent with the standard definition of pH, $-\log_{10}[H^+]$.

The model form of Equation 11 includes a linear term of all variables with minimal loss in the adjusted correlation coefficient. The linear portion of the model is equivalent to the classic chemical rate law (Eq. 10). Equation 11 (note base-10 logarithms) represents the best-fit model:

$$\begin{aligned}\log_{10}(\text{Rate } UO_2 \text{ or CSNF}) &= a_0 \cdot 1 + a_1 \cdot \text{IT} + a_2 \cdot PCO_3 + a_3 \cdot PO_2 + a_4 \cdot \text{PH} \\ &+ a_5 \cdot \text{LBU} + a_6 \cdot PO_2 \cdot \text{IT} + a_7 \cdot \text{LBU} \cdot \text{IT} + a_8 \cdot \text{LBU} \cdot PCO_3 \\ &+ a_9 \cdot \text{LBU} \cdot PO_2 + a_{10} \cdot \text{LBU} \cdot \text{PH} + a_{11} \cdot PCO_3^2 \end{aligned} \qquad \text{(Eq. 11)}$$

The term definitions, coefficients, and fitting statistics are in Table 14.

While the model in Equation 11, Table 14, has the best fit to the qualified alkaline data, a simpler model is recommended for TSPA-SR.

For pH > 7,

$$\text{Log}_{10}\, DR = a_0 + a_1 \cdot \text{IT} + a_2 \cdot \text{PCO}_3 + a_3 \cdot \text{PO}_2 \qquad \text{(Eq. 16)}$$

where $a_0 = 4.69$, $a_1 = -1085$, $a_2 = -0.12$, and $a_3 = -0.32$.

The recommended model for acid conditions is:

For pH ≤ 7,

$$\text{Log}_{10}\, DR = a_0 + a_1 \cdot \text{IT} + a_3 \cdot \text{PO}_2 + a_4 \cdot \text{PH} \qquad \text{(Eq. 18)}$$

where $a_0 = 7.13$, $a_1 = -1085$, $a_3 = -0.32$, and a4 = -0.41.

The range of validity for these models is ±1.5 orders of magnitude.

The estimated CSNF dissolution rates based on ^{99}Tc high-drip-rate tests and geometric surface area are in Table 27. If a roughness factor of three (Gray and Wilson 1995) is applied to make the surface areas similar to the results in Table 1, the estimates from Table 27 are 17 and 38 mg/(m^2·d), respectively. The intrinsic dissolution model in Equation 11 predicts a value of 22 mg/(m^2·d) at a pH of 8, 0.001 *M* carbonate, and 90°C for a fuel with a burnup of 30 MWd/kgU. This agreement between the model and ^{99}Tc release rates is good.

Estimates of spent-fuel dissolution rate using late-time data from Wilson's Series 3 tests are generally close to (within a factor of 6), but less than, those predicted by the model in Equation 11. The Wilson test fuels are like ATM-103, in that their burnup is about 30 MWd/kgU. The dissolution model predicts a rate of about 20 mg/(m^2·d) at 85°C and about 6 mg/(m^2·d) at 25°C. That estimates from Wilson's work are less than those predicted by the model can easily be explained by examining the water chemistry in each estimate. Wilson's tests were carried out in calcium and silicate-containing J-13 water. As previously emphasized, the tests on which the model is based do not have those mineral-forming components. The water chemistry used in the dissolution tests is more aggressive without the calcium and silicates. The results of those tests (Table 1) provide a basis for a conservative (bounding) spent-fuel dissolution model.

Gray (1999) has reported combined GIs and GBIs of ^{129}I that were approximately equal to the FGR fractions for LWR spent fuels. For ^{137}Cs, the combined GIs and GBIs were approximately one-third of the FGR fractions. In some of the fuels tested, the FGRs are high, between 7 and 18%. Recent performance assessments of the proposed repository at Yucca Mountain, TSPA-VA (CRWMS M&O 1998a) modeled 2% of the total inventories of ^{135}Cs, ^{137}Cs, ^{129}I, and ^{99}Tc as located in the gap and grain-boundary regions. Based on Gray's measurements (Gray 1999), the 2% inventory estimate may underestimate the real GIs and GBIs in some fuels. It is recommended that TSPA-SR replaces the 2% estimate for ^{129}I and ^{137}Cs inventories with these newly measure values (1 and 1/3 FGR fractions respectively).

There is substantial similarity between the corrosion products found in laboratory tests with UO_2 and commercial spent nuclear fuel and the mineral assemblages found at Nopal I in Pena Blanca, Mexico. Nopal I is most like Yucca Mountain in terms of geology and environment. In the laboratory tests and at Nopal I, the general paragenetic trend of oxidation mineral products is mixed uranium oxides, uranyl oxyhydroxides, and uranium silicates, including the more complex alkaline uranium silicates. β-uranophane dominates at long times in both laboratory and field studies.

INTENTIONALLY LEFT BLANK

8. INPUTS AND REFERENCES

ASTM C 1174-97. *Standard Practice for Prediction of the Long-Term Behavior of Materials, Including Waste Forms, Used in Engineered Barrier Systems (EBS) for Geological Disposal of High-Level Radioactive Waste.* West Conshohocken, Pennsylvania: American Society for Testing and Materials. TIC: 246015.

CRC 1991. *CRC* Handbook *of Chemistry and Physics, Lide, D.R., ed., 1991-1992.* 72nd Edition. Boca Raton, FL: CRC Press. TIC: 3595.

CRWMS M&O 1998a. "Waste Form Degradation, Radionuclide Mobilization, and Transport Through the Engineered Barrier System." Chapter 6 of *Total System Performance Assessment-Viability Assessment (TSPA-VA) Analyses Technical Basis Document.* B00000000-01717-4301-00006 REV 01. Las Vegas, Nevada: CRWMS M&O. ACC: MOL.19981008.0006.

CRWMS M&O 1998b. *Waste Form Degradation and Radionuclide Mobilization Expert Elicitation Project.* Las Vegas, Nevada: CRWMS M&O. ACC: MOL.19980804.0099.

CRWMS M&O 1999a. *Activity Evaluation For "1101213FM3 Waste Form Analyses & Models - PMR".* Activity Evaluation, December 14, 1999. Las Vegas, Nevada: CRWMS M&0. ACC: MOL.19991217.0048.

CRWMS M&O 1999b. *Classification of the MGR Uncanistered Spent Nuclear Fuel Disposal Container System.* ANL-UDC-SE-000001 REV 00. Las Vegas, Nevada: CRWMS M&O. ACC: MOL.19990928.0216.

CRWMS M&O 1999c. *Waste Package Materials Department Analysis and Modeling Reports Supporting the Waste Form PMR.* TDP-EBS-MD-000005 REV 00. Las Vegas, Nevada: CRWMS M&O. ACC: MOL.19991027.0145.

CRWMS M&O 2000. *Commercial Spent Nuclear Fuel Degradation in Unsaturated Drip Tests.* Input Transmittal WP-WP-99432.T. Las Vegas, Nevada: CRWMS M&O. ACC: MOL.20000107.0209.

de Pablo, J.; Casas, I.; Gimenez, J.; Molera, M.; and Torrero, M.D. 1997. "Effect of Temperature and Bicarbonate Concentration on the Kinetics of UO2(s) Dissolution Under Oxidizing Conditions." *Scientific Basis for Nuclear Waste Management XX:* Symposium held December 2–6, 1996, Boston, Massachusetts, U.S.A., 465, 535-542. Pittsburgh, Pennsylvania: Materials Research Society. TIC: 238884.

DOE (U.S. Department of Energy) 1998. *Quality Assurance Requirements and Description.* DOE/RW-0333P, Rev. 8. Washington, D.C.: U.S. Department of Energy, Office of Civilian Radioactive Waste Management. ACC: MOL.19980601.0022.

Finn, P.A.; Finch, R.; Buck, E.; and Bates, J. 1998. "Corrosion Mechanism of Spent Fuel under Oxidizing Conditions." *Scientific Basis for Nuclear Waste Management XXI,* Symposium held September 28-October 3, 1997, Davos, Switzerland. McKinley, I.G. and McCombie, C., eds., 506, 123-131. Warrendale, Pennsylvania: Materials Research Society. TIC: 240702.

Forsyth, R. 1997. *The SKB Spent Fuel Corrosion Program. An Evaluation of Results from the Experimental Programme Performed in the Studsvik Hot Cell Laboratory.* SKB TR 97-25. 81 p. Stockholm, Sweden: Swedish Nuclear Fuel and Waste Management Co. TIC: 246406.

Forsyth, R.S.; Werme, L.O.; and Bruno, J. 1986. "The Corrosion of Spent UO2 Fuel in Synthetic Groundwater." *Journal of Nuclear Materials*, 138, 1-15. Amsterdam, The Netherlands: Elsevier Science Publishers. TIC: 246407.

Grambow, B. 1989. *Spent Fuel Dissolution and Oxidation: An Evaluation of Literature Data.* SKB Technical Report 89-13. Stockholm, Sweden: Swedish Nuclear Fuel and Waste Management. TIC: 208579.

Gray, W.J. 1999. "Inventories of Iodine-129 and Cesium-137 in the Gaps and Grain Boundaries of LWR Spent Fuels." *Scientific Basis for Nuclear Waste Management XXII, Symposium held November 30-December 4, 1998, Boston, Massachusetts,* Wronkiewicz, D.J. and Joon, L.H., eds. *556,* 487-494. Warrendale, Pennsylvania: Materials Research Society. TIC: 246426.

Gray, W.J. and Wilson, C.N. 1995. *Spent Fuel Dissolution Studies FY 1991-1994.* PNL-10450. Richland, Washington: Pacific Northwest Laboratory. ACC: MOL.19960802.0035.

Grenthe, I.; Fuger, J.; Konings, R.J.M.; Lemire, R.J.; Muller, A.B.; Nguyen-Trung, C.; and Wanner, H. 1992. *Chemical Thermodynamics of Uranium.* Volume 1 of *Chemical Thermodynamics* . Wanner, H. and Forest, I., eds. Amsterdam, The Netherlands: North-Holland Publishing Company. TIC: 224074.

LL980601551021.042. Conversion of Uranium Dissolution Rates from Spent Fuel and Uranium Dioxide. Submittal date: 06/16/98.

LL980704251021.045. Additional Spent Fuel Flow-Through Tests. Submittal date: 07/17/98.

LL980711051021.048. Spent Fuel Dissolution Rates as a Function of Burnup and Water Chemistry. Submittal date: 08/05/98.

LL990200151021.071. Inventories of Iodine-129 and Cesium-137 in the Gaps and Grain Boundaries of LWR Spent Fuels. Submittal date: 02/11/99.

LL990707151021.075 1999. *Spent Fuel Flowthrough Dissolution Rate Data Report.* Richland, WA: Pacific Northwest National Laboratory.

LL990901851021.084. Spent Fuel Flowthrough Dissolution Rate Data Report. Submittal date: 09/08/1999.

LL991001251021.090. CSNF Waste Form Degradation: Unsaturated Drip Tests. Submittal date: 10/04/99.

LL000107951021.107. Nuclide Inventory in Spent Fuel: Data Sheet. Submittal date: 01/12/2000.

McKenzie, W.F. 1992. *UO_2 Dissolution Rates: A Review.* UCRL-ID-111663. Livermore, California: Lawrence Livermore National Laboratory. TIC: 246408.

Murphy, W.M. 1995. "Natural Analogs for Yucca Mountain." *Radwaste Magazine, 2* (6), 44–50. La Grange Park, Illinois: American Nuclear Society. TIC: 237929.

Pearcy, E.C. and Murphy, W.M. 1991. *Geochemical Natural Analogs Literature Review.* CNWR 90-008. San Antonio, Texas: Center for Nuclear Waste Regulatory Analyses. TIC: 213164.

Pearcy, E.C.; Prikryl, J.D.; Murphy, W.M.; and Leslie, B.W. 1994. "Alteration of Uraninite from the Nopal I Deposit, Pena Blanca District, Chihuahua, Mexico, Compared to Degradation of Spent Nuclear Fuel in the Proposed U.S. High-Level Nuclear Waste Repository at Yucca Mountain, Nevada." *Applied Geochemistry, 9*, 713–732. New York, New York: Elsevier Science. TIC: 236934.

Reed, D.T. and Bowers, D.L. 1990. "Alpha Particle-Induced Formation Of Nitrate in the Cm-Sulfate Aqueous System." *Radiochimica Acta, 51*, 119–125. Munich, Germany: R. Oldenbourg Verlag. TIC: 245894.

Shoesmith, D.W. 1999. *Fuel Corrosion Processes Under Waste Disposal Conditions.* AECL-12034. Pinawa, Manitoba, Canada: Whiteshell Laboratories. TIC: 246006.

Steward, S.A. and Mones, E.T. 1996. "Uranium Dioxide Dissolution Under Acidic Aqueous Conditions Comparison." *Seventh International Conference on High-Level Radioactive Waste Management,* 388–389. La Grange Park, Illinois: American Nuclear Society.

Stout, R.B. and Leider, H.R. 1998. *Waste Form Characteristics Report, CD-ROM Version.* UCRL-ID-132375. Livermore, California: Lawrence Livermore National Laboratory. TIC: 246106.

Stroes-Gascoyne, S. 1996. "Measurements of Instant-Release Source Terms For 137Cs, 90Sr, 99Tc, 129I, and 14C in used CANDU Fuels." *Journal of Nuclear Materials, 238*, 264–277. Amsterdam, The Netherlands: Elsevier Science. TIC: 245893.

Stumm, W. and Morgan, J.J. 1981. *Aquatic Chemistry – An Introduction Emphasizing Chemical Equilibria in Natural Waters.* New York, New York: John Wiley & Sons. TIC: 208448.

Tait, J.C. and Luht, J.L. 1997. *Dissolution Rates of Uranium from Unirradiated U02 and Uranium and Radionuclides from Used CANDU Fuel Using the Single-Pass Flow-Through Apparatus.* 06819-REP-01200-0006 R00. Toronto, Ontario, Canada: Ontario Hydro. TIC: 243164.

Torrero, M.E.; Baraj, E.; De Pablo, J.; Gimenez, J.; and Casas, I. 1997. "Kinetics of Corrosion and Dissolution of Uranium Dioxide as a Function of pH." *International Journal of Chemical Kinetics, 29* (4), 261–267. New York, New York: John Wiley & Sons. TIC: 246160.

Wilson, C.N. 1990. *Results from NNWSI Series 3 Spent Fuel Dissolution Tests.* PNL-7170. Richland, Washington: Pacific Northwest Laboratory. ACC: NNA.19900329.0142.

Wilson, C.N. and Gray, W. J. 1990. "Measurement of Soluble Nuclide Dissolution Rates from Spent Fuel." *Scientific Basis for Nuclear Waste Management XIII,* Symposium held November 27-30, 1989, Boston, Massachusetts. Oversby, V.M. and Brown, P.W., eds.,*176*, 489–498. Pittsburgh, Pennsylvania: Materials Research Society. TIC: 203658.

Wolf, S.F.; Bowers, D.L.; and Cunnane, J.C. 1999. *Analysis of Three Mile Island and Quad Cities Spent Nuclear Fuel Samples.* Argonne, Illinois: Argonne National Laboratory. TIC: 246100.

ATTACHMENT I

DOCUMENT INPUT REFERENCE SHEET (DIRS)

INTENTIONALLY LEFT BLANK

OFFICE OF CIVILIAN RADIOACTIVE WASTE MANAGEMENT

DOCUMENT INPUT REFERENCE SYSTEM

1. Document Identifier No./Rev.:	Change:	Title:
ANL-EBS-MD-000015 REV 00	N/A	CSNF Waste Form Degradation: Summary Abstraction

Input Document							8. TBVDue To		
2a.	2. Technical Product Input Source Title and Identifier(s) with Version	3. Section	4. Input Status	5. Section Used in	6. Input Description	7. TBV/TBD Priority	Unqual.	From Uncontrolled Source	Un-Confirmed
1	CRWMS M&O 1998a. "Waste Form Degradation, Radionuclide Mobilization, and Transport Through the Engineered Barrier System." Chapter 6 of *Total System Performance Assessment-Viability Assessment (TSPA-VA) Analyses Technical Basis Document.* B00000000-01717-4301-00006 REV 01. Las Vegas, Nevada: CRWMS M&O. ACC: MOL.19981008.0006.	p 6-60	N/A - Reference Only	6.5	Corroborative data, clad gap and inventory fraction.	N/A	N/A	N/A	N/A
2	de Pablo, J.; Casas, I.; Gimenez, J.; Molera, M.; and Torrero, M.D. 1997. "Effect of Temperature and Bicarbonate Concentration on the Kinetics of UO2(s) Dissolution Under Oxidizing Conditions." *Scientific Basis for Nuclear Waste Management XX: Symposium held December 2-6, 1996, Boston, Massachusetts, U.S.A., 465,* 535-542. Pittsburgh, Pennsylvania: Materials Research Society. TIC: 238884.	Table I	N/A - Reference Only	6.2	Corroborative data, CSNF Dissolution Rates	N/A	N/A	N/A	N/A
6	Murphy, W.M. 1995. "Natural Analogs for Yucca Mountain." *Radwaste Magazine, 2* (6), 44-50. La Grange Park, Illinois: American Nuclear Society. TIC: 237929.	General	N/A - Reference Only	6.6.1	Corroborative data	N/A	N/A	N/A	N/A

OFFICE OF CIVILIAN RADIOACTIVE WASTE MANAGEMENT

DOCUMENT INPUT REFERENCE SYSTEM

1. Document Identifier No./Rev.:	Change:	Title:
ANL-EBS-MD-000015 REV 00	N/A	CSNF Waste Form Degradation: Summary Abstraction

Input Document			4. Input Status	5. Section Used in	6. Input Description	7. TBV/TBD Priority	8. TBVDue To		
2a.	2. Technical Product Input Source Title and Identifier(s) with Version	3. Section					Unqual.	From Uncontrolled Source	Un-Confirmed
7	Forsyth, R.S.; Werme, L.O.; and Bruno, J. 1986. "The Corrosion of Spent UO2 Fuel in Synthetic Groundwater." *Journal of Nuclear Materials, 138*, 1-15. Amsterdam, The Netherlands: Elsevier Science Publishers. TIC: 246407.	Figure 2 plot	N/A - Reference Only	6.2.4	Corroborative data, acidic dissolution	N/A	N/A	N/A	N/A
8	Grenthe, I.; Fuger, J.; Konings, R.J.M.; Lemire, R.J.; Muller, A.B.; Nguyen-Trung, C.; and Wanner, H. 1992. *Chemical Thermodynamics of Uranium.* Volume 1 of *Chemical Thermodynamics* . Wanner, H. and Forest, I., eds. Amsterdam, The Netherlands: North-Holland Publishing Company. TIC: 224074.	Table V.43	N/A - Reference Only	6.1	Corroborative data, Uranyl carbonate reactio	N/A	N/A	N/A	N/A
10	Wilson, C.N. 1990. *Results from NNWSI Series 3 Spent Fuel Dissolution Tests.* PNL-7170. Richland, Washington: Pacific Northwest Laboratory. ACC: NNA.19900329.0142.	Tables A.1 to A.4	N/A - Reference Only	6.4	Corroborative data	N/A	N/A	N/A	N/A
11	Pearcy, E.C.; Prikryl, J.D.; Murphy, W.M.; and Leslie, B.W. 1994. "Alteration of Uraninite from the Nopal I Deposit, Pena Blanca District, Chihuahua, Mexico, Compared to Degradation of Spent Nuclear Fuel in the Proposed U.S. High-Level Nuclear Waste Repository at Yucca Mountain, Nevada." *Applied Geochemistry, 9*, 713-732. New York, New York: Elsevier Science. TIC: 236934.	Table 2 and figure 8	N/A - Reference Only	4.1.6,6.6	Corroborative data	N/A	N/A	N/A	N/A

OFFICE OF CIVILIAN RADIOACTIVE WASTE MANAGEMENT

DOCUMENT INPUT REFERENCE SYSTEM

1. Document Identifier No./Rev.:	Change:	Title:
ANL-EBS-MD-000015 REV 00	N/A	CSNF Waste Form Degradation: Summary Abstraction

Input Document			4. Input Status	5. Section Used in	6. Input Description	7. TBV/TBD Priority	8. TBVDue To		
2a.	2. Technical Product Input Source Title and Identifier(s) with Version	3. Section					Unqual.	From Uncontrolled Source	Un-Confirmed
12	Reed, D.T. and Bowers, D.L. 1990. "Alpha Particle-Induced Formation Of Nitrate in the Cm-Sulfate Aqueous System." *Radiochimica Acta, 51*, 119-125. München, Germany: R. Oldenbourg Verlag. TIC: 245894.	General	N/A - Reference Only	6.1	Corroborative data, pH changes from irradiated gas phase	N/A	N/A	N/A	N/A
14	Shoesmith, D.W. 1999. *Fuel Corrosion Processes Under Waste Disposal Conditions.* AECL-12034. Pinawa, Manitoba, Canada: Whiteshell Laboratories. TIC: 246006.	Entire	N/A - Reference Only	6.1	Supporting Information. Chemical basis of spent fuel dissolution.	N/A	N/A	N/A	N/A
15	Steward, S.A. and Mones, E.T. 1996. "Uranium Dioxide Dissolution Under Acidic Aqueous Conditions Comparison." *High Level Radioactive Waste Management, Proceedings of the Seventh Annual International Conference, Las Vegas, Nevada, April 29-May 3, 1996*, 388-389. La Grange Park, Illinois: American Nuclear Society. TIC: 226494.	Entire	N/A - Reference Only	6.2.4	corroborative data, acidic dissolution rates	N/A	N/A	N/A	N/A
16	Stroes-Gascoyne, S. 1996. "Measurements of Instant-Release Source Terms For 137Cs, 90Sr, 99Tc, 129I and 14C in Used CANDU Fuels." *Journal of Nuclear Materials, 238*, 264-277. Amsterdam, The Netherlands: Elsevier Science B.V. TIC: 245893.	Entire	N/A - Reference Only	6.5	corroborative data, gap and grain boundary inventories	N/A	N/A	N/A	N/A

OFFICE OF CIVILIAN RADIOACTIVE WASTE MANAGEMENT

DOCUMENT INPUT REFERENCE SYSTEM

1. Document Identifier No./Rev.:	Change:	Title:
ANL-EBS-MD-000015 REV 00	N/A	CSNF Waste Form Degradation: Summary Abstraction

Input Document			4. Input Status	5. Section Used in	6. Input Description	7. TBV/TBD Priority	8. TBVDue To		
2a.	2. Technical Product Input Source Title and Identifier(s) with Version	3. Section					Unqual.	From Uncontrolled Source	Un-Confirmed
17	Tait, J.C. and Luht, J.L. 1997. *Dissolution Rates of Uranium from Unirradiated U02 and Uranium and Radionuclides from Used CANDU Fuel Using the Single-Pass Flow-Through Apparatus.* 06819-REP-01200-0006 R00. Toronto, Ontario, Canada: Ontario Hydro. TIC: 243164.	Figures 3 to 21	N/A - Reference Only	6.2	Corroborative data, CSNF dissolution rates	N/A	N/A	N/A	N/A
18	Torrero, M.E.; Baraj, E.; De Pablo, J.; Gimenez, J.; and Casas, I. 1997. "Kinetics of Corrosion and Dissolution of Uranium Dioxide as a Function of pH." *International Journal of Chemical Kinetics, 29* (4), 261-267. New York, New York: John Wiley & Sons. TIC: 246160.	Table 1	N/A - Reference Only	6.2	Corroborative data, CSNF dissolution rates	N/A	N/A	N/A	N/A
20	Wolf, S.F.; Bowers, D.L.; and Cunnane, J.C. 1999. *Analysis of Three Mile Island and Quad Cities Spent Nuclear Fuel Samples.* Argonne, Illinois: Argonne National Laboratory. TIC: 246100.	Table 8, p.18	N/A - Reference Only	4.1.2	Corroborative data for ATM-109 burnup rate	N/A	N/A	N/A	N/A
26	Forsyth, R. 1997. *The SKB Spent Fuel Corrosion Program. An Evaluation of Results from the Experimental Programme Performed in the Studsvik Hot Cell Laboratory.* SKB TR 97-25. 81 p. Stockholm, Sweden: Swedish Nuclear Fuel and Waste Management Co. TIC: 246406.	Table 7-3	N/A - Reference Only	6.2	Corroborative data, CSFN dissolution rates	N/A	N/A	N/A	N/A

OFFICE OF CIVILIAN RADIOACTIVE WASTE MANAGEMENT

DOCUMENT INPUT REFERENCE SYSTEM

1. Document Identifier No./Rev.:	Change:	Title:
ANL-EBS-MD-000015 REV 00	N/A	CSNF Waste Form Degradation: Summary Abstraction

Input Document			4. Input Status	5. Section Used in	6. Input Description	7. TBV/TBD Priority	8. TBVDue To		
2a.	2. Technical Product Input Source Title and Identifier(s) with Version	3. Section					Unqual.	From Uncontrolled Source	Un-Confirmed
27	LL990707151021.075. Spent Fuel Flowthrough Dissolution Rate Data Report. Submittal date: 07/23/1999.	Tbl. 2, Fig. 1-9	N/A - Qualified-Verification Level 2	4.1.2, 6.2	Direct use data, CSNF dissolution rates.	N/A	N/A	N/A	N/A
31	DOE (U.S. Department of Energy) 1998. *Quality Assurance Requirements and Description.* DOE/RW-0333P, Rev. 8. Washington, D.C.: U.S. Department of Energy, Office of Civilian Radioactive Waste Management. ACC: MOL.19980601.0022.	Entire	N/A - Reference Only	2	DOE QA Requirements and Description	N/A	N/A	N/A	N/A
32	CRWMS M&O 1998b. *Waste Form Degradation and Radionuclide Mobilization Expert Elicitation Project.* Las Vegas, Nevada: CRWMS M&O. ACC: MOL.19980804.0099.	Appendix D	N/A - Reference Only	6.2	Elicitation Summary	N/A	N/A	N/A	N/A
38	LL990200151021.071. Inventories of I-129 and CS-137 in the Gaps and Grain Boundaries of LWR Spent Fuels. Submittal date: 02/11/1999.	Entire	N/A - . Reference Only	4.1.5,6.5	Plots of data in Table 10	N/A	N/A	N/A	N/A
41	LL980711051021.048. Spent Fuel Dissolution Rates as a Function of Burnup and Water Chemistry. Submittal date: 08/05/1998.	Entire	N/A - Qualified-Verification Level 2	4.1.2, 6.2	Direct Use Data. CSNF dissolution rates.	N/A	N/A	N/A	N/A
44	LL990901851021.084. Spent Fuel Flowthrough Dissolution Rate Data Report. Submittal date: 09/10/1999. Submit to RPC	Entire	N/A - Qualified-Verification Level 2	4.1.2, 6.2	Direct Use Data. CSNF dissolution rates	N/A	N/A	N/A	N/A

OFFICE OF CIVILIAN RADIOACTIVE WASTE MANAGEMENT

DOCUMENT INPUT REFERENCE SYSTEM

1. Document Identifier No./Rev.:	Change:	Title:
ANL-EBS-MD-000015 REV 00	N/A	CSNF Waste Form Degradation: Summary Abstraction

Input Document			4. Input Status	5. Section Used in	6. Input Description	7. TBV/TBD Priority	8. TBVDue To		
2a.	2. Technical Product Input Source Title and Identifier(s) with Version	3. Section					Unqual.	From Uncontrolled Source	Un-Confirmed
45	Stout, R.B. and Leider, H.R. 1998. *Waste Form Characteristics Report, CD-ROM Version.* UCRL-ID-132375. Livermore, California: Lawrence Livermore National Laboratory. TIC: 246106.	Numerous	N/A - Reference Only	Numerous	Numerous inputs for supporting information and data	N/A	N/A	N/A	N/A
46	CRWMS M&O 1999c. *Waste Package Materials Department Analysis and Modeling Reports Supporting the Waste Form PMR.* TDP-EBS-MD-000005 REV 00. Las Vegas, Nevada: CRWMS M&O. ACC: MOL.19991027.0145.	Entire	N/A - Reference Only	1	Development requirements	N/A	N/A	N/A	N/A
47	Gray, W.J. 1999. "Inventories of Iodine-129 and Cesium-137 in the Gaps and Grain Boundaries of LWR Spent Fuels." *Scientifc Basis for Nuclear Waste Management XXII, Symposium held November 30-December 4, 1998, Boston, Massachusetts,* Wronkiewicz, D.J. and Joon, L.H., eds. *556,* 487-494. Warrendale, Pennsylvania: Materials Research Society. TIC: 246426.	Entire	N/A - Reference Only	4.1.5,6.5,7	Corroborative information	N/A	N/A	N/A	N/A
48	Gray, W.J. and Wilson, C.N. 1995. *Spent Fuel Dissolution Studies FY 1991-1994.* PNL-10450. Richland, Washington: Pacific Northwest Laboratory. ACC: MOL.19960802.0035.	Entire	N/A - Reference Only	6.2.3,6.3.4,6.4,7	Corroborative information	N/A	N/A	N/A	N/A

OFFICE OF CIVILIAN RADIOACTIVE WASTE MANAGEMENT

DOCUMENT INPUT REFERENCE SYSTEM

1. Document Identifier No./Rev.:	Change:	Title:
ANL-EBS-MD-000015 REV 00	N/A	CSNF Waste Form Degradation: Summary Abstraction

Input Document			4. Input Status	5. Section Used in	6. Input Description	7. TBV/TBD Priority	8. TBVDue To		
2a.	2. Technical Product Input Source Title and Identifier(s) with Version	3. Section					Unqual.	From Uncontrolled Source	Un-Confirmed
50	Wilson, C.N. and Gray, W. J. 1990. "Measurement of Soluble Nuclide Dissolution Rates from Spent Fuel." *Scientific Basis for Nuclear Waste Management XIII, Symposium held November 27-30, 1989, Boston, Massachusetts,* Oversby, V.M. and Brown, P.W., eds. *176,* 489-498. Pittsburgh, Pennsylvania: Materials Research Society. TIC: 203658.	Entire	N/A - Reference Only	6.2.3,6.4	Corroborative information	N/A	N/A	N/A	N/A
52	LL980601551021.042. Comparison of Uranium Dissolution Rates from Spent Fuel and Uranium Dioxide. Submittal date: 06/16/1998.	Entire	N/A - Qualified-Verification Level 2	4.1.2	Direct use data. SNF dissolution rates.	:N/A	N/A	N/A	N/A
53	LL980704251021.045. Additional Spent Fuel Flow-Through Tests. Submittal date: 07/17/1998.	Entire	N/A - Qualified-Verification Level 2	4.1.2	Direct use data. SNF dissolution rates.	N/A	N/A	N/A	N/A
56	Pearcy, E.C. and Murphy, W.M. 1991. *Geochemical Natural Analogs Literature Review.* CNWR 90-008. San Antonio, Texas: Center for Nuclear Waste Regulatory Analyses. TIC: 213164.	Entire	N/A - Reference Only	6.6.1	Corroborative information	N/A	N/A	N/A	N/A

OFFICE OF CIVILIAN RADIOACTIVE WASTE MANAGEMENT

DOCUMENT INPUT REFERENCE SYSTEM

1. Document Identifier No./Rev.:	Change:	Title:
ANL-EBS-MD-000015 REV 00	N/A	CSNF Waste Form Degradation: Summary Abstraction

Input Document			4. Input Status	5. Section Used in	6. Input Description	7. TBV/TBD Priority	8. TBVDue To		
2a.	2. Technical Product Input Source Title and Identifier(s) with Version	3. Section					Unqual.	From Uncontrolled Source	Un-Confirmed
59	Finn, P.A.; Finch, R.; Buck, E.; and Bates, J. 1998. "Corrosion Mechanism of Spent Fuel under Oxidizing Conditions." *Scientific Basis for Nuclear Waste Management XXI, Symposium held September 28-October 3, 1997, Davos, Switzerland,* McKinley, I.G. and McCombie, C., eds. *506,* 123-131. Warrendale, Pennsylvania: Materials Research Society. TIC: 240702.	Entire	N/A - Reference Only	6.3.1	Corroborative information	N/A	N/A	N/A	N/A
60	ASTM C 1174-97. 1997. *Standard Practice for Prediction of the Long-Term Behavior of Materials, Including Waste Forms, Used in Engineered Barrier Systems (EBS) for Geological Disposal of High-Level Radioactive Waste.* West Conshohocken, Pennsylvania: American Society for Testing and Materials. TIC: 246015.	Entire	N/A - NRC Guidance/Codes & Standards	4.3	Corroborative information	N/A	N/A	N/A	N/A
61	McKenzie, W.F. 1992. *UO2 Dissolution Rates: A Review.* UCRL-ID-111663. Livermore, California: Lawrence Livermore National Laboratory. TIC: 246408.	Entire	N/A - Reference Only	6.2	corroborative information	N/A	N/A	N/A	N/A

OFFICE OF CIVILIAN RADIOACTIVE WASTE MANAGEMENT

DOCUMENT INPUT REFERENCE SYSTEM

1. Document Identifier No./Rev.:	Change:	Title:
ANL-EBS-MD-000015 REV 00	N/A	CSNF Waste Form Degradation: Summary Abstraction

Input Document			4. Input Status	5. Section Used in	6. Input Description	7. TBV/TBD Priority	8. TBVDue To		
2a.	2. Technical Product Input Source Title and Identifier(s) with Version	3. Section					Unqual.	From Uncontrolled Source	Un-Confirmed
63	Grambow, B. 1989. *Spent Fuel Dissolution and Oxidation: An Evaluation of Literature Data.* SKB Technical Report 89-13. Stockholm, Sweden: Swedish Nuclear Fuel and Waste Management. TIC: 208579.	Entire	N/A - Reference Only	6.2,6.2.3,6.2.4	Corroborative information	N/A	N/A	N/A	N/A
66	CRWMS M&O 2000. *Commercial Spent Nuclear Fuel Degradation in Unsaturated Drip Tests.* Input Transmittal WP-WP-99432.T. Las Vegas, Nevada: CRWMS M&O. ACC: MOL.20000107.0209.	Entire	N/A - Reference Only	Entire	Data Transmittal Report	N/A	N/A	N/A	N/A
67	LL991001251021.090. Draft - CSNF Waste Form Degradation: Unsaturated Drip Tests - G2020 Analysis and Modeling Report . Submittal date: 10/04/1999.	Entire	N/A - Reference Only	4.1.3	Corroborative information.	N/A	N/A	N/A	N/A
68	Stumm, W. and Morgan, J.J. 1981. *Aquatic Chemistry – An Introduction Emphasizing Chemical Equilibria in Natural Waters.* New York, New York: John Wiley & Sons. TIC: 208448.	Fig. 4.3 p 181	N/A - Reference Only	6.2.3	Carbonate-pH correlation	N/A	N/A	N/A	N/A
71	CRWMS M&O 1999b. *Classification of the MGR Uncanistered Spent Nuclear Fuel Disposal Container System.* ANL-UDC-SE-000001 REV 00. Las Vegas, Nevada: CRWMS M&O. ACC: MOL.19990928.0216.	p.7	N/A - Qualified/Confirmed/Controlled	2	Quality classification	N/A	N/A	N/A	N/A

OFFICE OF CIVILIAN RADIOACTIVE WASTE MANAGEMENT

DOCUMENT INPUT REFERENCE SYSTEM

1. Document Identifier No./Rev.:	Change:	Title:
ANL-EBS-MD-000015 REV 00	N/A	CSNF Waste Form Degradation: Summary Abstraction

Input Document			4. Input Status	5. Section Used in	6. Input Description	7. TBV/TBD Priority	8. TBVDue To		
2a.	2. Technical Product Input Source Title and Identifier(s) with Version	3. Section					Unqual.	From Uncontrolled Source	Un-Confirmed
73	CRC 1991. *CRC Handbook of Chemistry and Physics, Lide, D.R., ed., 1991-1992.* 72nd Edition. Boca Raton, FL: CRC Press. TIC: 3595.	Table 15-33	N/A - Reference Only	4.1.3	Corroborative information.	N/A	N/A	N/A	N/A
74	CRWMS M&0 1999a. *Activity Evaluation For "1101213FM3 Waste Form Analyses & Models - PMR".* Activity Evaluation, December 14, 1999. Las Vegas, NV: CRWMS M&0. ACC: MOL.19991217.0048.	Entire	N/A - Reference Only	2	Development of analysis	N/A	N/A	N/A	N/A
75	LL000107951021.107. Nuclide Inventory in Spent Fuel: Data Sheet. Submittal date: 01/12/2000.	Entire	N/A - . Qualified-Verification Level 2	4.1.5	Gap and grain boundary inventories	N/A	N/A	N/A	N/A